LOCAL L 1 SUB-FINSLER GEOMETRY IN DIMENSION 3: NON-GENERIC CASES

Fazia Harrache, Francesca Chittaro, Mohamed Aidene

LOCAL L^1 SUB-FINSLER GEOMETRY IN DIMENSION 3: NON-GENERIC CASES

FAZIA HARRACHE, FRANCESCA C. CHITTARO, AND MOHAMED AIDÈNE

Abstract. We study the local geometry of the sub-Finsler structure induced by a sub-Riemannian metric on a 3-dimensional manifold. We provide a description of the upper part of the cut locus for short geodesics, in some non generic cases.

1. Introduction

Consider a pair of smooth vector fields f, g on $\mathbb{R}^3$ such that f, g and their Lie brackets $[f, g]$ are linearly independent at every point of $\mathbb{R}^3$. For every $\boldsymbol{q} \in \mathbb{R}^3$, define on $\mathrm{span}\{f(\boldsymbol{q}), g(\boldsymbol{q})\}$ some norm $h_{\boldsymbol{q}}$, smoothly depending on $\boldsymbol{q}$. This norm endows the whole $\mathbb{R}^3$ with a distance function, defined in the following way: given two points $\boldsymbol{q}_0, \boldsymbol{q}_1 \in \mathbb{R}^3$, their distance is defined as

$$d(\boldsymbol{q}_0, \boldsymbol{q}_1) = \inf \left\{ \int_0^1 h_{\gamma(t)}(\dot\gamma(t))dt \ : \ \left\{ \begin{array}{c} \gamma \in AC([0,1], \mathbb{R}^3) \\ \dot\gamma(t) \in \mathrm{span}\{f(\gamma(t)), g(\gamma(t))\} \text{ a.e. } t \\ \gamma(0) = \boldsymbol{q}_0, \ \gamma(1) = \boldsymbol{q}_1. \end{array} \right. \right\}. \tag{1}$$

If the norm $h_{\boldsymbol{q}}$ is the restriction to $\mathrm{span}\{f(\boldsymbol{q}), g(\boldsymbol{q})\}$ of some Riemannian norm on $\mathbb{R}^3$, the optimal control problem (1) is the well known sub-Riemannian problem (see for instance the books [4, 19] and references therein). If instead $h_{\boldsymbol{q}}$ is not related to a scalar product on the span of f and g, we are in the more general case of sub-Finsler geometry.

Sub-Finsler geometry is a rather new research fields, and few publications are now available. We mention the paper [11], in which the authors study the unit sphere of left-invariant sub-Finsler metrics on Lie groups, and the papers [13, 14], where $h_{\boldsymbol{q}}$ is a positive homogeneous function on the distribution, smooth outside the zero section; the generic three dimensional case and the Engel group in dimension four are studied.

In the papers [6, 7, 8, 9, 18], the sub-Finsler problem is approached from the viewpoint of geometric control; in particular, thanks to a suitable time reparametrisation, the problem of finding the shortest path between two endpoints can be reformulated as a minimum-time problem for a control system linear in the control, with some suitable constraints on the set of admissible controls. In particular, in [9] the time-optimal synthesis (from the origin) is provided for three celebrated distributions in dimension 2 and 3, that is, the Grushin, Heisenberg and Martinet distribution. In [8], the Pontryagin extremals for a free nilpotent distribution of rank 2 and step 3 in $\mathbb{R}^5$ are analysed.

The papers [6, 7] deal with generic distributions in dimension 2 and 3. In particular, in [7] the authors consider a generic rank 2 step 2 distribution in $\mathbb{R}^3$, endowed with a maximum norm, and study the local time optimal synthesis from the origin, that is, the structure of the small spheres and the local cut locus; the Heisenberg system studied in [9] corresponds to the nilpotent part of such distributions. The analysis is carried out by means of a perturbative expansion in terms of a small parameter, linked to the final time, in the spirit of the results [2, 10, 12] obtained for the conjugate locus of the contact sub-Riemannian case in dimension 3 (see also [22] for an analogous result in dimension 5). In the cited paper, the authors identify two invariants of the distribution (called respectively C_1 and C_2) and provide a complete characterization of the cut locus of short geodesics in the case in which $C_1 C_2 \neq 0$.

In this paper, we are concerned with the sub-Finsler L^1 problem, that is, we assume that the norm of any vector $X = \alpha f(\boldsymbol{q}) + \beta g(\boldsymbol{q})$ is defined by $h_{\boldsymbol{q}}(X) = |\alpha| h_{\boldsymbol{q}}(f(\boldsymbol{q})) + |\beta| h_{\boldsymbol{q}}(g(\boldsymbol{q}))$. The induced metric structure is called a sub-Finsler L^1 metric. Up to a change of variables in the set

of controls, this problem is completely equivalent to the one studied in [7], where the L^∞ norm is instead considered.

We are also restricting ourselves to L^1 sub-Finsler structures which are *compatible with a sub-Riemannian metric* (according to Definition 2); loosely speaking, we require that the manifold is endowed with a Riemannian structure, and that the vector fields f and g are obtained from an orthonormal frame by applying a *constant* non-singular linear transformation. Thanks to this choice, we can take advantage of the Agrachev-Gauthier normal form of the vector fields f and g (see [5, 12]), which permits us to considerably simplify the computations. The choice of focusing on such structures has also other advantages: first of all, thanks to the symmetries of the vector fields, it is sufficient to compute the analytic expression of a rather reduced number of trajectories, and recover the other ones by applying suitable coordinate changes and permutations in the invariants; the same can be done for several other computations (such as the computation of Maxwell points and of wavefronts). Moreover, we can single out six main invariants (called A, C_1, C_2, D_1, E_1, where C_1 and C_2 are equivalent to their homonyms in [7]), linked to the geometric invariant of the sub-Riemannian structure, and provide a complete characterisation of the upper part of the cut locus based on the values of these invariants. Finally, it can be proved ([16]) that, restricting to this particular class of sub-Finsler structures, it is possible to obtain the same results of [7], at least for what concerns the upper part of the local sphere (that is, for final points such that $|z| \geq |xy|/2$). Therefore, in this paper we are concerned with the special case the invariant C_1 is null, while $C_2 \neq 0$ (thanks to the symmetries of the problem, the case in which $C_1 \neq 0$ and $C_2 = 0$ can be recovered by a suitable change of variables and rearrangement of the invariants of the distribution). As in [7], we are interested in the local problem, that is, we are studying the optimality of short geodesics; following the cited papers [2, 7, 12], we analyse the jets of the trajectories of the control system with respect to some small parameter (linked to the final time), and provide a detailed description of the upper part of the cut locus of the jets of the geodesics, in the case in which the invariant C_1 is null, but both invariants E_1 and D_1 are nonzero.

Adapting the same techniques of [12], it is possible to prove that the condition $C_1 \neq 0$ is generically true (in the sense specified in Section 2.1.1); in particular, for a generic L^1 sub-Finsler structure compatible with a sub-Riemannian structure, the set of points $\boldsymbol{q} \in M$ such that $C_1 = 0$ has codimension 1 in M. We can also prove that the subset characterised by $D_1 = E_1 = 0$ has codimension 2 in the set of points for which $C_1 = 0$. The assumption $D_1 E_1 \neq 0$ is thus generically true in the subset of degenerate cases.

The structure of the paper is the following: in Section 2 we state the problem under concern, we provide the normal form of the vector fields f and g and we start the investigation of the time-optimal synthesis, by applying the Pontryagin Maximum Principle (PMP); finally, we recall the structure of the optimal trajectories of the nilpotent case, already studied in [9]. In Section 3 we compute the jets of the bang-bang extremals and of the switching times; we also briefly discuss the notions of local and global optimality, and we provide a definition for the cut and the conjugate locus. The short Section 4 contains a summary of the methods used to locate the cut locus of the geodesics; the analysis is thus carried out Sections 5-6-7.

In Section 8 we discuss the problem which are still left to analyse.

The Appendices contain the results of some useful computations and the analysis of the intersections of the fronts.

2. Statement of the problem and preliminary analysis

Let us consider a smooth 3 dimensional connected sub-Riemannian manifold $(g, \mathcal{D}, M)$, where $\mathcal{D} \subset TM$ is a smooth 2-dimensional distribution of constant non-holonomic degree 2 ([4, 17]), and $g : \mathcal{D} \times \mathcal{D} \to \mathbb{R}$ is a positive definite quadratic form, smoothly depending on $\boldsymbol{q} \in M$, that defines a scalar product on $\mathcal{D}_{\boldsymbol{q}}$ for every $\boldsymbol{q}$ in M.

In the paper [12], the authors construct a suitable change of variables that provides normal coordinates and a normal form for the sub-Riemannian structure $(g, \mathcal{D}, M)$. More precisely, [12, Theorem 3.1] states that for every $\boldsymbol{q} \in M$ there exist local coordinates $(\boldsymbol{x}, \boldsymbol{y}, \boldsymbol{z})$ centred at $\boldsymbol{q}$ and

an orthonormal basis ℓ, g for $g_{\boldsymbol{q}}$ that can be written as

$$\ell = \begin{pmatrix} 1+y^2\beta(x,y,z) \\ -xy\beta(x,y,z) \\ -\frac{y}{2}(1+\gamma(x,y,z)) \end{pmatrix} \qquad g = \begin{pmatrix} -xy\beta(x,y,z) \\ (1+x^2)\beta(x,y,z) \\ \frac{x}{2}(1+\gamma(x,y,z)) \end{pmatrix}, \tag{2}$$

where $\beta, \gamma : \mathbb{R}^3 \to \mathbb{R}$ are two smooth functions satisfying

$$\beta(0,0,z) = \gamma(0,0,z) = 0 \quad \forall z \in \mathbb{R} \tag{3}$$

$$\frac{\partial \gamma}{\partial x}(0,0,z) = \frac{\partial \gamma}{\partial y}(0,0,z) = 0 \quad \forall z \in \mathbb{R}. \tag{4}$$

Remark 1. *The jets of the functions β and γ are closely connected with some geometric invariants of the sub-Riemannian manifold $(g, \mathcal{D}, M)$, such as the curvature (see* [5, 12]*).*

We now endow $\mathcal{D}$ with a smooth L^1 norm, in which the vector fields ℓ, g still play a special role; such a L^1 metric will be said *compatible with the sub-Riemannian structure.*

Definition 1. *Let U be a neighbourhood in M. Consider two vector fields f, g on U such that $f(\boldsymbol{q})$ and $g(\boldsymbol{q})$ are linearly independent and belong to $\mathcal{D}_{\boldsymbol{q}}$ for every $\boldsymbol{q} \in U$. The pair (f, g) defines a local L^1 norm, in the following way: the L^1 norm of both f and g is set to 1 and, for every vector $X \in \mathcal{D}_{\boldsymbol{q}}$, the L^1 norm of X is defined as*

$$\|X\|_1 = |\lambda_1| + |\lambda_2|,$$

where λ_1 and λ_2 are the unique real numbers such that $X = \lambda_1 f(\boldsymbol{q}) + \lambda_2 g(\boldsymbol{q})$.

Definition 2. *We say that the L^1 metric associated with (f, g) is compatible with $g_{\boldsymbol{q}}$ there exists a constant non-singular two dimensional square matrix M such that*

$$\begin{pmatrix} f \\ g \end{pmatrix} = M \begin{pmatrix} \ell \\ g \end{pmatrix}. \tag{5}$$

Up to rescaling the L^1 norm, we can always assume that $\det M = 1$. The most particular case of a compatible L^1 metric is the one in which $f = \ell$ and $g = g$.

As in the sub-Riemannian case, the norm $\|\cdot\|_1$ endows U with a distance function. Indeed, given two points $\mathbf{x}_0$ and $\mathbf{x}_1 \in U$, their distance is defined as the minimum of the functional

$$J(\boldsymbol{u}) = \int_0^1 |u_1(t)| + |u_2(t)| \, dt$$

over all measurable L^1 functions $\boldsymbol{u} = (u_1, u_2) : [0,1] \to \mathbb{R}^2$ such that the trajectories of the control system

$$\dot{\boldsymbol{\xi}}(t) = \big(u_1(t) f + u_2(t) g\big) \circ \boldsymbol{\xi}(t) \tag{6}$$

satisfy $\boldsymbol{\xi}(0) = \mathbf{x}_0$ and $\boldsymbol{\xi}(1) = \mathbf{x}_1$ (if the minimum does not exist, the distance is set to $+\infty$).

Thanks to the fact that $\mathcal{D}$ is a non-holonomic distribution and to Rashevsky-Chow Theorem (see for instance [3, 17]), a solution of the control system (6) connecting $\mathbf{x}_0$ with $\mathbf{x}_1$ and completely contained in U always exists.

Applying a suitable time reparametrisation, the problem under investigation can be rewritten as the following minimum-time problem:

$$\text{minimise } T \text{ subject to}$$

$$\dot{\boldsymbol{\xi}}(t) = u_1(t) f(\boldsymbol{\xi}(t)) + u_2(t) g(\boldsymbol{\xi}(t)), \tag{7a}$$

$$\boldsymbol{\xi}(0) = \mathbf{x}_0, \quad \boldsymbol{\xi}(T) = \mathbf{x}_1,$$

$$\boldsymbol{u} : [0, T] \to Q \quad \text{measurable}, \tag{7b}$$

where $Q = \{(u_1, u_2) \in \mathbb{R}^2 : |u_1| + |u_2| \leq 1\}$ and the final time T is free. A straightforward application of Filippov's theorem (see for instance [3]) guarantees that the minimum is attained for every pair $(\mathbf{x}_0, \mathbf{x}_1)$ belonging to U. Without loss of generality, in the following we set $\mathbf{x}_0 = (0,0,0)$.

2.1. **The normal form.** In this section we perform a coordinate change that allows us to obtain a nice symmetric form of the two vector fields f, g defining the sub-Finsler structure of M.

Proposition 1. *Let $(\mathbf{x}, \mathbf{y}, \mathbf{z})$ be the normal coordinates in which $\mathbf{f}$ and $\mathbf{g}$ assume the form (2). There exists a change of coordinates $\Phi : (\mathbf{x}, \mathbf{y}, \mathbf{z}) \mapsto (x, y, z)$ such that $\mathbf{z} = z$ and*

$$f = \frac{\partial}{\partial x} + yW \qquad g = \frac{\partial}{\partial y} - xW, \tag{8}$$

where W is a smooth vector field of the form

$$\begin{pmatrix} L_{11}x + L_{12}y \\ L_{21}x + L_{22}y \\ -\frac{1}{2} + L_{31}x + L_{32}y \end{pmatrix}$$

and $L_{ij} : \mathbb{R}^3 \to \mathbb{R}$ are smooth functions satisfying $L_{ij}(0, 0, z) = 0$ for every z.

Proof. The proofs relies on straightforward computations. Let

$$M = \begin{pmatrix} \mu_1 & \mu_2 \\ \mu_3 & \mu_4 \end{pmatrix} \tag{9}$$

be the matrix appearing in equation (5), and assume without loss of generality that $\det M = 1$. Set

$$\begin{pmatrix} x \\ y \end{pmatrix} = M^{-1} \begin{pmatrix} \mathbf{x} \\ \mathbf{y} \end{pmatrix}, \qquad z = \mathbf{z}.$$

Then it is immediate to verify that

$$f = \frac{\partial}{\partial x} + yH(\Phi^{-1}(x, y, z)) \qquad g = \frac{\partial}{\partial y} - xH(\Phi^{-1}(x, y, z)),$$

where $H(\mathbf{x}, \mathbf{y}, \mathbf{z}) = \beta(\mathbf{x}, \mathbf{y}, \mathbf{z})\Big(\mathbf{y}\frac{\partial}{\partial \mathbf{x}} - \mathbf{x}\frac{\partial}{\partial \mathbf{y}}\Big) - \frac{1}{2}(1 + \gamma(\mathbf{x}, \mathbf{y}, \mathbf{z}))\frac{\partial}{\partial \mathbf{z}}$.

From (3) and (4), it is easy to see that

$$\beta(\Phi^{-1}(0, 0, z)) = \gamma(\Phi^{-1}(0, 0, z)) = 0 \quad \forall z \in \mathbb{R}$$
$$\frac{\partial\big(\gamma \circ \Phi^{-1}\big)}{\partial x}(0, 0, z) = \frac{\partial\big(\gamma \circ \Phi^{-1}\big)}{\partial y}(0, 0, z) = 0 \quad \forall z \in \mathbb{R},$$

and the proposition is proved. □

Remark 2. *By straightforward computations it is easy to prove that, possibly shrinking U, the vector fields f, g and $[f, g]$ are linearly independent on U.*

The functions L_{ij}, $i = 1, 2, 3$, $j = 1, 2$, can be written as

$$L_{ij}(x, y, z) = \mathrm{ax}_{ij}x + \mathrm{ay}_{ij}y + \frac{1}{2}\begin{pmatrix} x & y & z \end{pmatrix} \begin{pmatrix} \omega_{xxij} & \omega_{xyij} & \omega_{xzij} \\ \omega_{yxij} & \omega_{yyij} & \omega_{yzij} \\ \omega_{zxij} & \omega_{zyij} & \omega_{zzij} \end{pmatrix} \begin{pmatrix} x \\ y \\ z \end{pmatrix} + \phi_{ij}(x, y, z),$$

where ϕ_{ij} are smooth functions vanishing at all points $(0, 0, z)$, together with all their first and second order derivatives with respect to x, y.

Remark 3. *The constants $\mathrm{ax}_{ij}, \mathrm{ay}_{ij}, \omega_{\cdot\cdot ij}$ are called the invariants of the metric.*

Remark 4. *Without loss of generality, in (9) we can choose $\mu_2 = 0$, so that $\mu_1 = \frac{1}{\mu_4} \neq 0$. This correspond to apply a rotation around the z axis, which makes f collinear to $\mathbf{f}$. This operation does not impact the structure of the small spheres.*

We finally remark that the control system (7b) inherits some symmetry properties from the vector fields (8), as the following Lemma shows.

Lemma 1. *Let $\theta = \frac{k\pi}{2}$, $k \in 1,2,3$, denote with $\hat{R}_\theta$ (respectively, R_θ) the matrix of the (counterclockwise) rotation of angle θ in the two dimensional Euclidean space (respectively, around the axis z in three dimensional Euclidean space). Consider the vector fields*

$$\widetilde{f} = \begin{pmatrix} 1 + y(x\widetilde{L}_{11}(\mathbf{x}) + y\widetilde{L}_{12}(\mathbf{x})y) \\ y(x\widetilde{L}_{21}(\mathbf{x}) + y\widetilde{L}_{22}(\mathbf{x})y) \\ -\frac{y}{2} + y(x\widetilde{L}_{31}(\mathbf{x}) + y\widetilde{L}_{32}(\mathbf{x})y) \end{pmatrix} \quad \widetilde{g} = \begin{pmatrix} -x(x\widetilde{L}_{11}(\mathbf{x}) + y\widetilde{L}_{12}(\mathbf{x})) \\ 1 - x(x\widetilde{L}_{21}(\mathbf{x}) + y\widetilde{L}_{22}(\mathbf{x})) \\ \frac{x}{2} - x(x\widetilde{L}_{31}(\mathbf{x}) + y\widetilde{L}_{32}(\mathbf{x})) \end{pmatrix} \tag{10}$$

where

$$\begin{pmatrix} \widetilde{L}_{11}(\mathbf{x}) & \widetilde{L}_{12}(\mathbf{x}) \\ \widetilde{L}_{21}(\mathbf{x}) & \widetilde{L}_{22}(\mathbf{x}) \\ \widetilde{L}_{31}(\mathbf{x}) & \widetilde{L}_{32}(\mathbf{x}) \end{pmatrix} = R_\theta^{-1} \begin{pmatrix} L_{11}(R_\theta\mathbf{x}) & L_{11}(R_\theta\mathbf{x}) \\ L_{21}(R_\theta\mathbf{x}) & L_{22}(R_\theta\mathbf{x}) \\ L_{31}(R_\theta\mathbf{x}) & L_{32}(R_\theta\mathbf{x}) \end{pmatrix} \hat{R}_\theta. \tag{11}$$

Let $\widetilde{\boldsymbol{u}} : [0,T] \to Q$ be some measurable function and $\widetilde{\boldsymbol{\xi}}(\cdot)$ denote the solution of the Cauchy problem

$$\begin{cases} \dot{\widetilde{\boldsymbol{\xi}}}(t) = (\widetilde{u}_1\widetilde{f} + \widetilde{u}_2\widetilde{g})) \circ \widetilde{\boldsymbol{\xi}}(t), \\ \widetilde{\boldsymbol{\xi}}(0) = (0,0,0). \end{cases}$$

Then $R_\theta\widetilde{\boldsymbol{\xi}}(t)$ is the solution of the Cauchy problem (7a) *corresponding to the control $\boldsymbol{u}(t) = R_\theta\widetilde{\boldsymbol{u}}(t)$ with initial condition equal to $(0,0,0)$.*

The proof is just a straightforward computation, and is thus omitted. A summary of the transformations undergone by the main invariants is provided in Appendix B.1.

2.1.1. *Genericity.* In this section, we briefly discuss the notion of genericity we are considering, thus clarifying the statements done in the introduction. The whole section relies on the results of the article [12].

Let $\mathrm{SubR}(M)$ denote the set of all sub-Riemannian structures on the manifold M, endowed with the Whitney topology ([15]). The set of all the sub-Finsler L^1 structures compatible with some sub-Riemannian structure on M, that we denote with $\overline{\mathrm{SF}}_1(M)$, can be identified with $\mathbb{R}^2 \times \mathrm{SubR}(M)$ (see Remark 4), endowed with the product topology.

Following [12, Theorem 1.3, Corollary 1.4, Corollary 2.8], we write the function γ in (2) as $\gamma(x,y,z) = c_1x^2 + c_2y^2 + 2c_3xy + V(x,y) + \varphi(x,y,z)$, where V is a cubic function and φ, together with its partial derivatives with respect to x, y of order less than 4, vanishes at $(0,0,z)$. By easy computations, we can see that $\mathrm{ax}_{31} = \frac{c_1}{\mu_1^2}$, $\mathrm{ay}_{32} = c_1\mu_3^2 + \frac{c_2}{\mu_1^2} - 2c_3\mu_1\mu_3$ and $\mathrm{ax}_{32} = \mathrm{ay}_{31} = -c_1\mu_1\mu_3 + c_3$.

Therefore, we can adapt the proof of [12, Theorem 1.5] and conclude that, for a generic sub-Finsler L^1 metric compatible with a sub-Riemannian structure, the set of points $\boldsymbol{q} \in M$ such that the normal form (8) has $\mathrm{ax}_{31} = 0$ (respectively, $\mathrm{ay}_{32} = 0$) form a 2-dimensional submanifold of M. Therefore, asking $\mathrm{ax}_{31}\mathrm{ay}_{32} \neq 0$, as done in [7], is a genericity assumptions.

In this paper, we are interested in sub-Finsler structure for which $\mathrm{ax}_{31} = 0$, but some other invariants (called D_1 and E_1 and defined in equation (16)) are non-zero. By easy computations, it can be proved that E_1 and D_1 are linear combinations of the invariants of the original sub-Riemannian metric (more precisely, the terms called V and l in [12]). Adapting again [12, Theorem 1.5], we get that, for a generic sub-Finsler L^1 metric compatible with a sub-Riemannian structure, the set of points $\boldsymbol{q} \in M$ such that the normal form (8) has $\mathrm{ax}_{31} = D_1 = E_1 = 0$ has codimension 3 in M.

In other words, the assumption we are doing is generically true if we restrict ourselves to the non-generic set of points $\boldsymbol{q}$ for which the normal form has $\mathrm{ax}_{31} = 0$.

2.2. **Pontryagin Maximum Principle.** Let us now focus on problem (7); we fix some $\boldsymbol{q}_0 \in M$ and we restrict ourselves to a neighbourhood U of $\boldsymbol{q}_0$ in which the normal coordinates centred at $\boldsymbol{q}_0$ are well defined; we then we perform the change of variable described in Proposition 1.

To find the optimal trajectories of problem (7), we apply the Pontryagin Maximum Principle (PMP) (see for instance [3, 4]) : we denote with $\boldsymbol{p} = (p_x, p_y, p_z)$ the adjoint vector (or costate, or

covector) and we write the control-dependent Hamiltonian

$$h(\boldsymbol{p}, \mathbf{x}, \boldsymbol{u}) = u_1 F(\boldsymbol{p}, \mathbf{x}) + u_2 G(\boldsymbol{p}, \mathbf{x}),$$

with $F(\boldsymbol{p}, \mathbf{x}) = \langle \boldsymbol{p}, f(\mathbf{x}) \rangle$ and $G(\boldsymbol{p}, \mathbf{x}) = \langle \boldsymbol{p}, g(\mathbf{x}) \rangle$. Pontryagin Maximum Principle states that, if $\widehat{\boldsymbol{\xi}} : [0, T] \to M$ is an optimal solution for the minimum-time problem (7), and $\widehat{\boldsymbol{u}}$ is its associated control function, then there exists a nowhere zero Lipschitz curve $\widehat{\boldsymbol{p}}(t)$ such that

$$\dot{\widehat{\boldsymbol{p}}}(t) = -\frac{\partial h}{\partial \mathbf{x}}(\widehat{\lambda}(t), \widehat{\boldsymbol{u}}(t)) \quad \dot{\widehat{\boldsymbol{\xi}}}(t) = \frac{\partial h}{\partial \boldsymbol{p}}(\widehat{\lambda}(t), \widehat{\boldsymbol{u}}(t)) \qquad \forall t \tag{12a}$$

$$h(\widehat{\boldsymbol{\lambda}}(t), \widehat{\boldsymbol{u}}(t)) = \max_{\boldsymbol{v} \in Q} h(\widehat{\boldsymbol{\lambda}}(t), \boldsymbol{v}) \qquad \text{a.e. } t \tag{12b}$$

$$h(\widehat{\boldsymbol{\lambda}}(t), \widehat{\boldsymbol{u}}(t)) \equiv \nu \qquad \forall t, \tag{12c}$$

where $\widehat{\boldsymbol{\lambda}}(t) = (\widehat{\boldsymbol{p}}(t), \widehat{\boldsymbol{\xi}}(t))$ and $\nu \in \{0, 1\}$. With a little abuse of terminology, when we say that a trajectory satisfies the PMP we mean that it is an admissible trajectory for the control system (7a) and that it satisfies equations (12), for some nowhere zero Lipschitz curve $\boldsymbol{p}(\cdot)$. Analogously, given a pair $\boldsymbol{\lambda}(\cdot) = (\boldsymbol{p}(\cdot), \boldsymbol{\xi}(\cdot))$, where $\boldsymbol{\xi}$ is an admissible trajectory for the control system (7a), the adjoint covector is nowhere zero and $\boldsymbol{\lambda}$ satisfies equations (12), we say that $\boldsymbol{\lambda}(\cdot)$ is an *extremal*. The trajectories that satisfy the PMP (that is, the projections of extremals) are called *geodesics*.

Remark 5. *Thanks to Remark 2, it is straightforward to prove that ν cannot be zero, therefore we set $\nu = 1$. In particular, for every extremal associated with a trajectory starting from the origin, at least one between $|p_x(0)|$ and $|p_y(0)|$ is equal to 1.*

Equations (12b)-(12c) imply that the control associated with an extremal takes values on the boundary of Q, i.e., internal control are not admitted. The value of the control is determined by the relative values of F and G along the extremal: let $I \subset [0, T]$ be some interval, and $\boldsymbol{\lambda} : I \to \mathbb{R}^6$ an extremal of (7); then

- if $|F(\boldsymbol{\lambda}(t))| \neq |G(\boldsymbol{\lambda}(t))| \ \forall t \in I$, then, on I, the control takes value on one of the vertices of Q (for instance, if $F(\boldsymbol{\lambda}(t)) > |G(\boldsymbol{\lambda}(t))|$, then $\boldsymbol{u} = (1, 0)$). In this case, $\boldsymbol{\lambda}|_I$ is said to be a *regular bang arc*.
- if $|F(\boldsymbol{\lambda}(t)| = |G(\boldsymbol{\lambda}(t))| \ \forall t \in I$, then the control takes values on one of the sides of Q, and, in particular, it is not uniquely determined. Indeed, assume for instance that $F(\boldsymbol{\lambda}(t)) = G(\boldsymbol{\lambda}(t)) > 0 \ \forall t \in I$: then any control of the form $(\alpha, 1 - \alpha), \alpha \in [0, 1]$, realizes the maximum in equation (12b). In this case, $\boldsymbol{\lambda}|_I$ is a *singular arc*.

When an extremal crosses transversely one of the surfaces $\{F = G\}$ or $\{F = -G\}$, the control switches, that is, its value jumps from one vertex of Q to another one; in particular, by continuity of the extremals and from the fact that F and G cannot be both zero along an extremal, a control satisfying PMP can switch only from one vertex of Q to a neighbouring one. For these reasons, F and G are called the *switching functions*, and the graphs of $F - G$ and $F + G$ are called *switching surfaces*. The derivatives of the switching functions along an extremal are given by

$$\frac{d}{dt} F(\boldsymbol{\lambda}(t)) = -u_2(t) \Theta(\boldsymbol{\lambda}(t)), \quad \frac{d}{dt} G(\boldsymbol{\lambda}(t)) = u_1(t) \Theta(\boldsymbol{\lambda}(t)),$$

where $\Theta(\boldsymbol{p}, \mathbf{x}) = \langle \boldsymbol{p}, [f, g](\mathbf{x}) \rangle$.

The symmetric properties of the normal form (8) are inherited also by the extremals, as the Lemma here below states.

Lemma 2. *Assume that $(\boldsymbol{p}(t), \boldsymbol{\xi}(t))$ is an extremal of the optimal control problem (7), associated with the control function $\boldsymbol{u}(t)$*

Then the triple $(\widetilde{\boldsymbol{p}}(t), \widetilde{\boldsymbol{\xi}}(t)) = (R_\theta^{-1} \boldsymbol{p}(t), R_\theta^{-1} \boldsymbol{\xi}(t))$ satisfies the PMP for the minimum time problem associated with the system

$$\dot{\widetilde{\boldsymbol{\xi}}}(t) = (\widetilde{u}_1 \widetilde{f} + \widetilde{u}_2 \widetilde{g}) \circ \widetilde{\boldsymbol{\xi}}(t),$$

where $\widetilde{f}$ and $\widetilde{g}$ are the vector fields defined in (10) and $\widetilde{\boldsymbol{u}}(t) = \widehat{R}_\theta^{-1} \boldsymbol{u}(t)$.

2.3. **Optimality of geodesics.** It is rather clear that, if an admissible trajectory is time-minimising between its two endpoints, it is time-minimising also between any two intermediate points of its. On the contrary, in general a geodesic is not time-minimising on its whole length, but at some point it ceases to be optimal; the point where a geodesics loses its optimality is called a *cut point*. More precisely, following [4, 7], we can define the cut time and the cut point as follows:

Definition 3. *Let $\boldsymbol{\xi}$ be an admissible curve of the control system* (7a)*. Define*

$$t_{\mathrm{cut}}(\boldsymbol{\xi}) = \sup\left\{t > 0 : \boldsymbol{\xi}|_{[0,t]} \text{ is time-minimising}\right\}.$$

If $t_{\mathrm{cut}}(\boldsymbol{\xi}) < +\infty$, we say that $\boldsymbol{\xi}(t_{\mathrm{cut}})$ is the cut point to $\boldsymbol{\xi}(0)$ along $\boldsymbol{\xi}$.

Moreover, we call the cut locus *(to $\mathbf{x}_0$) the set of all cut points of geodesics starting from a point $\mathbf{x}_0 \in \mathbb{R}^3$.*

Definition 4. *Using Arnold's terminology, the points reached in the same time by more than one geodesic (with same initial point) are called Maxwell points.*

The set of all Maxwell points of geodesics starting from a point $\mathbf{x}_0 \in \mathbb{R}^3$ is called the Maxwell set to $\mathbf{x}_0$.

In Sub-Riemannian geometry and, in general, optimal control, it is worth investigating also the local optimality of geodesics, with respect to some suitable topology; in this paper we are interested in optimality in the strong (i.e. C^0) topology: we say that an admissible trajectory $\boldsymbol{\xi}$ is locally optimal if there exists a neighbourhood $\mathcal{U}$ of its graph in $\mathbb{R}^3$ such that $\boldsymbol{\xi}$ is time minimising among all trajectories with graph contained in $\mathcal{U}$. This notion of optimality is referred to as *strong-local optimality* (see for instance [4, 20]), in opposition to *weak-local optimality*, where other topologies (e.g. C^1, $W^{1,1}$) in the space of trajectories are considered.

In sub-Riemannian geometry and in some optimal control problems, a usual method to detect the loss of local optimality is to look for the points of non invertibility of the exponential map (see for instance [3, 4]). For the problem under concern, the exponential map is well-defined only locally around regular bang-bang extremals, and it is piecewise smooth. Indeed, consider a quadruple $(\boldsymbol{p}_0, T) \in \mathbb{R}^4$ such that the solution of the Hamilton equation (12a) with initial condition $(\boldsymbol{p}_0, \mathbf{x}_0)$ crosses the switching surfaces only a finite number of times in the interval $[0, T]$, and that all these intersections are transversal (that is, the extremal is not tangent to the switching surface). More precisely, we assume that there exist m times $0 < t_1 < \cdots < t_m < T$ such that the extremal $\boldsymbol{\lambda}$ with $\boldsymbol{\lambda}(0) = (p_x^0, p_y^0, p_z^0, 0, 0, 0)$ satisfies $|F(\boldsymbol{\lambda}(t))| \neq |G(\boldsymbol{\lambda}(t))|$ $\forall t \in [0,t] \setminus \{t_1, \dots, t_m\}$, $|F(\boldsymbol{\lambda}(t_k))| = |G(\boldsymbol{\lambda}(t_k))|$ for every k, and $\frac{d}{dt}(F-G)(\boldsymbol{\lambda}(t_k)) \neq 0$ whenever $F(\boldsymbol{\lambda}(t_k)) = G(\boldsymbol{\lambda}(t_k))$ (respectively, $\frac{d}{dt}(F+G)(\boldsymbol{\lambda}(t_k)) \neq 0$ whenever $F(\boldsymbol{\lambda}(t_k)) = -G(\boldsymbol{\lambda}(t_k))$). We denote with $\boldsymbol{u}^1, \dots, \boldsymbol{u}^{m+1}$ the controls associated with the extremal $\boldsymbol{\lambda}$ on the subintervals $(0, t_1), \dots, (t_m, T)$. Thanks to the structure of the extremal, we have that $\boldsymbol{u}^1, \dots, \boldsymbol{u}^{m+1} \in \{(1,0), (0,1), (-1,0), (0,-1)\}$. A straight application of the implicit function theorem yields the following result.

Lemma 3. *There exist a neighbourhood $\mathcal{U}$ of $\boldsymbol{p}^0$ in $\mathbb{R}^3$ and m smooth functions $\mathfrak{t}_k$, $k = 1, \dots, m$, such that $\mathfrak{t}_k(\boldsymbol{p}^0) = t_k$ and, for every $\boldsymbol{p} \in \mathcal{U}$, there exists a bang-bang extremal $\boldsymbol{\lambda}_{\boldsymbol{p}}$ with initial point equal to $(\boldsymbol{p}, \mathbf{x}_0)$ such that the control associated with $\boldsymbol{\lambda}_{\boldsymbol{p}}|_{(\mathfrak{t}_{k-1}(\boldsymbol{p}), \mathfrak{t}_k(\boldsymbol{p}))}$ is $\boldsymbol{u}^k$.*

Proof. Without loss of generality, assume that $p_x^0 = 1$, $|p_y^0| < 1$ and $p_z^0 > 0$ (recall indeed that $|F(\boldsymbol{\lambda}(0))| \neq |G(\boldsymbol{\lambda}(0))|$). Define the map $\varphi_1 : \mathbb{R}^3 \times \mathbb{R} \to \mathbb{R}$ as

$$\varphi_1(\boldsymbol{p}, t) = (F - G) \circ \exp(t\vec{F})(\boldsymbol{p}).$$

By assumptions, $\varphi_1(\boldsymbol{p}_0, t_1) = 0$ and $\frac{d}{dt}\varphi_1(\boldsymbol{p}^0, t_1) \neq 0$. We can then apply the implicit function theorem to prove the existence of a neighbourhood $\mathcal{U}$ and a $\mathfrak{t}_1 : \mathcal{U} \to \mathbb{R}$ as in the statement of the lemma.

Without loss of generality, assume that $\frac{d}{dt}\varphi_1(\boldsymbol{p}_0, t_1)$ is negative; this, together with the assumptions on the extremal $\boldsymbol{\lambda}$, implies that $\dot{\boldsymbol{\lambda}}(t) = \vec{G}(\boldsymbol{\lambda}(t))$ for $t \in (t_1, t_2)$. Define $\varphi_2(\boldsymbol{p}, t) = (F+G) \circ \exp\left((t - \mathfrak{t}_2(\boldsymbol{p}))\vec{G}\right) \circ \exp\left(\mathfrak{t}_1(\boldsymbol{p})\vec{F}\right)(\boldsymbol{p})$. By assumptions on $\boldsymbol{\lambda}$, we see that $\varphi_2(\boldsymbol{p}_0, t_2) = 0$ and $\frac{d}{dt}\varphi_2(\boldsymbol{p}_0, t_2) \neq 0$, so that we can again apply the implicit function theorem and deduce the existence of $\mathfrak{t}_2$ as in the thesis.

We proceed in the same way for all other switching times. □

Possibly shrinking $\mathcal{U}$ and taking a smaller T, we can define the exponential map on $\mathcal{U} \times [0, T]$ as follows

$$\text{Exp}(\boldsymbol{p}, t) = \begin{cases} \exp((u_1^1 f + u_2^1 g)t)(\mathbf{x}_0) & \text{if } t \in [0, \mathfrak{t}_1(\boldsymbol{p})] \\ \exp((u_1^k f + u_2^k g)(t - \mathfrak{t}_k(\boldsymbol{p}))) \circ \text{Exp}(\boldsymbol{p}, \mathfrak{t}_{k-1}(\boldsymbol{p}))(\mathbf{x}_0) & \text{if } t \in [\mathfrak{t}_{k-1}(\boldsymbol{p}), \mathfrak{t}_k(\boldsymbol{p})], \\ & 2 \leq k \leq m. \end{cases} \tag{13}$$

The exponential map (13) is smooth on $\mathcal{U} \times [0, T]$, except at the points $(\boldsymbol{p}, \mathfrak{t}_k(\boldsymbol{p}))$, $k = 1, \dots, m$. Indeed, for every $(\boldsymbol{p}, t)$ of this form, the plane $\{(\delta\boldsymbol{p}, \delta t) \in \mathbb{R}^3 \times \mathbb{R}\}$ is divided into two semi-planes by the straight line $\{\delta t = \langle d\mathfrak{t}_k(\boldsymbol{p})\delta p\rangle\}$, and the differential of the exponential map has different analytic expressions on the two semiplanes.

Let us compute the differential of the exponential map outside these points; as explained in Remark 5, and thanks to the hypothesis that $|F(\boldsymbol{p}_0)| \neq |G(\boldsymbol{p}_0)|$, we know that one (and only one) between $|p_x^0|$ or $|p_y^0|$ is equal to 1; without loss of generality, we can assume that $p_x^0 = 1$ and $|p_y^0| < 1$. In particular, to compute the differential of the exponential map, we consider only variations along t, p_x and p_z.

It is easy to see that the differential of $\text{Exp}(\boldsymbol{p}, t)$ is singular when $t \leq \mathfrak{t}_2(\boldsymbol{p})$. Indeed, if $t \leq \mathfrak{t}_1(\boldsymbol{p})$, then $\text{Exp}(\boldsymbol{p}, t)$ does not depend explicitly on $\boldsymbol{p}$. If instead $t \in (\mathfrak{t}_1(\boldsymbol{p}), (\mathfrak{t}_2(\boldsymbol{p})]$, then

$$\text{DExp}_{(\boldsymbol{p},t)}[\delta t, \delta p_x, \delta p_z] = g(\text{Exp}(\boldsymbol{p}, t))\delta t + \langle d\mathfrak{t}_1(\boldsymbol{p}), \delta\boldsymbol{p}\rangle \big(-g(\text{Exp}(\boldsymbol{p}, t)) + \exp((t - \mathfrak{t}_1(\boldsymbol{p})g)_* f(\exp(\mathfrak{t}_1(\boldsymbol{p})))(\mathbf{x}_0)\big).$$

Let $\delta\boldsymbol{p}$ be a non-trivial variation (in (p_y, p_z)) such that $\langle d\mathfrak{t}_1(\boldsymbol{p}), \delta\boldsymbol{p}\rangle = 0$, $\delta\boldsymbol{p} \neq 0$; it is immediate to see that the variation $(\delta\boldsymbol{p}, 0)$, belongs to the kernel of $\text{DExp}_{(\boldsymbol{p},t)}$.

However, the singularity of $\text{DExp}_{(\boldsymbol{p},t)}$ for $t \leq \mathfrak{t}_2(\boldsymbol{p})$ does not reflect a proper loss of optimality. Consider indeed a sufficiently small neighbourhood (in the space of p_y and p_z) of the point $(1, p_y^0, p_z^0)$, with $|p_y^0| < 1$, and compute

$$\frac{\partial \mathfrak{t}_1}{\partial p_y^0}(\boldsymbol{p}^0) = \frac{1}{\Theta(\boldsymbol{\lambda}(t_1))} \frac{\partial \varphi_1(\boldsymbol{p}, t)}{\partial p_y^0}(\widehat{\lambda}(t_1), t_1) = \frac{1}{\Theta(\boldsymbol{\lambda}(t_1))}\big(1 + \mathcal{O}(x)\big).$$

If we consider short times, we can then apply the implicit function theorem again, to prove that there exists a locally defined smooth function $\eta : \mathbb{R} \to \mathbb{R}$ such that $\eta(p_z^0) = p_y^0$ and $\mathfrak{t}_1(1, p_y, p_z)$ is constant if $p_y = \eta(p_z)$. In other words, the set $\mathcal{U} \cap \{p_x \equiv 1\}$ is foliated by level curves of $\mathfrak{t}_1$. Then, all geodesics associated with the extremals emanating from covectors belonging to one of these curves coincide up to their second switching point. This is due to the fact that there are several extremals associated with the same trajectory: the singularity of the exponential map does not reveal a loss of local optimality of the geodesics [1].

In order to obtain information on when the geodesics cease to be locally optimal, we then focus on the differential of the exponential map after the second switching time. Since local optimality cannot be lost along a bang arc (see [20]), we concentrate of what happens at the switching points. We recall the following fact.

Lemma 4. *Le $\boldsymbol{v} \in \mathbb{R}^n$ and consider two matrices A_+, A_- such that $\det A_+ > 0$, $\det A_- < 0$ and $A_+\boldsymbol{v} = A_-\boldsymbol{v}$*

Define the two semi-planes $\Pi_+ = \{\boldsymbol{w} \in \mathbb{R}^n : \boldsymbol{w} \cdot \boldsymbol{v} \geq 0\}$ and $\Pi_- = \{\boldsymbol{w} \in \mathbb{R}^n : \boldsymbol{w} \cdot \boldsymbol{v} \leq 0\}$ and the piecewise defined linear map $A : \mathbb{R}^n \to \mathbb{R}^n$ as

$$A\boldsymbol{w} = \begin{cases} A_+\boldsymbol{w} & \text{if } \boldsymbol{w} \in \Pi_+ \\ A_-\boldsymbol{w} & \text{if } \boldsymbol{w} \in \Pi_-. \end{cases}$$

The map A is not invertible.

Motivated by this Lemma, we adopt the following definition of conjugate time (let us remark that it is the same proposed in [7]).

[1] It is indeed typical of bang-bang extremals that the exponential map is singular along the first arcs, without direct implications on the loss of optimality, which requires the use of other tools, such as the second variation, to study their local optimality (see for instance [1, 20])

Definition 5. *Let $\boldsymbol{\lambda}$ be a regular bang-bang extremal for the optimal control problem* (7)*. The first conjugate time along $\boldsymbol{\lambda}$ is defined as*

$$t_{\mathrm{conj}}(\boldsymbol{\lambda}) = \inf\left\{t > 0 : \exists\ t_1 < t < t_2 \text{ such that } \mathrm{JExp}(\boldsymbol{p}^0, t_1)\mathrm{JExp}(\boldsymbol{p}^0, t_2) < 0\right\},$$

where $\mathrm{JExp}(\boldsymbol{p}^0, t)$ denotes the Jacobian [2] *of $\mathrm{Exp}(\boldsymbol{p}_0, t)$ and $\boldsymbol{\lambda} = (\boldsymbol{p}^0, \mathbf{x}_0)$.*

The first conjugate point along $\boldsymbol{\lambda}$ is the point reached by the projection of $\boldsymbol{\lambda}$ at first conjugate time. The set of all conjugate points associated to extremals with initial condition equal to $\mathbf{x}_0$ is called the first conjugate locus.

2.4. **The Heisenberg system.** The simplest case of the optimal control problem (7) corresponds to the nilpotent approximation of the vector fields f and g (also known as Heisenberg group, see for instance [4, 17]), that is

$$f = \not{f} = \begin{pmatrix} 1 \\ 0 \\ -y/2 \end{pmatrix} \qquad g = \not{g} = \begin{pmatrix} 0 \\ 1 \\ x/2 \end{pmatrix}.$$

The time-optimal problem for such a system has already been studied in [9, 11, 18]. Since it constitutes a starting point for the study of the generic cases, it is worth recalling the main properties of its time-optimal synthesis from the initial point $\mathbf{x}_0 = (0, 0, 0)$.

First of all, we notice that the control system does not depend on z, so that the adjoint vector p_z is constant along every extremal; moreover, $\Theta(\boldsymbol{p}, \mathbf{x}) \equiv p_z$. This fact has two consequences:

- Singular arcs are characterised by $p_z \equiv 0$; therefore, if an extremal contains a singular arc, then the whole extremal is singular.
- Given any bang-bang concatenation, the sequence of its associated controls is uniquely determined by the initial one and the sign of p_z: indeed, if $p_z > 0$ (respectively, $p_z < 0$), the controls follow the vertices of Q in the counterclockwise (respectively, clockwise) sense.

We notice moreover that the problem exhibits a discrete symmetry: it is invariant for rotations of $k\pi/2$, $k \in \mathbb{Z}$ around the vertical axis (z); moreover, it turns out that the unit sphere (that is, the set of all points reachable in time 1 from the origin) is symmetric with respect to the xy plane, and that the geodesics that reach positive (respectively, negative) z are projections of extremals with $p_z \geq 0$ (respectively, $p_z \leq 0$). For these reasons, we discuss only the extremals whose initial adjoint vector $\boldsymbol{p}(0) = (p_x^0, p_y^0, p_z)$ satisfies $p_x^0 = 1$, $p_y^0 \in [-1, 1]$ and $p_z \geq 0$; indeed, all other extremals can be recovered from these ones applying a suitable transformation.

First of all, consider any extremal with $p_y^0 \in [-1, 1)$ and $p_z > 0$: then, since $F(\boldsymbol{\lambda}(0)) = 1 > |p_y^0| = |G(\boldsymbol{\lambda}(0))|$, PMP implies that there exists some $\mathbb{T}_1 > 0$ such that on the interval $[0, \mathbb{T}_1)$ the control associated with the extremal is $(1, 0)$; in particular, $\mathbb{T}_1$ is the smallest (positive) time satisfying $F(\boldsymbol{\lambda}(\mathbb{T}_1)) = G(\boldsymbol{\lambda}(\mathbb{T}_1))$, which, by computations, turns out to be $\mathbb{T}_1 = \frac{1-p_y^0}{p_z}$.

For $t \in (\mathbb{T}_1, \mathbb{T}_2)$, where $\mathbb{T}_2 = \mathbb{T}_1 + 2/p_z$, the control associated with the extremal is equal to $(0, 1)$; $\mathbb{T}_2$ is indeed the smallest time greater than $\mathbb{T}_1$ such that $F(\boldsymbol{\lambda}(\mathbb{T}_2)) = -G(\boldsymbol{\lambda}(\mathbb{T}_2))$. For times greater than $\mathbb{T}_2$, the control switches every $\Delta T = 2/p_z$, following the vertexes of Q in the counterclockwise sense.

In the special case $p_x^0 = p_y^0 = 1$, explicitly integrating the Hamiltonian system and applying equation (12b), it is easy to see that the control associated with such extremals is equal to $(0, 1)$ on the interval $(0, \Delta T)$, and then it switches every ΔT, following the same sequence as above.

Let $(\widehat{\boldsymbol{p}}, \widehat{\boldsymbol{\xi}})$ be an extremal such that $\boldsymbol{p}(0) = (1, \widehat{p}_y^0, \widehat{p}_z)$, with $\widehat{p}_y^0 \in [-1, 1)$; integrating the system, we see that, for $t \in [\mathbb{T}_4, 8/\widehat{p}_z]$, the expression of the geodesic is given by

$$\begin{cases} x(t) = t - 4\Delta T \\ y(t) = 0 \\ z(t) = \Delta T^2, \end{cases}$$

[2] we stress that we consider the variations along the time and two components of the covector, that is, we do not consider variations along the component of the covector between p_x^0 and p_y^0 that is equal to ± 1. If both have absolute value equal to one, we must consider one-sided variations along only one of them.

that is, its value depends only on t and on $\widehat{p}_z$, but not on $\widehat{p}_y^0$. In particular, at $t = \mathbb{T}_4 = \frac{7-\widehat{p}_y^0}{\widehat{p}_z}$, $\widehat{\boldsymbol{\xi}}$ meets all geodesics with $\boldsymbol{p}(0) = (1, p_y^0, \widehat{p}_z)$ and $\widehat{p}_y^0 < p_y^0 \leq 1$, and coincides with them up to the time $8/\widehat{p}_z$. Moreover, for every $\epsilon > 0$, we can always find some $p_y^0 > \widehat{p}_y^0$ such that the graph of the corresponding trajectory is ϵ-close in the C^0 norm to the graph of $\widehat{\boldsymbol{\xi}}$. In other words, at $t = \mathbb{T}_4$ the trajectory $\widehat{\boldsymbol{\xi}}$ loses its local optimality.

To verify if a geodesics loses its global optimality before its fourth switching time, we must look for intersections of the trajectory under study with some geodesics trajectories whose graph does not belong to a neighbourhood of its graph, that is, whose initial control is not $(1, 0)$. By computations, it is possible to prove that such intersections occur either at the fourth switching time, either at $8/p_z$. Therefore, for every trajectory, the fourth switching time $\mathbb{T}_4$ is the cut time.

To complete the analysis, we now consider a singular extremal with $p_x^0 = p_y^0 = 1$ and $p_z = 0$. As already said, every control of the form $(\alpha(t), 1 - \alpha(t))$, with $\alpha(t) \in [0, 1]$ $\forall t$, satisfies PMP. First of all, we notice that $x(T) + y(T) = \int_0^T u_1(t) + u_2(t)\, dt = T$, so that a singular extremal is necessarily optimal (as every point $\mathbf{x}_f$ cannot be reached in a time less than $|x_1| + |y_1|$). Moreover, it is possible to prove that $z(T) \leq x(T)y(T)/2$, and, conversely, that every point $(x_1, y_1, z_1) \in \mathbb{R}^3$ with $|z_1| \leq |x_1 y_1|/2$ can be reached by a singular trajectory. In particular, the minimum time for reaching such points is $|x_1| + |y_1|$.

Applying suitable rotations in the xy-plane and/or a reflection in the z-coordinate, we recover all optimal geodesics for the Heisenberg system.

3. Generic case: bang-bang geodesics with controls switching in counterclockwise sense

3.1. **Local developments.** As already anticipated in the introduction, we are interested in the local geometry of the sub-Finsler metric associated with $\{f, g\}$, or, equivalently, in the local optimal synthesis for the minimum time problem (7). Indeed, if we consider any possible endpoint, many issues concerning the completeness of the vector fields, the existence of the minimum, the validity of the normal form, together with major difficulties in the integration of the system, may arise. Concerning the structure of the extremals, differently from the nilpotent case, where the only possible geodesics are regular bang-bang (with control switching from vertex to vertex of Q always in the same sense) and singular (with $p_z \equiv 0$), many other behaviours are possible, such as bang-singular concatenations or bang-bang extremals with controls switching several times between the same two vertices of Q (see for instance Section 8 and [7]).

On the other hand, as in the sub-Riemannian case ([2, 12, 22]), it is interesting to see how a small perturbation of the nilpotent system affects the shape of the conjugate and the cut locus. We then study the optimal synthesis from some initial point $\mathbf{x}_0$ (corresponding to the origin in local coordinates) for *small times*. By straightforward computations, it is possible to prove that, for T small enough, every admissible trajectory of the control system (6) with controls in Q satisfies $|x(t)|, |y(t)|, |z(t)| < 1$, $t \in [0, T]$. In particular, for T small enough, the nilpotent part in f, g dominates, and the trajectories are close to those described in Section 2.4.

Moreover, when we restrict to short times, we reduce the possible behaviours of the extremals. Indeed, by computations we can prove that

$$\Theta(\boldsymbol{\lambda}(t)) = p_z(t) + \big(1 + p_z(t)\big)\mathcal{O}(x(t)^2, y(t)^2, z(t)),$$

which implies that the sign of Θ is constant in the time interval $[0, T]$, unless we have $p_z^0 = \mathcal{O}(T^2)$. In the first case, the corresponding extremals are associated with controls that switch from vertex to vertex of Q following the same sense (determined by the sign of Θ), as for the nilpotent system. In the second case, as F and G vary very slowly along the extremal, the associated control is constant or may vary only on one side of Q (for instance, if both F and G are positive along the extremal, we have $u_1(t) + u_2(t) \equiv 1$ on $[0, T]$), see Section 8 for a brief description of such situations.

By straightforward computations, we can prove that the geodesics associated with extremal of the first kind satisfy the bound $|z(t)| \geq \frac{|x(t)y(t)|}{2} + \mathcal{O}(x(t)^4, y(t)^4)$ (as for the Heisenberg system), and that those associated with extremals of the second kind the bound $|z(t)| \leq \frac{|x(t)y(t)|}{2} + \mathcal{O}(x(t)^4, y(t)^4)$. As already said in the introduction, in this paper we focus on these extremals or, equivalently, we study the upper part of the sphere, that is, the part with $|z(t)| > \frac{|x(t)y(t)|}{2}$.

In short times, these geodesics are characterised by very large values of $p_z(0)$ (that is, of the same order of magnitude of the inverse of the final time). In order to (approximately) compute such extremals, we derive an asymptotic expansion of the solution of the Hamiltonian system in powers of the small parameter $\rho_0 = 1/p_z(0)$.

Let $(\boldsymbol{p}(t), \boldsymbol{\xi}(t))$ be an extremal of (7) with $p_z(0) \gg 1$, and let $\boldsymbol{u}(t)$ be its associated control function. Following the same techniques used in [2, 7, 12], we perform the time reparametrisation

$$\tau(t) = \int_0^t p_z(s)\, ds, \tag{14}$$

and we define the new variables

$$\widehat{p}_x = \frac{p_x}{p_z} \qquad \hat{p}_y = \frac{p_y}{p_z} \qquad \rho = \frac{1}{p_z} \qquad \widehat{\Theta} = \frac{\Theta}{p_z}.$$

Notation. *In the paper we are dealing with two time-scales: the real time t and the reparametrised time τ, which are related by equation* (14)*. In order to avoid ambiguities, we will use normal fonts $(t, T, \boldsymbol{T}, \dots)$ to denote the real time, and script or Greek fonts $(\tau, \boldsymbol{\tau}, \mathscr{T}, \mathcal{T})$ to denote the reparametrised time. In particular, the symbol $\mathbb{T}_k$ denotes the k-th switching time, and the symbol $\mathscr{T}_k$ is devoted to the k-th reparametrised switching time.*

As the relation (14) *is invertible, sometimes we will write t as a function of τ, obviously satisfying $t(\tau) = \int_0^\tau \rho(s)\, ds$.*

In these new variables, Hamiltonian system (12a) can be rewritten as

$$\begin{aligned}
\frac{dx}{d\tau} &= u_1\rho + \rho\Psi_1(x,y,z) & \frac{d\widehat{p}}{d\tau} &= -\rho\frac{u_2}{2} + \rho\Xi_4(x,y,z,p_x,p_y,p_z)\\
\frac{dy}{d\tau} &= u_2\rho + \rho\Psi_2(x,y,z) & \frac{d\widehat{q}}{d\tau} &= \rho\frac{u_1}{2} + \rho\Xi_5(x,y,z,p_x,p_y,p_z)\\
\frac{dz}{d\tau} &= \rho\Psi_3(x,y,z) & \frac{d\rho}{d\tau} &= -\rho^2(u_2x - u_1y)\Xi_6(x,y,z,p_x,p_y,p_z)
\end{aligned}$$

where, for every k, Ψ_k and Ξ_k are functions satisfying $\Psi(0,0,z) = 0$ and $\Xi(0,0,z,p_x,p_y,p_z) = 0$.

In order to compute the jets of the extremals we now write $(\boldsymbol{p}(\tau), \boldsymbol{\xi}(\tau))$ as a power series in $\rho_0 = \rho(0)$, as follows:

$$\begin{cases} x(\tau) = \sum_{k=1}^4 \rho_0^k x_k(\tau) + X_6(\tau,\rho_0)\rho_0^5 \\ y(\tau) = \sum_{k=1}^4 \rho_0^k y_k(\tau) + Y_6(\tau,\rho_0)\rho_0^5 \\ z(\tau) = \sum_{k=1}^5 \rho_0^k z_k(\tau) + Z_7(\tau,\rho_0)\rho_0^6 \end{cases} \qquad \begin{cases} p_x(\tau) = \sum_{k=1}^4 \rho_0^k p_{xk}(\tau) + P_{x5}(\tau,\rho_0)\rho_0^6 \\ p_y(\tau) = \sum_{k=1}^4 \rho_0^k p_{yk}(\tau) + P_{y5}(\tau,\rho_0)\rho_0^6 \\ \rho(\tau) = \sum_{k=1}^5 \rho_0^k \rho_k(\tau) + R_6(\tau,\rho_0)\rho_0^6, \end{cases} \tag{15}$$

where the functions here above are smooth in their variables. Plugging (15) into the Hamiltonian system, we obtain the corresponding differential equation for each of the functions in the development here above. We can then integrate term by term, in order to obtain the expression of the functions of τ in (15).

The power series for the switching times are computed analogously. Consider, for instance, an extremal with $p_x(0) = 1$ and $|p_y(0)| < 1$. The switching (reparametrised) time $\mathscr{T}_1$ is determined by the condition $F(t(\mathscr{T}_1)) = G(t(\mathscr{T}_1)) = 1$. Plugging the developments for $(\boldsymbol{p}(\tau), \boldsymbol{\xi}(\tau))$ into $\widehat{\Theta}$, we can compute the coefficients $\widehat{\Theta}_k$ in the expression

$$\widehat{\Theta} = 1 + \widehat{\Theta}_1\rho_0 + \widehat{\Theta}_2\rho_0^2 + \widehat{\Theta}_3\rho_0^3 + \cdots.$$

Developing $\mathscr{T}_1$ in powers of ρ_0 and imposing, at each order in ρ_0,

$$\begin{aligned} 1 = G(t(\mathscr{T}_1)) &= p_y(0) + \int_0^{\mathscr{T}_1} \widehat{\Theta}(\boldsymbol{p}(\tau), \mathbf{x}(\tau)) d\tau \\ &= p_y(0) + \int_0^{\mathscr{T}_1^0} (1 + \rho_0 \widehat{\Theta}_1 + \cdots) d\tau + \int_{\mathscr{T}_1^0}^{\mathscr{T}_1^0 + \rho_0 \mathscr{T}_1^1} (1 + \rho_0 \Theta_1 + \cdots) d\tau + \cdots, \end{aligned}$$

we can identify all the coefficients $\mathscr{T}_1^k$ of the development of $\mathscr{T}_1$. We proceed in the same way for the other switching times.

Based on Lemmas 1-2, there is no need of computing the switching times for the geodesics with $p_x(0) \neq 1$, as they can be easily recovered from those just computed, by application of the permutation of the invariants (equation (11)).

We end this section by classifying the four different kind of bang-bang geodesics associated with extremals with large positive $p_z(0)$, according to their initial velocity. For every $\rho_0 > 0$ small enough, we define the set

$$\Gamma_f^{\rho_0} = \left\{ \boldsymbol{\xi} : [0, 10\rho_0] \to \mathbb{R}^3 : \begin{cases} \boldsymbol{\lambda} = (\boldsymbol{p}, \boldsymbol{\xi}) \text{ satisfies PMP for the problem (7) with control } \boldsymbol{u} \\ \boldsymbol{\xi}(0) = (0,0,0) \\ \boldsymbol{p}(0) = (1, p_y^0, p_z^0) \ \text{ with } p_y^0 \in [-1,1) \text{ and } p_z^0 \geq \frac{1}{\rho_0} - 1 \\ \exists\ 0 < \mathscr{T}_1 < \cdots < \mathscr{T}_5 \leq 20\rho_0 \ \text{ such that } \begin{cases} \boldsymbol{u}|_{(0,\mathscr{T}_1)} = \boldsymbol{u}|_{(\mathscr{T}_4,\mathscr{T}_5)} = (1,0) \\ \boldsymbol{u}|_{(\mathscr{T}_1,\mathscr{T}_2)} = (0,1) \\ \boldsymbol{u}|_{(\mathscr{T}_2,\mathscr{T}_3)} = (-1,0) \\ \boldsymbol{u}|_{(\mathscr{T}_3,\mathscr{T}_4)} = (0,-1) \end{cases} \end{cases} \right\}.$$

$\Gamma_f^{\rho_0}$ is actually a formal definition for the set of bang-bang geodesics with $p_z(0)$ large enough and that behave qualitatively as the bang-bang geodesics of the nilpotent case with initial velocity f and switch at least five time in the time interval $[0, 10\rho_0]$. In an analogous way, we can define also $\Gamma_{-f}^{\rho_0}$, $\Gamma_g^{\rho_0}$ and $\Gamma_{-g}^{\rho_0}$. Since in the following ρ_0 will always be fixed, we will drop the super-script ρ_0 from the definition of these sets.

In the following, we will sometimes shorten the expression "a geodesic belonging to the set Γ." by saying "a Γ. geodesic".

3.2. **First considerations on local optimality.** As already remarked in Section 2.3, the Jacobian of the exponential map gives information about the local optimality of geodesics with at least three bang arcs, as it is null for geodesics with one or two arcs.

For what concerns geodesics with constant bang control (i.e., only one bang arc), it is easy to see that all of them are optimal: indeed, if for instance $\boldsymbol{u} = (1,0)$, then $\boldsymbol{\xi}(t) = (t,0,0)$, and t is the minimum time for reaching the point $(t,0,0)$. On the other hand, using, for instance, the criterion given in [20], it is possible to see that regular bang-bang geodesics with large $p_z(0)$ and two bang arcs are locally optimal (see [20, Remark 3.5]). Finally, in [23] it has been proved that regular bang-bang geodesics with large $p_z(0)$ and more than five bang arcs cannot be locally optimal.

Summing up, we can concentrate on the computation of the Jacobian of the exponential map for bang-bang geodesics with 5 bang arcs. By long but simple computations, it is possible to compute the power expansion of the Jacobian, which turns out to be constant (with respect to time), at least up to the order we computed, along each bang arc. For extremals corresponding to geodesics in the sets $\Gamma_{\pm f}$, we obtain

$$\mathrm{JExp}|_{(p_y^0, p_z^0, \tau)} = \begin{cases} 0 & \tau \in [0, \mathscr{T}_2(p_y^0, p_z^0)) \\ 4\rho_0^3 + \mathcal{O}(\rho_0^4) & \tau \in (\mathscr{T}_2(p_y^0, p_z^0), \mathscr{T}_3(p_y^0, p_z^0)) \\ 8\rho_0^3 + \mathcal{O}(\rho_0^4) & \tau \in (\mathscr{T}_3(p_y^0, p_z^0), \mathscr{T}_4(p_y^0, p_z^0)) \\ 256 \mathrm{ax}_{31} \rho_0^5 + 32\big(D_1 p_y^0 \pm E_1\big)\rho_0^6 + \mathcal{O}(\rho_0^7) & \tau \in (\mathscr{T}_4(p_y^0, p_z^0), \mathscr{T}_5(p_y^0, p_z^0)) \\ -8\rho_0^3 & \tau \in (\mathscr{T}_5(p_y^0, p_z^0), \mathscr{T}_6(p_y^0, p_z^0)) \\ -8\rho_0^3 + \mathcal{O}(\rho_0^4) & \tau \in (\mathscr{T}_5(p_y^0, p_z^0), \mathscr{T}_6(p_y^0, p_z^0)), \end{cases}$$

where

$$D_1 = 9\mathrm{ax}_{21} - 15\omega_{xx31} \qquad E_1 = 3\mathrm{ax}_{11} - 3\mathrm{ax}_{22} - 3\mathrm{ay}_{21} + 5\omega_{xx32} + 5\omega_{xy31} + 5\omega_{yx31}. \tag{16}$$

Analogously, for extremals corresponding to geodesics in the sets $\Gamma_{\pm g}$, we obtain

$$J\mathrm{Exp}|_{(p_x^0,p_z^0,\tau)} = \begin{cases} 0 & \tau \in [0, \mathscr{T}_2(p_x^0,p_z^0)) \\ 4\rho_0^3 + \mathcal{O}(\rho_0^4) & \tau \in (\mathscr{T}_2(p_x^0,p_z^0), \mathscr{T}_3(p_x^0,p_z^0)) \\ 8\rho_0^3 + \mathcal{O}(\rho_0^4) & \tau \in (\mathscr{T}_3(p_x^0,p_z^0), \mathscr{T}_4(p_x^0,p_z^0)) \\ 256\mathrm{ay}_{32}\rho_0^5 - 32\big(D_2p_x^0 \mp E_2\big)\rho_0^6 + \mathcal{O}(\rho_0^7) & \tau \in (\mathscr{T}_4(p_x^0,p_z^0), \mathscr{T}_5(p_x^0,p_z^0)) \\ -8\rho_0^3 & \tau \in (\mathscr{T}_5(p_x^0,p_z^0), \mathscr{T}_6(p_x^0,p_z^0)) \\ -8\rho_0^3 + \mathcal{O}(\rho_0^4) & \tau \in (\mathscr{T}_5(p_x^0,p_z^0), \mathscr{T}_6(p_x^0,p_z^0)), \end{cases} \tag{17}$$

where

$$D_2 = -9\mathrm{ay}_{12} - 15\omega_{yy32} \qquad E_2 = -3\mathrm{ax}_{12} - 3\mathrm{ay}_{11} - 3\mathrm{ay}_{22} - 5\omega_{xy32} - 5\omega_{yx32} - 5\omega_{yy31}.$$

We this obtain the following results.

Proposition 2. *If* $\mathrm{ax}_{31} < 0$*, then* $\mathscr{T}_4$ *is the conjugate time for all extremals corresponding to geodesics in the sets* $\Gamma_{\pm f}$*; if* $\mathrm{ax}_{31} > 0$*, the conjugate time for these extremals coincides with* $\mathscr{T}_5$*.*

Analogously, the conjugate time for all extremals corresponding to geodesics in the sets $\Gamma_{\pm g}$ *coincides with* $\mathscr{T}_4$ *if* $\mathrm{ay}_{32} < 0$ *and with* $\mathscr{T}_5$ *if* $\mathrm{ay}_{32} > 0$*.*

Proposition 3. *Assume that* $\mathrm{ax}_{31} = 0$ *and* $|E_1| \neq |D_1|$*. If* $E_1 < -|D_1|$ *(respectively,* $E_1 > |D_1|$*), then the fourth (respectively, fifth) switching time is the conjugate time for every geodesic in the set* Γ_f*. If* $|E_1| < |D_1|$*, then the switching time of all geodesics of the kind* Γ_f *with* $D_1p_y^0 + E_1 < 0$ *(respectively,* $D_1p_y^0 + E_1 > 0$*) is their fourth (respectively, fifth) switching time.*

Remark 6. *Proposition 3 can be suitably adapted to describe the conjugate times of geodesics in the sets* Γ_{-f} *and* $\Gamma_{\pm g}$ *in the degenerate cases* $\mathrm{ax}_{31} = 0$ *and* $\mathrm{ay}_{32} = 0$*.*

Remark 7. *If* $\mathrm{ax}_{31} = 0$ *and* $0 < |E_1| < |D_1|$*, to detect the conjugate times for the geodesic with initial covector* $p_y^0 = -\frac{E_1}{D_1}$*, a higher order development of the Jacobian is needed; in particular, it involves the functions* ϕ_{ij} *in the normal form of the vector fields. As it is only one trajectory, and since we are interested in the cut points, we neglect this analysis.*

Remark 8. *As stated in Proposition 2, if* $\mathrm{ax}_{31} \neq 0$*, there is a symmetry in the behaviour of the geodesics belonging to the set* Γ_f *and those belonging to the set* Γ_{-f}*. If instead* $\mathrm{ax}_{31} = 0$*, this symmetry is broken: assume for instance that* $E_1 > |D_1|$*. Then, for the trajectories of the set* Γ_f*,* JExp *does not change sign at* $\mathscr{T}_4$*, whereas it does for trajectories of the set* Γ_{-f}*, for which the fourth switching time is the conjugate time.*

As will be detailed in the following, this fact appears also in the shape of the cut locus, which is no more symmetric, as it is when both ax_{31} *and* ay_{32} *are nonzero (see for instance* [7, 16]*).*

For the purpose of future computations, in analogy with [7] we set

$$C_1 = 8\mathrm{ax}_{31} \qquad C_2 = 8\mathrm{ay}_{32},$$
$$A = 4\mathrm{ax}_{32} + 4\mathrm{ay}_{31}$$

Together with E_1, E_2, D_1 and D_2, these are the main invariants that provide a complete classification of the cut locus. We also define the following constants

$$\begin{aligned} c &= 4\mathrm{ax}_{12} + 7\mathrm{ax}_{21} + 4\mathrm{ay}_{11} - 12\mathrm{ay}_{22} + 15\omega_{xx31} + 20\omega_{xy32} + 20\omega_{yx32} + 20\omega_{yy31} \\ d &= 4\mathrm{ax}_{22} + \mathrm{ay}_{12} + 4\mathrm{ay}_{21} + 15\omega_{yy32} \\ c_2 &= 12\mathrm{ax}_{11} - 4\mathrm{ax}_{22} - 7\mathrm{ay}_{12} - 4\mathrm{ay}_{21} + 20\omega_{xx32} + 20\omega_{xy31} + 20\omega_{yx31} + 15\omega_{yy32} \\ d_2 &= 4\mathrm{ax}_{12} + \mathrm{ax}_{21} + 4\mathrm{ay}_{11} - 15\omega_{xx31}, \end{aligned}$$

which do not affect the classification of the cut locus, but often appear in the computations.

As already anticipated, the invariants C_1 and C_2 play the same role as their homonyms in [7], where the case in which $C_1C_2 \neq 0$ has been studied in details. In this paper, we are pushing further the analysis, setting $C_1 = 0$ (thanks to Lemmas 1-2, the case in which $C_1 \neq 0$ and $C_2 = 0$ is completely analogous). To avoid more degenerate cases, and based on the genericity properties stated in Section 2.1.1, we thus assume that $D_1E_1 \neq 0$.

Summing up, these are our assumptions on the invariants.

Assumption 1. *The invariants A, C_2, D_1 and E_1 are non zero. Moreover, we assume that $|A| \neq |C_2|$ and $|D_1| \neq |E_1|$.*

The invariant C_1 is null.

Remark 9. *As already pointed out in Section 2.1.1, asking an invariant to be nonzero boils down to avoid a codimension one set in M.*

The cases we neglect are surely interesting (for instance, if $A = 0$ there may be some remarkable differences in the part of the cut locus closer to vertical axis); however, the assumptions on A do not affect the value of the Jacobian of the exponential map, and asking $|E_1| = |D_1|$ can be seen as a limit situation of the case $|E_1| > |D_1|$.

Therefore, in this paper we concentrate on the cases for which Assumption 1 holds true.

3.3. **Suspension of the fronts.** In the spirit of [7], to characterise the Maxwell locus we look for the self intersection of the front at some fixed time $\boldsymbol{T}$; in particular, we can restrict the study to the suspension of the front, that is, the intersection of the set $\mathrm{Exp}(\cdot, \boldsymbol{T})$ with the plane where the vertical coordinate z is equal to some prescribed constant (that we usually set to be equal to $4\zeta^2$, where ζ is some positive constant of the same order of magnitude of ρ_0)

We focus on Γ_f geodesics, as the behaviour of the others can be recovered applying suitable rotations and permutations of the parameters, as explained in Lemmas 1-2.

We fix a small positive parameter ζ and a time $\boldsymbol{T} = T_1\zeta + T_2\zeta^2 + T_3\zeta^3 + T_4\zeta^4 + \mathcal{O}(\zeta^5)$, then we look at the intersection of the front at time $\boldsymbol{T}$ with the plane $z = 4\zeta^2$. Inspired by the nilpotent case, we see that self-intersections of the front that cause a loss of optimality may occur near the fourth switching time or between the fourth and the fifth switching times. Therefore, we choose $T_1 \in (6, 10)$ and we consider only the geodesics that are projection of extremals with $p_z^0 = 1/\rho_0$, where $\rho_0 = \zeta + \mathcal{O}(\zeta^2)$: for such trajectories, $\boldsymbol{T}$ lies between the third and the fifth switching time.

The details on the computation of the suspensions are given in Appendix A.1; here below, we just analyse the results.

As the geodesics are defined by piecewise functions (the analytic expression is different on each interval between two switching times), to compute the suspension of the front we must distinguish between the trajectories whose control at time $\boldsymbol{T}$ has already switched four times from those whose control has not yet. First of all, we focus on trajectories for which $\boldsymbol{T}$ is smaller than their fourth switching time, which means to restrict to $p_y^0 \in [-1, 7 - T_1]$. We call the set containing the value at $\boldsymbol{T}$ of all such geodesics the *fourth bang front*.

By a simple computation , we can see that, at the first order in ζ, the suspension of the fourth bang front on the plane $\{z = 4\zeta^2\}$ is given by the curve

$$\{(s\zeta, \big(-3s + 2\sqrt{2s^2 + 2sT_1 + 16}\big)\zeta) : s \in [T_1 - 8, 0]\}.$$

In particular, for the purpose of detection of Maxwell points, the interesting part of this front is the one near the origin (in the affine plane $z = 4\zeta^2$), that is, for $T_1 \sim 8$ and $p_y^0 \sim -1$; therefore, we set $T_1 = 8$ and $p_y^0 = -1 + \sum_{k\geq 1} \mu_k \rho_0^k$. For such parameters, the intersection of the front with the plane $z = 4\zeta^2$ is given by

$$\begin{cases} x(\boldsymbol{T}) &= -\mu_1\zeta^2 - \big(4C_2 + 4A + \mu_2\big)\zeta^3 + \mathcal{O}(\zeta^4) \\ y(\boldsymbol{T}) &= -(T_2 + \mu_1)\zeta^2 - \big(T_3 + \frac{1}{6}(8C_2 - 16C_1 + 3(T_2\mu_1 + \mu_1^2 + 2\mu_2))\big)\zeta^3 + \mathcal{O}(\zeta^4). \end{cases} \tag{18}$$

In particular, at the leading order in ζ it is segment of slope equal to $+1$.

We now compute the suspension of the part of the front made by the value at time $\boldsymbol{T}$ of trajectories of the set Γ_f for which $\boldsymbol{T}$ is greater than the fourth switching time and less than the

fifth one. We call this set the *fifth bang front*. Its suspension to the plane $\{z = 4\zeta^2\}$ is given by

(19)
$$\begin{cases} x(\boldsymbol{T}) &= (T_1-8)\zeta + T_2\zeta^2 + \Big(T_3 + \big(2(p_y^0)^2 + 2(T_1-8)p_y^0 - \frac{2}{3}\big)C_1 - \frac{8}{3}C_2 - 2(T_1-8)A\Big)\zeta^3 \\ &+ \big(T_4 + \frac{4}{3}D_1(p_y^0)^3 + 2E_1(p_y^0)^2 + 2T_2C_1p_y^0 - 2AT_2 + (T_1-8)(D_1(p_y^0)^2 + 2E_1p_y^0 - \frac{1}{3}\boldsymbol{c}) \\ &- \frac{2}{3}(E_1 + 2\boldsymbol{d})\big)\zeta^4 + \mathcal{O}(\zeta^5) \\ y(\boldsymbol{T}) &= 4\big(A - C_1p_y^0\big)\zeta^3 + \big(\frac{2}{3}\boldsymbol{c} - 2D_1(p_y^0)^2 - 4E_1p_y^0\big)\zeta^4 + \mathcal{O}(\zeta^5). \end{cases}$$

As already observed in [7], if $C_1 \neq 0$ this front is at the leading order an arc of parabola of length $\mathcal{O}(\zeta^3)$. If instead $C_1 = 0$, the lowest order term not constant with respect to p_y^0 is of order four. In particular, $y(\boldsymbol{T})$ is, up to some constant, an arc of parabola with vertex in $p_y^0 = -\frac{E_1}{D_1}$. Then, if $\big|\frac{E_1}{D_1}\big| \geq 1$, we have that $\frac{\partial y(\boldsymbol{T})}{\partial p_y^0} \neq 0$ for every $p_y^0 \in (-1,1)$, so that $x(\boldsymbol{T})$ can be written as a smooth function of $y(\boldsymbol{T})$. If instead $\big|\frac{E_1}{D_1}\big| < 1$, then $y(\boldsymbol{T})$ is not monotone on the interval $[-1,1]$. In particular, from

$$\frac{\partial x(\boldsymbol{T})}{\partial p_y^0}\Big|_{p_y^0=-\frac{E_1}{D_1}} = \frac{\partial y(\boldsymbol{T})}{\partial p_y^0}\Big|_{p_y^0=-\frac{E_1}{D_1}} = 0$$
$$\frac{\partial^2 x(\boldsymbol{T})}{\partial (p_y^0)^2}\Big|_{p_y^0=-\frac{E_1}{D_1}} = -4E_1 + 2(T_1-8) \qquad \frac{\partial^2 y(\boldsymbol{T})}{\partial (p_y^0)^2}\Big|_{p_y^0=-\frac{E_1}{D_1}} = -4D_1,$$

and the fact that we assumed $D_1 \neq 0$, we deduce that the front has a cusp for $p_y^0 = -\frac{E_1}{D_1}$ (see [21]). For $p_y^0 \neq -\frac{E_1}{D_1}$, we have

$$\frac{dx}{dy} = -p_y^0 + \frac{1}{2}(T_1-8) \qquad \frac{d^2x}{dy^2} = \frac{1}{4(D_1p_y^0 + E_1)}.$$

We can then distinguish six main cases.

$\boldsymbol{A_\pm}$. These are the cases in which $|E_1| > |D_1|$ and $E_1 > 0$ (respectively, $E_1 < 0$). As remarked before, the front of the fifth arc is a smooth curve. In particular, $\frac{d^2x}{dy^2}$ has the same sign as E_1 for $q_0 \in [-1,1]$.

$\boldsymbol{B_\pm}$. These are the cases in which $D_1 > |E_1|$ and $E_1 > 0$ (respectively, $E_1 < 0$). We have

$$\frac{\partial y(\boldsymbol{T})}{\partial q_0} > 0 \quad \frac{d^2x}{dy^2} < 0 \qquad \text{if } q_0 \in \Big[-1, -\frac{E_1}{D_1}\Big)$$
$$\frac{\partial y(\boldsymbol{T})}{\partial q_0} < 0 \quad \frac{d^2x}{dy^2} > 0 \qquad \text{if } q_0 \in \Big(-\frac{E_1}{D_1}, 1\Big].$$

An example of such a front (for $T_1 = 8$) is plotted in Figure 2.

$\boldsymbol{C_\pm}$. These are the cases in which $D_1 < -|E_1|$ and $E_1 > 0$ (respectively, $E_1 < 0$). We have

$$\frac{\partial y(\boldsymbol{T})}{\partial q_0} < 0 \quad \frac{d^2x}{dy^2} > 0 \qquad \text{if } q_0 \in \Big[-1, -\frac{E_1}{D_1}\Big)$$
$$\frac{\partial y(\boldsymbol{T})}{\partial q_0} > 0 \quad \frac{d^2x}{dy^2} < 0 \qquad \text{if } q_0 \in \Big(-\frac{E_1}{D_1}, 1\Big].$$

An example of such a front (for $T_1 = 8$) is plotted in Figure 3.

To recover the front of the trajectories of kind Γ_{-f}, we apply a rotation of π around the axis z and a suitable permutation of the invariants. Notice that this permutation, that leaves A, C_1 and C_2 unchanged, sends D_1 into $-D_1$ and E_1 into $-E_1$. The suspension of the front thus is

(20)
$$\begin{cases} x(\boldsymbol{T}) &= -(T_1-8)\zeta - T_2\zeta^2 - \Big(T_3 + (2(p_y^0)^2 - 2(T_1-8)p_y^0 - \frac{2}{3})C_1 - \frac{8}{3}C_2 - 2(T_1-8)A\Big)\zeta^3 \\ &+ \big(-T_4 - \frac{4}{3}D_1(p_y^0)^3 + 2E_1(p_y^0)^2 + 2T_2C_1p_y^0 + (T_1-8)(D_1(p_y^0)^2 - 2E_1p_y^0 - \frac{2}{3}\boldsymbol{c}) \\ &+ 2AT_2 - \frac{2}{3}(E_1 + \boldsymbol{d})\big)\zeta^4 + \mathcal{O}(\zeta^5) \\ y(\boldsymbol{T}) &= -4\big(A + C_1p_y^0\big)\zeta^3 + \big(\frac{2}{3}\boldsymbol{c} - 2D_1(p_y^0)^2 + 4E_1p_y^0\big)\zeta^4 + \mathcal{O}(\zeta^5). \end{cases}$$

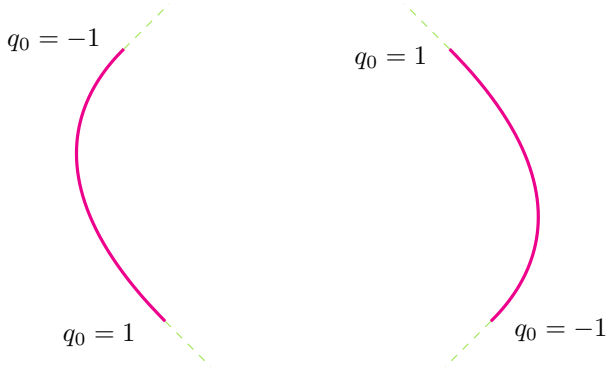

FIGURE 1. Suspensions of the fronts (fifth arc) of the kind A_+ (on the left) and A_- (on the right), at the time $\boldsymbol{T} = 8\zeta + \mathcal{O}(\zeta^2)$. In green: the tangents at $q_0 = 0, 1, -1$.

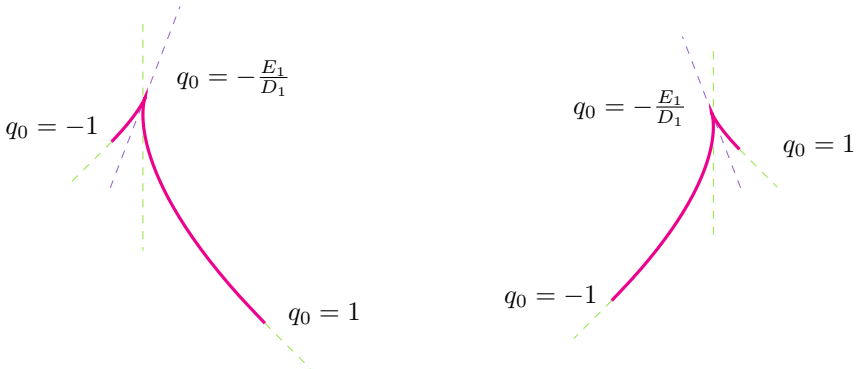

FIGURE 2. Suspensions of the fronts (fifth arc) of the kind B_+ (on the left) and B_- (on the right), at the time $\boldsymbol{T} = 8\zeta + \mathcal{O}(\zeta^2)$. In green: the tangents at $q_0 = 0, 1, -1$. In purple: the tangent at $q_0 = -\frac{E_1}{D_1}$ (the cusp).

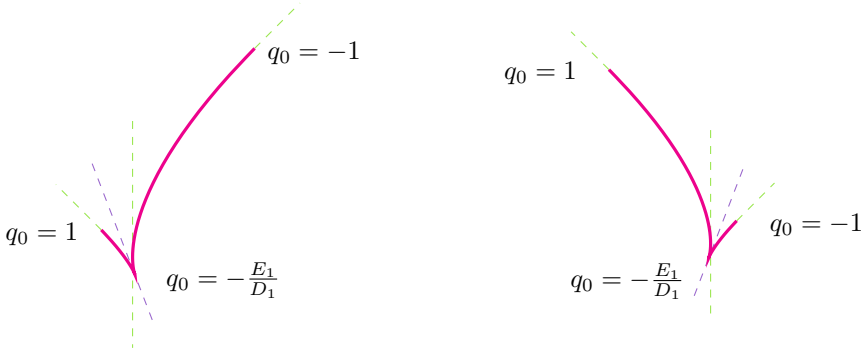

FIGURE 3. Suspensions of the fronts (fifth arc) of the kind C_+ (on the left) and C_- (on the right), at the time $\boldsymbol{T} = 8\zeta + \mathcal{O}(\zeta^2)$. In green: the tangents at $q_0 = 0, 1, -1$. In purple: the tangent at $q_0 = -\frac{E_1}{D_1}$ (the cusp).

The comparison between equations (19) and (20) highlights the phenomenon described in Remark 8, that is, the breaking of the symmetry between trajectories of the sets Γ_f and Γ_{-f} for order higher than the third one.

Notation. In the following, we will use the following notations :

- $\mathcal{F}_4(\boldsymbol{T})$ (respectively, $\bar{\mathcal{F}}_4(\boldsymbol{T}), \mathcal{G}_4(\boldsymbol{T}), \bar{\mathcal{G}}_4(\boldsymbol{T})$)) denotes the fourth bang front at time $\boldsymbol{T}$ of the trajectories of the set Γ_f (respectively, $\Gamma_{-f}, \Gamma_g, \Gamma_{-g}$), that is, the set
$$\left\{ \boldsymbol{\xi}(\boldsymbol{T}) : \begin{array}{l} \boldsymbol{\xi}(\cdot) \in \Gamma_f \\ \mathbb{T}_3(\boldsymbol{\xi}) \leq \boldsymbol{T} \leq \mathbb{T}_4(\boldsymbol{\xi}) \end{array} \right\},$$
where $\mathbb{T}_3(\boldsymbol{\xi})$ and $\mathbb{T}_4(\boldsymbol{\xi})$ denote the third and fourth switching times of the geodesics $\boldsymbol{\xi}$.
- $\mathcal{F}_5(\boldsymbol{T})$ (respectively, $\bar{\mathcal{F}}_5(\boldsymbol{T}), \mathcal{G}_5(\boldsymbol{T}), \bar{\mathcal{G}}_5(\boldsymbol{T})$)) denotes the fifth bang front at time $\boldsymbol{T}$ of the trajectories of the set Γ_f (respectively, $\Gamma_{-f}, \Gamma_g, \Gamma_{-g}$). The definition is analogous to the previous one.

To avoid heavy notations, in the following we are omitting the dependence on the time $\boldsymbol{T}$ from the symbols denoting the fronts.

3.3.1. *Self-intersections of the front of geodesics of the set Γ_f.* In the cases $B_\pm$ and $C_\pm$, corresponding to the cases when $|E_1| < |D_1|$, a peculiar phenomenon arises: the self-intersections between the fourth and the fifth bang front of bang-bang geodesics with the same initial control (that is, belonging to the same set Γ_f), which do not happen when $C_1C_2 \neq 0$. Here below, we explain in details the case B_+, that is, $0 < E_1 < D_1$, which is illustrated in Figures 4-5 [3]; the other cases can be easily derived by applying the suitable symmetries and the corresponding permutation of the invariants.

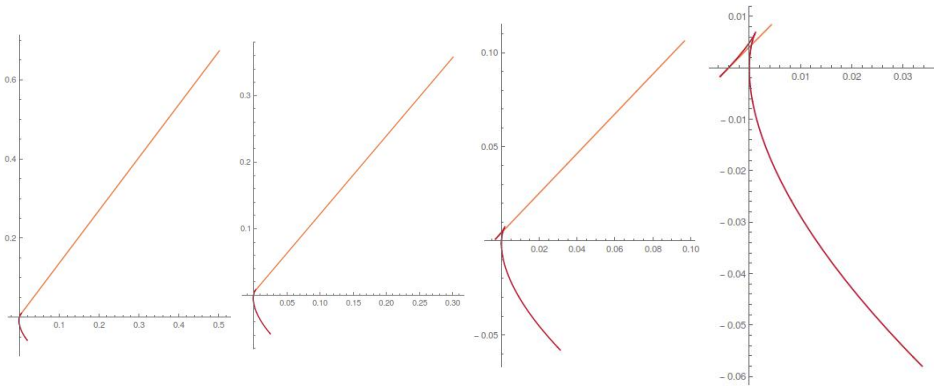

FIGURE 4. Suspension of the front of geodesics of the set Γ_f, for $D_1 > E_1 > 0$. In orange, the fourth bang arc ($\mathcal{F}_4$); in red, the fifth bang arc ($\mathcal{F}_5$). From left to right: $T = 7.5\zeta$, $T = 7.7\zeta$, $T = 7.9\zeta$ and $T = 7.99\zeta$.

Consider two geodesics $\boldsymbol{\xi}_f$ and $\widetilde{\boldsymbol{\xi}}_f$ of the set Γ_f, and assume that their adjoint covectors at time $t = 0$ are respectively $(1, \gamma, 1/\rho_0)$, with $\gamma = \gamma_0 + \sum_{k\geq 1} \gamma_k \rho_0^k$, and $(1, \eta, 1/\widetilde{\rho}_0)$, with $\eta = \eta_0 + \sum_{k\geq 1} \eta_k \rho_0^k$ and $\widetilde{\rho}_0 = \rho_0 + \sum_{k\geq 1} \alpha_k \rho_0^k$. We assume that $\gamma_0 \leq \eta_0$.

We evaluate both $\boldsymbol{\xi}_f$ and $\widetilde{\boldsymbol{\xi}}_f$ near the fourth switching time of $\boldsymbol{\xi}_f$, that is, at some time $\boldsymbol{T} = (7 - \gamma_0)\rho_0 + \mathcal{O}(\rho_0^2)$. Whenever $\gamma_0 < \eta_0$, then, we can choose (higher order terms in) $\boldsymbol{T}$ and a small enough ρ_0 such that $\boldsymbol{T}$ is smaller than the fourth switching time of $\boldsymbol{\xi}_f$ and greater than the fourth switching time of $\widetilde{\boldsymbol{\xi}}_f$.

We now solve the equation $\boldsymbol{\xi}_f(\boldsymbol{T}) = \widetilde{\boldsymbol{\xi}}_f(\boldsymbol{T})$ by equating the jets at each order. We find that γ_0 and η_0 must satisfy one of these equations:

$$\begin{aligned} \gamma_0 &= \eta_0 \\ \gamma_0 + 2\eta_0 &= -3\frac{E_1}{D_1} \end{aligned} \tag{21}$$

[3] We stress that these and the following pictures are illustrating the phenomena only qualitatively, as proportions between the length of the arcs are not fully respected.

If $\gamma_0 = \eta_0$, carrying on the computations we find also $\alpha_k = 0\ \forall k \leq 3$ and $\boldsymbol{T}$ equal (up to the third order in ρ_0) to the switching time (higher order are not inspected): indeed, $\boldsymbol{\xi}_f$ and $\widetilde{\boldsymbol{\xi}}_f$ are (up to higher order terms) the same trajectory, and we are evaluating it at the switching time between the fourth and the fifth arc. If instead $\gamma_0 + 2\eta_0 = -3\frac{E_1}{D_1}$, combining the equality with the constraints $\eta_0, \gamma_0 \in [-1, 1]$ and $\gamma_0 \leq \eta_0$, we obtain that this intersection may occur for $\gamma_0 \in [-1, -\frac{E_1}{D_1}]$ and $\eta_0 \in [-\frac{E_1}{D_1}, \frac{1}{2} - \frac{3E_1}{2D_1}]$. We also find

$$\boldsymbol{T} = (7 - \gamma_0)\rho_0 - \gamma_1\rho_0^2 + \Big(\frac{20}{3}C_2 - 8A\gamma_0\Big)\rho_0^3 + \mathcal{O}(\rho_0^4)$$
$$\widetilde{\rho}_0 = \rho_0 - \frac{9}{4}A\Big(\gamma_0 + \frac{E_1}{D_1}\Big)\rho_0^3 + \mathcal{O}(\rho_0^4)$$

The suspension at $z = 4\zeta^2$ of this intersection is given by the equation

(22)
$$\begin{cases} x = -(1+\gamma_0)\zeta - \gamma_1\zeta^2 + \big((\gamma_0 - 3)C_2 + (1 + 12\gamma_0 - 5\gamma_0^2)\frac{A}{4} - \gamma_2\big)\zeta^3 + \mathcal{O}(\zeta^4) \\ y = 4A\zeta^3 + \mathcal{O}(\zeta^4), \end{cases} \qquad \gamma_0 \in \Big[-1, -\frac{E_1}{D_1}\Big],$$

which is, up to fourth orders in ζ, a horizontal segment of length $\Big(1 - \frac{E_1}{D_1}\Big)\zeta + \mathcal{O}(\zeta^2)$.

We now focus on the geodesics of the set Γ_{-f}. From equation (17) we can see that, along the fifth bang arc, the Jacobian of the exponential map is negative if $p_y^0 \in \big[-1, \frac{E_1}{D_1}\big)$ and positive for $p_y^0 \in \big(\frac{E_1}{D_1}, 1\big]$. In this case there is no intersection between the fourth and the fifth front of the same strategy, as can be seen in Figure 5.

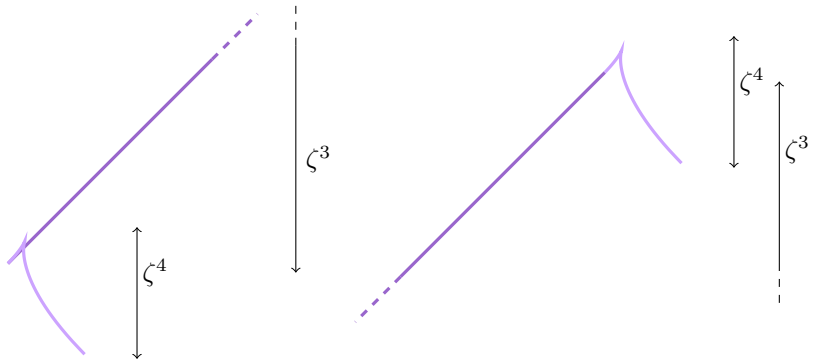

FIGURE 5. On the left (right): self intersection (suspension) of the front of trajectories of the set Γ_f (Γ_{-f}). Purple: front of the fourth bang arc; lavanda: front of the fifth bang arc.

The same computations hold also for the case B_- (only the picture is different, as in this case the interval $\big[-1, -\frac{E_1}{D_1}\big]$ is longer than the interval $\big[-\frac{E_1}{D_1}, 1\big]$).

The cases $C_\pm$ are completely analogous (in particular, the case C_+ corresponds to the case B_-, to which a rotation of π around the z axis, and the corresponding permutation of the invariants, are applied. Same for the case C_- with respect to B_+).

4. Local structure of the conjugate and cut locus for small spheres

In order to detect Maxwell points, we must look for the intersections of a geodesic with other ones with a different initial control (that is, belonging to another set $\Gamma_\cdot$). To reduce the set in which we carry out the research, we get inspired by the behaviour of the geodesics in the nilpotent case: consider for instance, in the nilpotent case, a bang-bang geodesic with initial control $(1, 0)$, that is, associated with an adjoint covector $(1, p_y^0, p_z^0)$, with $p_y^0 \in [-1, 1)$. We recall that, at time $\mathbb{T}_4$, this geodesics meets the geodesic associated with the adjoint covector $(1, 1, p_z^0)$ (whose initial

control is $(0,1)$, see Section 2.4); at time $t = 8/p_z^0$, all geodesics with $p_z(0) = p_z^0$ meet at the point $(0, 0, 4/(p_z^0)^2)$. This suggests that, in the generic case, geodesics in the set Γ_f may lose global optimality near their fourth switching time by intersection with geodesics in the set Γ_g, or, near the time $8/p_z(0)$, by intersecting also geodesics belonging to the sets Γ_{-f} and Γ_{-g}.

In order to reduce the number of eventual intersections to study, we will rely on the following facts. First of all, we neglect intersections involving arcs that are surely not optimal (for instance, if $C_2 < 0$, we do not consider the fifth bang fronts of geodesics of the set $\Gamma_{\pm g}$). Then, we exploit the information given by the invariants A and C_2 to locate the fifth bang fronts: roughly, the front $\mathcal{F}_5$ (respectively, $\bar{\mathcal{F}}_5$) is contained in a horizontal strip of width $\mathcal{O}(\zeta^4)$ centred around $4A\zeta^3$ (respectively, $-4A\zeta^3$), and the front $\mathcal{G}_5$ (respectively, $\bar{\mathcal{G}}_5$) is contained in the vertical strip of width $4C_2\zeta^3 + \mathcal{O}(\zeta^4)$ centred around $4A\zeta^3$ (respectively, $-4A\zeta^3$), see equations (19)-(20)-(50).

Once the intersections among geodesics with different initial velocity are detected, we must identify, for each geodesic, which intersection occurs before the other ones; this intersection (if it occurs before the conjugate point) is the cut point. In order to determine which intersection occurs before the others, we will explicitly compute the time or we will rely on some geometric considerations (for instance, that the suspension of some front is constrained in a strip in the plane and is translating in a specific direction as time increases).

Based on this analysis, we can give a detailed description of the upper part of the cut locus, under Assumption 1. With respect to the generic case $C_1 \neq 0$, we highlight the following differences:

- the intersection of the cut-locus with the plane $\{z = 4\zeta^2\}$ is no more symmetric with respect to the origin (or the point $(4c_{110}\zeta^2, -8c_{200}\zeta^2)$ in [7]);
- when $|D_1| > |E_1|$, there are some pieces of the cut locus that have a length of order $\mathcal{O}(\zeta^4)$;
- the suspension of the cut locus is no more C^1 (but is is piecewise C^1);
- the (suspension of the) upper part of the cut-locus could be disconnected.

In the following, we analyse the following three cases: $E_1 < -|D_1|$ (case $\boldsymbol{A}_-$), $D_1 > E_1 > 0$ (case $\boldsymbol{B}_+$) and $-D_1 < E_1 < 0$ (case $\boldsymbol{B}_-$). The other three cases can be obtained from these ones, just exchanging the behaviours of the part of the front made of trajectories of the class Γ_f with the one made of trajectories of the class Γ_{-f}; at this order of jets, this corresponds to a rotation of an angle π with respect to the vertical axis.

Notation. For the sake of readability, in the following we will sometimes omit to specify that we are providing only the leading terms in the development with respect to ζ; in particular, this will be done in two cases: when we specify the intersection points (for instance, the value of the intersection between the fronts $\mathcal{F}_4$, $\mathcal{G}_4$ and $\bar{\mathcal{G}}_4$ is given by equation (28) up to fifth order terms in ζ); when we describe the behaviour of the geodesics according to the value of the initial adjoint vector (for instance, when we say that the geodesics with $p_y^0 \in [-1, -1 + c\zeta^2]$ behave in some particular way, we mean $p_y^0 \in [-1, -1 + c\zeta^2 + \mathcal{O}(\zeta^3)]$).

5. $E_1 < -|D_1|$ (CASE $\boldsymbol{A}_-$)

From Proposition 3, the conjugate time of all geodesics belonging to the set Γ_f coincides with the fourth switching time, whereas the conjugate time of geodesics belonging to the set Γ_{-f} coincides with the fourth switching time. For what concerns the geodesics in the sets $\Gamma_{\pm g}$, it depends on the sign of C_2. We are analysing these two cases separately.

5.1. $C_2 < 0$**.** Let us first look for the intersection of geodesics of the set Γ_f with those of the set Γ_g. We fix $\rho_0 > 0$ small enough, $\gamma \in [-1, 1)$ and a time $\boldsymbol{T} > 0$. Let $\boldsymbol{\xi}_f$ be the geodesics associated with an extremal with initial covector $(1, \gamma, 1/\rho_0)$, and $\boldsymbol{\xi}_g$ be some geodesic (of Γ_g) with initial covector $(\beta, 1, 1/\widehat{\rho}_0)$, where $\beta = \beta_0 + \sum_{k\geq 1} \beta_k \rho_0^k$ and $\widehat{\rho}_0 = \rho_0 + \sum_{k\geq 2} \alpha_k \rho_0^k$. We define the reparametrised times

$$\mathcal{T} = \delta_0 + \delta_1\rho_0 + \delta_2\rho_0^2 + \cdots \quad \text{and} \quad \widehat{\mathcal{T}} = \widehat{\delta}_0 + \widehat{\delta}_1\rho_0 + \widehat{\delta}_2\rho_0^2 + \cdots \tag{23}$$

such that

$$\boldsymbol{T} = \int_0^{\mathscr{T}} \rho(s)ds = \int_0^{\widehat{\mathscr{T}}} \widehat{\rho}(s)ds. \tag{24}$$

Since, from the analysis of the nilpotent case, we know that these intersections occur close to the fourth switching time of $\boldsymbol{\xi}_f$, we set $\delta_0 = \widehat{\delta}_0 = 7-\gamma$. Then, plugging the expansion of $\widehat{\rho}_0$ in powers of ρ_0 and equations (23) into equation (24), imposing the equality at each power of ρ_0, we obtain the expression of $\widehat{\delta}_k$ in terms of the coefficients δ_k and α_k, for $k \geq 1$.

Using equations (51)-(52)-(53), we compute the jets of the trajectories $\boldsymbol{\xi}_f$ and $\boldsymbol{\xi}_g$ at the (reparametrised) times $\mathscr{T}$ and $\widehat{\mathscr{T}}$, and we impose the equality, up to the fourth order in ρ_0 for x, y, and to the fifth one for z, for each of the three coordinates. Thanks to this, we recover the values for the coefficients $\alpha_k, \beta_k, \delta_k$, as functions of the invariants and of γ. In particular, we obtain

$$\beta = 1 + 2(1-\gamma)C_1\rho_0^2 + 2(1-\gamma)\big(E_1 + \frac{\gamma+2}{3}D_1\big)\rho_0^3 + \mathcal{O}(\rho_0^4).$$

As $|\beta| \leq 1$, this intersection occurs only if $C_1 \leq 0$ and, if $C_1 = 0$, if $E_1 + \frac{\gamma+2}{3}D_1 \leq 0$. We obtain also

$$\mathscr{T}_4 - \mathscr{T} = 2(\gamma-1)C_1\rho_0^2 + 2(\gamma-1)\big(E_1 + \frac{1+2\gamma}{3}D_1)\rho_0^3,$$

where $\mathscr{T}_4$ is the (reparametrised) fourth switching time of the trajectory $\boldsymbol{\xi}_f$; then, this intersection happens only if $C_1 \leq 0$ and, if $C_1 = 0$, if

$$E_1 + \frac{1+2\gamma}{3}D_1 \leq 0. \tag{25}$$

Finally, we fix some $\zeta \sim \rho_0$, and we compute the suspension of the intersections to the plane $\{z = 4\zeta^2\}$. If $C_1 = 0$, we obtain

$$\begin{cases} x = -(1+\gamma)\zeta + \big((1+12\gamma-5\gamma^2)\frac{A}{4} + (\gamma-3)C_2\big)\zeta^3 + \mathcal{O}(\zeta^4) \\ y = 4A\zeta^3 - \frac{2}{3}\big(D_1\gamma^2 + (3E_1+D_1)(1+\gamma) - c\big)\zeta^4 + \mathcal{O}(\zeta^5). \end{cases} \tag{26}$$

At its leading order in ζ it is a horizontal segment of length $\sim 2\zeta$.

By computations, it is easy to prove that in the case $\boldsymbol{A}_-$ the intersection between the arcs $\bar{\mathcal{F}}_4$ and $\bar{\mathcal{G}}_4$ cannot occur (see Appendix A.2-α) for details).

The intersections of the geodesics in the set $\Gamma_{\pm g}$ (near the fourth switching time) with those of the set $\Gamma_{\mp f}$ are analysed in Section A.2. The suspensions of these intersections are given by

$$\begin{cases} x = \pm(4A + 2(1+\gamma)C_2)\zeta^3 + \mathcal{O}(\zeta^4) \\ y = \mp(1+\gamma)\zeta \mp \big((1+12\gamma-5\gamma^2)\frac{A}{4} - \frac{1}{24}(5-9\gamma-9\gamma^2+5\gamma^3)C_2\big)\zeta^3 + \mathcal{O}(\zeta^4), \end{cases} \tag{27}$$

where $\gamma = -p_x^0$ for the geodesics in Γ_g and $\gamma = p_x^0$ for the geodesics in Γ_{-g}.

Computing the limits of equations (26)-(27) as $\gamma \to -1$, that is, near the origin, we see that the reciprocal position of the intersections depend on the sign of the invariant A. Indeed, if $A > 0$, then the three fronts $\mathcal{F}_4$, $\mathcal{G}_4$ and $\bar{\mathcal{G}}_4$ meet at the point

$$\Big(-4A\zeta^3 - \frac{4}{3}\big(2E_1 + d\big)\zeta^4, 4A\zeta^3 - \frac{4}{3}\big(2E_2 + d_2\big)\zeta^4\Big), \tag{28}$$

as can be computed using equations (18)-(49). This suggests that, near the origin of the plane of the suspension, the cut locus is made the intersections between the trajectories Γ_g and those in the set Γ_{-g}. To study them, we proceed as above: we consider a geodesic of the set Γ_g, associated with an extremal with initial adjoint vector equal to $(\beta, 1, 1/\rho_0)$, and geodesic in the set Γ_{-g} associated with an extremal with initial adjoint vector equal to $(\mu, -1, 1/\widetilde{\rho}_0)$, where $\mu = \sum_{k\geq 0}\mu_k\rho_0^k$ and $\widetilde{\rho}_0 = \rho_0 + \mathcal{O}(\rho_0^2)$; since we are close to the origin, also we set $\beta = \sum_{k\geq 0}\beta_k\rho_0^k$ and $\boldsymbol{T} = 8\rho_0 + \mathcal{O}(\rho_0^2)$.

Equating the jets of the two geodesics, we find the following constraints

$$\mu_0 = -1 \quad \beta_0 = 1$$
$$\mu_1 = \beta_1 = 0$$
$$\mu_2 - \beta_2 = 8A,$$

that implies that this intersections occur only for $A \geq 0$; its suspension is given by

$$\begin{cases} x = (4A + \mu_2)\zeta^3 + \mathcal{O}(\zeta^4) \\ y = -(4A + \mu_2)\zeta^3 + \mathcal{O}(\zeta^4). \end{cases} \tag{29}$$

We are left to analyse the behaviour of the geodesics in the set Γ_{-f}. As we must neglect their intersections with the geodesics from Γ_f (which may occur only after the conjugate time of the Γ_f geodesics), and they cannot intersect the geodesics from Γ_{-g} (because of (41)-(42)), we shall investigate their intersection with the trajectories of the set Γ_g. More precisely, for ρ_0 and $\boldsymbol{T}$ fixed, we consider a trajectory of the set Γ_{-f} with initial covector $(-1, p_y^0, 1/\rho_0)$ and a trajectory of the set Γ_g with initial covector $(\beta, 1, 1/\widehat{\rho}_0)$, where as usual $\beta = \sum_{k\geq 0} \beta_k \rho_0^k$ and $\widehat{\rho}_0 = \rho_0 + \sum_{k\geq 2} \alpha_k \rho_0^k$. We recall that, in the nilpotent case, such intersections occur only for $\gamma \sim 1$ and $\boldsymbol{T} \leq 8\rho_0 + \mathcal{O}(\rho_0^2)$; this suggests us to consider the fifth bang arc of the geodesics of the set Γ_{-f}. Imposing the equality of the jets of the two trajectories, we find the constraints

$$\beta_0 = 1, \quad \beta_1 = 0, \quad \beta_2 = -8A,$$

so that this intersection occurs only if $A \geq 0$. The suspension of the intersections to the plane $\{z = 4\zeta^2\}$ is given by

$$\begin{cases} x = 4A\zeta^3 + \big(-\frac{2}{3}D_1(p_y^0)^3 + (E_1 + D_1)(p_y^0)^2 - 2E_1 p_y^0 - \frac{1}{3}(D_1 + 5E_1 + 4\mathcal{d})\big)\zeta^4 + \mathcal{O}(\zeta^4) \\ y = -4A\zeta^3 - \big(2D_1(p_y^0)^2 - 4E_1 p_y^0 - \frac{2}{3}\mathcal{c}\big)\zeta^4 + \mathcal{O}(\zeta^5). \end{cases}$$

In particular, the tangent to this curve is given by

$$\frac{dy}{dx} = \frac{y\prime(p_y^0)}{x\prime(p_y^0)} = -\frac{2}{1 - p_y^0} + \mathcal{O}(\zeta).$$

Computing its limits for $p_y^0 \to \pm 1$, we see that junction of this curve with the other ones composing the suspensions of the cut locus is C^1.

Summing up, we can say that

- all geodesics of the set Γ_f lose their optimality during the fourth arc, intersecting the trajectories of the sets Γ_{-g}, if $p_y^0 \in [-1, -1 - 4C_2\rho_0^2]$ and Γ_g, otherwise.
- all geodesics of the set Γ_{-f} lose their optimality after the fourth switching time, by intersecting the trajectories from Γ_g;
- the geodesics of the set Γ_g lose their optimality during their fourth bang arc, when intersecting the fourth arcs of Γ_f (for $p_x^0 \in [1 + 4\big(E_1 + \frac{D_1}{3}\big)\rho_0^2, 1]$), Γ_{-g} (for $p_x^0 \in [1 - 8A\rho_0^2, 1 + 4\big(E_1 + \frac{D_1}{3}\big)\rho_0^2, 1]$) and the trajectories of the set Γ_{-f}.
- the geodesics of the set Γ_{-g} lose their optimality during their fourth bang arc, when intersecting the fourth arcs of Γ_f and Γ_g.

The suspension of the cut locus has three branches, each of that is C^1. Its graph is shown in Figures 6-7.

If $A < 0$, the trajectories of the set Γ_g do not meet the trajectories of the set Γ_{-g} before the conjugate time (see Appendix A.2-δ)); on the other hand, using the expressions (18), (49) and (20), we can prove that the three fronts $\mathcal{F}_4$, $\bar{\mathcal{G}}_4$ and $\bar{\mathcal{F}}_5$ meet at the point

$$\Big(-4A\zeta^3 - \frac{4}{3}(2E_1 + \mathcal{d})\zeta^4, -4A\zeta^3 - 2\big(2E_1 + D_1 - \frac{1}{3}\mathcal{c}\big)\zeta^4\Big).$$

Reasoning as above, we thus look for the intersections of the trajectories Γ_f with those Γ_{-f} (see Appendix A.2-γ)–A.2-ε)). We conclude that, as in the preceding case, the cut locus has three branches and each branch of the cut locus is C^1. This case is shown in Figure 6.

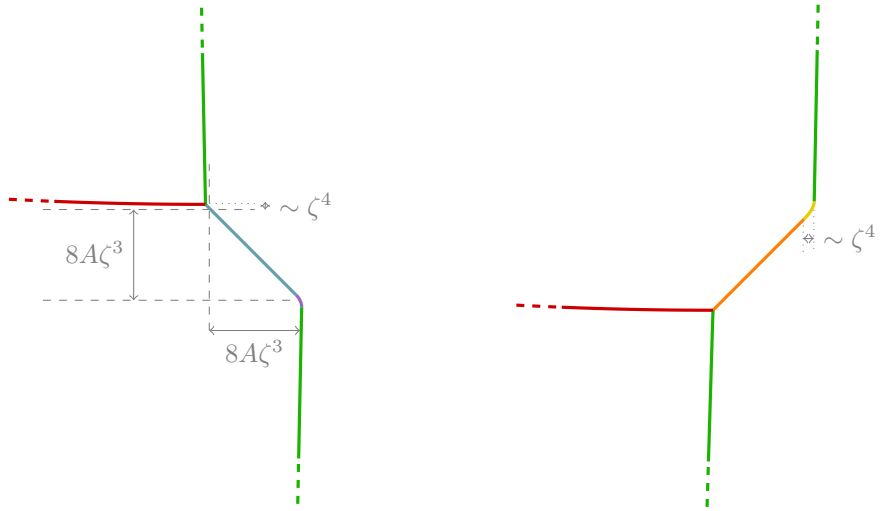

FIGURE 6. Suspension of the cut locus for the case A_- with $C_2 < 0$. On the left, $A > 0$, on the right, $A < 0$. Red: $\mathcal{F}_4 \cap \mathcal{G}_4$; green: $\bar{\mathcal{G}}_4 \cap \mathcal{F}_4$ and $\mathcal{G}_4 \cap \bar{\mathcal{F}}_4$; sugarpaper: $\mathcal{G}_4 \cap \bar{\mathcal{G}}_4$; purple: $\mathcal{G}_4 \cap \bar{\mathcal{F}}_5$; orange: $\mathcal{F}_4 \cap \bar{\mathcal{F}}_4$; yellow: $\mathcal{F}_4 \cap \bar{\mathcal{F}}_5$.

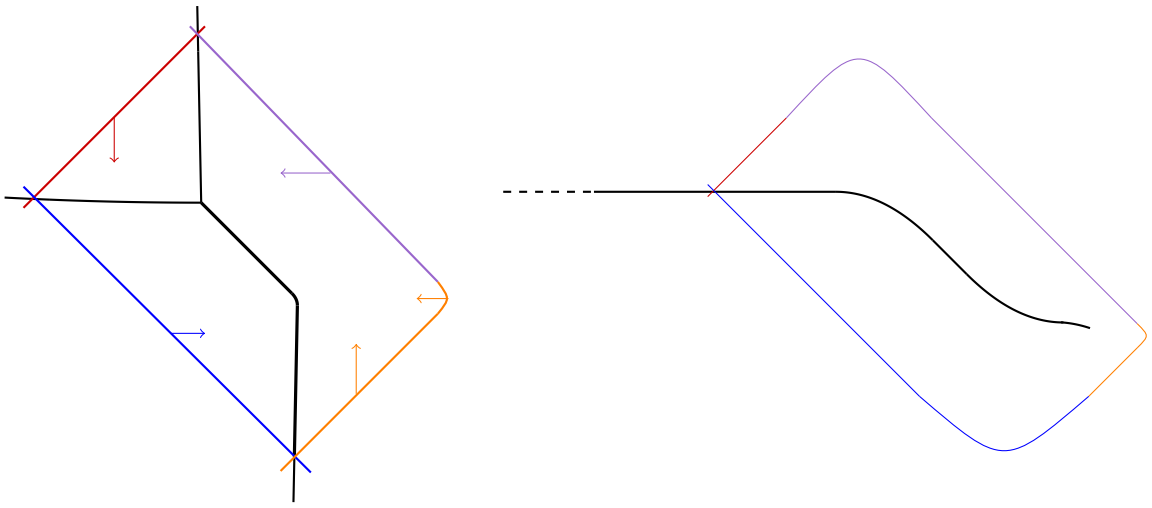

FIGURE 7. The formation of the cut locus in the cases A_- with $C_2 < 0$ and $A > 0$ (on the left) and A_- with $A > C_2 > 0$ (on the right). In red (respectively, blue, orange, purple) the front $\mathcal{F}$ (respectively $\mathcal{G}, \bar{\mathcal{F}}, \bar{\mathcal{G}}$)

5.2. $C_2 > 0$. When $C_2 > 0$, the conjugate time of the trajectories of the sets $\Gamma_{\pm g}$ is the fifth conjugate time. Moreover, the intersections between the fourth bang front of Γ_g (respectively, Γ_{-g}) geodesics with the fourth front of geodesics of the set Γ_{-f} (respectively, Γ_f) do not occur. We thus focus on the part of the wavefront made by the geodesics in Γ_g that have already passed the fourth switching time. From equation (50), we can see that the front is constrained between the vertical lines $\{x = (A - C_2)\zeta^3\}$ and $\{x = (A + C_2)\zeta^3\}$ (up to fourth order terms in ζ). For the fifth bang front of Γ_{-g} geodesics an analogous bound holds. Then, to understand how the fronts coming from different strategies may intersect, we must look at the relative values of A and C_2; in particular, as in the case in which $C_1 \neq 0$, we have four cases.

$A > C_2$. The cut locus has one branch and is given by the concatenation of the following intersections:

$$\mathcal{F}_4 \cap \mathcal{G}_4, \quad \mathcal{G}_4 \cap \bar{\mathcal{G}}_5, \quad \mathcal{G}_4 \cap \bar{\mathcal{G}}_4, \quad \bar{\mathcal{G}}_4 \cap \mathcal{G}_5 \quad \bar{\mathcal{F}}_5 \cap \mathcal{G}_5.$$

In order to prove this, first of all we notice that all geodesics of the set Γ_f lose their optimality during the fourth bang arc, by intersections with the geodesics of Γ_g (as $C_2 > 0$ forbids the intersection with the front $\bar{\mathcal{G}}_4$ and $A > 0$ forbids those with the fronts $\bar{\mathcal{F}}_4$ and $\bar{\mathcal{F}}_5$).

From (46), we can see that the intersection $\mathcal{G}_4 \cap \bar{\mathcal{G}}_5$ is, up to higher order terms in ζ, an arc of parabola (with concavity $-C_2$) connecting the points $(-4(A + C_2)\zeta^3, 4A\zeta^3)$ and $(-4(A - C_2)\zeta^3, 4(A - C_2)\zeta^3)$; moreover, the tangent at the curve is given by

$$\frac{y\prime(p_x^0)}{x\prime(p_x^0)} = \frac{p_x^0 - 1}{2}$$

(here p_x^0 refers to the first component of the adjoint vector at time 0 of the trajectory Γ_{-g}). Analogously, the suspension of the intersection $\bar{\mathcal{G}}_4 \cap \mathcal{G}_5$ can be recovered by applying to the intersection $\mathcal{G}_4 \cap \bar{\mathcal{G}}_5$ a rotation of π around the z axis and its corresponding permutation of the invariants. In particular, it is an arc of parabola of concavity C_2 joining to the intersection $\mathcal{G}_4 \cap \bar{\mathcal{G}}_4$ at the point $(4(A + C_2)\zeta^3, -4A\zeta^3)$. Recalling that the intersection $\mathcal{G}_4 \cap \bar{\mathcal{G}}_4$ is a segment of slope -1 (see equation (44)), we get that the junctions at the points $(-4(A + C_2)\zeta^3, 4A\zeta^3)$ and $(-4(A - C_2)\zeta^3, 4(A - C_2)\zeta^3)$ are C^1. We thus conclude that the geodesics of the set Γ_g lose optimality in the following ways:

- if $p_x^0 \geq 1 + 4(E_1 + 1/3D_1)\zeta^3 + \mathcal{O}(\zeta^4)$, the geodesic loses its optimality by intersecting $\mathcal{F}_4$.
- if $1 - 4C_2\zeta^2 \leq p_x^0 \leq 1 + 4(E_1 + 1/3D_1)\zeta^3$, then the geodesic loses its optimality by intersecting $\bar{\mathcal{G}}_5$ (see equation (46)).
- for $1 - 8A\zeta^2 \leq p_x^0 \leq 1 - 4C_2\zeta^2$,then the geodesic loses its optimality during its fifth bang arc, by intersecting $\bar{\mathcal{G}}_4$ (see equation (44)).
- finally, all geodesics of the kind Γ_g with $-1 + \varepsilon \leq p_x^0 \leq 1 - 8A\zeta^2 + \mathcal{O}(\zeta^3)$, where $\varepsilon > 0$ is going to be determined here below, lose their optimality during the fifth bang arc, by intersecting the fourth bang front of Γ_{-g}.

To understand what happens for $p_x^0 \in [-1, -1 + \varepsilon)$, we must study the intersection the front $\mathcal{G}_5$ with the front $\bar{\mathcal{F}}_5$: let us consider their expressions at some time $\boldsymbol{T} = T_1\zeta + T_2\zeta^2 + T_3\zeta^3 + T_4\zeta^4 + \mathcal{O}(\zeta^5)$ (equations (20) and (50)). By naively imposing the equality of the jets of both coordinates up to the fourth order in ζ, we obtain the constraints

$$T_1 = 8, \qquad T_2 = 0, \qquad T_3 = -4A - \frac{4}{3}C_2, \qquad g_0 = -1$$

and the two pairs of solutions

$$q_0 = 1, \qquad T_4 = 4(E_1 - E_2) - \frac{4}{3}(D_1 + D_2)$$
$$q_0 = -\frac{1}{2} + \frac{3E_1}{2D_1}, \qquad T_4 = \frac{3}{2D_1}\Big(E_1 + \frac{D_1}{3}\Big)^2 - 4\Big(E_2 + \frac{D_2}{3}\Big).$$

The first pair is not surprising: consider indeed the Γ_g geodesics associated with the initial covector $(p_x^0, 1, 1/\rho_0)$ at its fourth switching time $(9 + p_x^0)\rho_0 + \mathcal{O}(\rho_0)$. Its limit for $p_x^0 \to -1$ is indeed the Γ_{-f} geodesics (with initial covector $(-1, 1, 1/\rho_0)$) at its fifth switching time $7 + p_y^0$. This in particular tells us that, fixing $g_0 = -1$, $q_0 = 1$ and T_k in such a way that $\boldsymbol{T}$ corresponds to the fifth switching time for the first trajectory (or the fourth switching time for the second one), then the system (20)=(50) is satisfied at each order in ζ.

Since there are only two pair of solutions, it seems that the fronts intersect only in two points (that is, only two pairs of geodesics intersect); this would mean that the geodesics of the set Γ_{-f} have no Maxwell points before the conjugate time (as other intersections do not occur). A finer analysis is thus in order: to do so, we set $g_0 = -1 + \eta(q_0, \zeta)$ and $\boldsymbol{T} = 8\zeta + \big(-4A - \frac{4}{3}C_2\big)\zeta^3 + T(q_0, \zeta)$, where η and T are functions, that we assume bounded for $q_0 \in [-1, 1]$ and ζ sufficiently small; we

then substitute these expressions in $\mathcal{G}_5$. The system (20)=(50) becomes

$$\begin{cases} 4C_2(1+g_0) - T(q_0,\zeta) + \big(-\frac{4}{3}D_1q_0^3 + 2E_1q_0^2 + 2E_1 - 2D_2g_0^2 + 4E_2g_0 + \frac{2}{3}D_2\big)\zeta = \mathcal{O}(\zeta^2) \\ 2C_2(1-g_0^2) - T(q_0,\zeta) + \big(\frac{4}{3}D_2g_0^3 - 2E_2g_0^2 - 2E_2 - 2D_1q_0^2 + 4E_1q_0 + \frac{2}{3}D_1\big)\zeta = \mathcal{O}(\zeta^2), \end{cases}$$

where the right-hand sides of the equations here above depend on η, q_0 and T. Summing the two equations and factorising the result, we obtain the equation

(30)
$$\eta(q_0,\zeta)^2\big(3C_2 + (3D_2 + 3E_2 - 2D_2\eta(q_0,\zeta))\zeta\big) + (1-q_0)^2\big(-2D_1q_0 + 3E_1 - D_1\big)\zeta - R(\eta,T,q_0,\zeta) = 0,$$

where

$$R\Big(0, \mathbb{T}_4 - 8\zeta - \big(-4A - \frac{4}{3}C_2\big)\zeta^3, -1, \zeta\Big) = 0 \ \forall\zeta,$$
$$\lim_{\zeta\to 0}\frac{R(\eta,T,q_0,\zeta)}{\zeta^2} = 0$$

(here $\mathbb{T}_4$ denotes the fourth switching time of the Γ_g geodesics). Let us now neglect higher order terms in ζ, that is, let us study the equation

$$\eta(q_0,\zeta)^2\big(3C_2 + (2D_2\eta(q_0,\zeta) - D_2 + 3E_2)\zeta\big) + (1-q_0)^2\big(-2D_1q_0 + 3E_1 - D_1\big)\zeta = 0, \tag{31}$$

which is a cubic equation for η. For $q_0 = 1$, the equation (31) has the double root $\{\eta = 0\}$ and the simple one $\{\eta = -\frac{3}{2} - \frac{3E_2}{2D_2} - \frac{3C_2}{2D_1}\frac{1}{\zeta}\}$, where the latter is not an admissible value for the adjoint vector if ζ is small enough. Since $(-2D_1q_0 - D_1 + 3E_1) < 0$ for every $q_0 \in [-1,1]$, we can see that, for $q_0 \neq 1$, the constant root of (31) splits into two distinct roots, one strictly greater and one strictly smaller than 1, continuously depending on q_0; it is easy to prove that, if ζ is small enough, then the latter is always greater than -1.

This argument holds also for equation (30). Indeed, R is null for $g_0 = -1$, $q_0 = 1$ and $\boldsymbol{T}$ equal to the switching time; then, for every $q_0 \in [-1,1)$ there exists $\bar\zeta$ such that

$$(1-q_0)^2(-2D_1q_0 + 3E_1 - D_1) - R(\eta,T,q_0,\zeta) > 0$$

for $\zeta < \bar\zeta$, $|\eta| < 1/2$ and T close enough to the switching time. Then the graph of the function defined in the right-hand side of (30) is close to the one of the function defined in the right-hand side of (31); possibly further shrinking ζ, we can say that equation (30) has the root

$$\eta(q_0,\zeta) = \left(\sqrt{\zeta}\sqrt{\frac{D_1 - E_1}{C_2 + (D_2+E_2)\zeta}} + \mathcal{O}(\zeta)\right)(1-q_0) + \mathcal{O}((q_0+1)^2). \tag{32}$$

This also provides the following expansions for T:

$$T(q_0,\zeta) = 4\sqrt{C_2(D_1 - E_1)}(1-q_0)\sqrt{\zeta} + \mathcal{O}(\zeta),$$

which gives an estimate for the parameter $\varepsilon = 2\sqrt{\zeta}\sqrt{\frac{D_1-E_1}{C_2}} + \mathcal{O}(\zeta)$.

The suspension of the intersection between the fronts $\mathcal{G}_5$ and $\bar{\mathcal{F}}_5$ is thus obtained by substituting the values of $\boldsymbol{T}$ into equation (20)

$$\begin{cases} x(\boldsymbol{T}) &= 4(A+C_2)\zeta^3 - 4\sqrt{C_2(D_1-E_1)}(1-q_0)\zeta^{7/2} + \mathcal{O}(\zeta^4) \\ y(\boldsymbol{T}) &= -4A\zeta^3 + \mathcal{O}(\zeta^4), \end{cases} \qquad q_0 \in [-1,1].$$

Remark 10. *The usual procedure of developing the component p_x^0 of the covector of the trajectory of the set Γ_g in powers of ζ (or ρ_0, which has the same order of magnitude) in this case does not work. Indeed, as equation* (32) *shows, p_x^0 should be rather developed in powers of $\sqrt{\zeta}$.*

This is due to the fact that we are studying the intersection of a front of length $\mathcal{O}(\zeta^3)$ with one length $\mathcal{O}(\zeta^4)$, differently from the other cases.

We can conclude that all geodesics of the set Γ_{-f} lose their optimality during the fifth bang front, by intersecting the fifth bang front of Γ_g, and that the intersection $\mathcal{G}_5 \cap \bar{\mathcal{F}}_5$ participate to the cut locus. We notice however that its junction with the part of intersection $\mathcal{G}_5 \cap \bar{\mathcal{G}}_4$ belonging to the cut locus is not C^1.

Finally, the lost of optimality of the geodesics of the set Γ_{-g} is analogous to the one of the trajectories Γ_g (with the difference that they do not meet other trajectories than those of the set Γ_g).

The shape of the cut locus is depicted in Figure 8.

$0 < A < C_2$. This case is very similar to the precedent one, with one major exception: if $A < C_2$, then the intersection between the fourth arcs of the geodesics of the sets Γ_g and Γ_{-g} does not occur; on the other hand, the front $\mathcal{G}_5$ meets the front $\bar{\mathcal{G}}_5$.

Moreover, the arc of parabola $\mathcal{G}_4 \cap \bar{\mathcal{G}}_5$ is the intersection of optimal geodesics only when those of the set Γ_g are associated with an initial covector $p_x^0 \leq \frac{2A}{C_2} - 1$. This can be proved by comparing the intersection times and taking into account that the intersection $\mathcal{G}_5 \cap \bar{\mathcal{G}}_5$ requires $p_x^0 \geq \frac{2A}{C_2} - 1$ to exist (see Appendix A.2-ζ)-η) for details). The arc of parabola contained in the cut locus joins the points $(-4(A + C_2)\zeta^3, 4A\zeta^3)$ and $(4(A - C_2)\zeta^3, (-4A^2/C_2 + 4A)\zeta^3)$. Analogously, the arc of parabola given by $\bar{\mathcal{G}}_4 \cap \mathcal{G}_5$ participates to the cut locus connecting the points $(4(A+C_2)\zeta^3, -4A\zeta^3)$ and $(-4(A - C_2)\zeta^3, (4A^2/C_2 - 4A)\zeta^3)$.

The points $(4(A-C_2)\zeta^3, (-4A^2/C_2+4A)\zeta^3)$ and $(-4(A-C_2)\zeta^3, (4A^2/C_2-4A)\zeta^3)$ are connected by the intersection $\mathcal{G}_5 \cap \bar{\mathcal{G}}_5$, which is a segment of slope $-A/C_2$ (see Appendix A.2 -η)).

Thus, the cut locus has one branch and is given by the concatenation of the following intersections:

$$\mathcal{F}_4 \cap \mathcal{G}_4, \quad \mathcal{G}_4 \cap \bar{\mathcal{G}}_5, \quad \mathcal{G}_5 \cap \bar{\mathcal{G}}_5, \quad \bar{\mathcal{G}}_4 \cap \mathcal{G}_5, \quad \bar{\mathcal{F}}_5 \cap \mathcal{G}_5.$$

It can be easily verified that all junctions are C^1, except the one involving $\bar{\mathcal{F}}_5 \cap \mathcal{G}_5$.

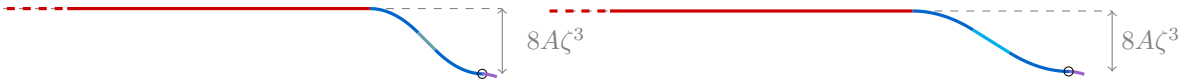

FIGURE 8. Suspension of the cut locus for the case A_- with $C_2 > 0$ and $A > 0$. On the left, $A > C_2$, on the right $0 < A < C_2$; red: $\mathcal{F}_4 \cap \mathcal{G}_4$; blue: $\mathcal{G}_4 \cap \bar{\mathcal{G}}_5$ and $\bar{\mathcal{G}}_4 \cap \mathcal{G}_5$; sugarpaper: $\mathcal{G}_4 \cap \bar{\mathcal{G}}_4$; purple $\mathcal{G}_5 \cap \bar{\mathcal{F}}_5$; cyan: $\mathcal{G}_5 \cap \bar{\mathcal{G}}_5$. The circles denote the points where the junction is not C^1.

$-C_2 < A < 0$. We will show here below that the cut locus has one branch and is given by the concatenation of the following intersections:

$$\mathcal{F}_4 \cap \mathcal{G}_4, \quad \mathcal{F}_4 \cap \mathcal{G}_5, \quad \mathcal{G}_5 \cap \bar{\mathcal{G}}_5, \quad \bar{\mathcal{F}}_4 \cap \bar{\mathcal{G}}_5, \quad \bar{\mathcal{F}}_5 \cap \bar{\mathcal{G}}_5.$$

First of all, we recall that, when A is negative, the geodesics of the sets Γ_g and Γ_{-g} meet (eventually) after the fourth switching time of both. Then, to detect the loss of optimality of the geodesics of the set Γ_g, we study their intersections with those of the set Γ_f. Consider the geodesics of the set Γ_g associated with the initial covector $(p_x^0, 1, 1/\zeta)$. If $p_x^0 \geq 1 + 4\big(E_1 + D_1/3\big)\zeta^3 + \mathcal{O}(\zeta^4)$, then it loses its local optimality before the fourth switching time, by intersecting a geodesic of Γ_f. If $p_x^0 \in [1 + \frac{2A}{C_2}, 1 + 4\big(E_1 + D_1/3\big)\zeta^3]$, then it loses optimality after the fourth switching time, by intersecting a geodesic of the set Γ_f with initial adjoint vector $(1, \widetilde{p}_y^0, 1/\widetilde{\rho}_0)$, with $\widetilde{p}_y^0 \leq -1 - 8A\zeta^3$ and $\widetilde{\rho}_0 = \zeta + \mathcal{O}(\zeta^2)$ (see Section A.2-κ)); from (48), we see that this intersection is an arc of parabola; in particular, the arc joining the points $(4(A - C_2)\zeta^3, 4A\zeta^3)$ and $(-4(A + C_2)\zeta^3, 4(A + A^2/C_2)\zeta^3)$ belongs to the cut locus. We can repeat the same reasoning for the fronts $\bar{\mathcal{F}}_4$ and $\bar{\mathcal{G}}_5$ and see that the symmetric arc of parabola joining the points $(-4(A - C_2)\zeta^3, -4A\zeta^3)$ and $(4(A + C_2)\zeta^3, -4(A + A^2/C_2)\zeta^3)$ belongs to the cut locus.

Finally, all trajectories of the set Γ_g with $p_x^0 \in [-1, 1 + \frac{2A}{C_2}]$ lose their optimality along the fifth bang arc, by intersecting the fifth bang front $\bar{\mathcal{G}}_5$.

It is left to prove how the trajectories of the set Γ_{-f} with initial covector $(-1, p_y^0, \zeta)$, for $p_y^0 \leq 1 + 8A\zeta^3$, lose optimality. By geometric considerations on the position of the fronts, the only possibility is an intersection with the front $\bar{\mathcal{G}}_5$. To find such intersection, we proceed exactly as in the case $A > C_2$, that is, we impose equality of the jets of the fronts $\bar{\mathcal{F}}_5$ and $\bar{\mathcal{G}}_5$. This gives rise

to the following system

$$\begin{cases} (1+g_0)^2(3C_2-(3E_2+(2g_0-1)D_2)\zeta)+(q_0+1)^2(-2D_1q_0+3E_1+D_1)=\mathcal{O}(\zeta^2) \\ T(q_0,\zeta)+2(g_0^2-1)C_2-2\big(D_1q_0^2+(1+g_0^2)E_2+\frac{2}{3}D_2g_0^3-2E_1q_0-\frac{1}{3}D_1\big)\zeta=\mathcal{O}(\zeta^2), \end{cases} \tag{33}$$

where we recall that q_0 denotes the second component of the initial covector of the trajectory of the set Γ_{-f}, and g_0 the first component of the initial covector of the trajectory of the set Γ_{-g}. If we neglect the higher order terms in ζ, we see that the first equation has an evident solution at $g_0=-1,\ q_0=-1$. Proceeding as we did above, we substitute $g_0=-1+\eta(q_0,\zeta)$ in the equation, thus obtaining a cubic equation for η, with constant term $(q_0+1)^2(-2D_1q_0+3E_1+D_1)$. Since the constant term is negative for every $q_0\in(-1,1]$, then the double root $\{\eta=0\}$ splits into two, one of which is always strictly greater than -1 and strictly smaller than 1 for $q_0\in[-1,1)$ and ζ small enough. As in the precedent case, choosing ζ small enough we obtain the following asymptotic expansion for the solutions of (33)

$$g_0(q_0,\zeta)=-1+\sqrt{\zeta}\sqrt{\frac{-D_1-E_1}{C_2}}(1+q_0)+\mathcal{O}(\zeta)$$
$$T(q_0,\zeta)=4A-\frac{4}{3}C_2+4\sqrt{\zeta}\sqrt{-C_2(D_1+E_1)}(1+q_0)+\mathcal{O}(\zeta),$$

which gives the following expression for the suspension:

$$\begin{cases} x=-4(A-C_2)\zeta^3-4(q_0+1)\sqrt{-C_2(D_1+E_1)}\zeta^{7/2}+\mathcal{O}(\zeta^4) \\ y=-4A\zeta^3+\mathcal{O}(\zeta^4) \end{cases} \tag{34}$$

As above, we can prove that all the junctions, except the one with (34), are C^1, up to higher order terms. The shape of the cut locus is shown in Figure 9.

$A<-C_2<0$. This case looks alike the precedent one, with two differences: first of all, the arc of parabola (48) (as well as its symmetric) participates to the cut locus for every $q_0\in[-1,1]$; then, part of the cut locus closer to the origin of the plane $\{z=4\eta^2\}$ is given by the intersection $\mathcal{F}_4\cap\bar{\mathcal{F}}_4$, which is studied in Section A.2-γ).

The cut locus has one branch and is given by the concatenation of the following intersections:

$$\mathcal{F}_4\cap\mathcal{G}_4,\quad \mathcal{F}_4\cap\mathcal{G}_5,\quad \mathcal{F}_4\cap\bar{\mathcal{F}}_4,\quad \bar{\mathcal{F}}_4\cap\bar{\mathcal{G}}_5,\quad \mathcal{F}_5\cap\bar{\mathcal{G}}_5.$$

The shape of the cut locus is shown in Figure 9. As above, we can prove that all the junctions, except the one with (34), are C^1.

FIGURE 9. Suspension of the cut locus for the case A_- with $C_2>0$ and $A<0$. On the left, $-C_2<A<0$: red: $\mathcal{F}_4\cap\mathcal{G}_4$; purple: $\mathcal{F}_4\cap\mathcal{G}_5$ and $\bar{\mathcal{F}}_4\cap\bar{\mathcal{G}}_5$; cyan: $\mathcal{G}_5\cap\bar{\mathcal{G}}_5$; dark green: $\bar{\mathcal{F}}_5\cap\bar{\mathcal{G}}_5$. On the right $A<-C_2$: red: $\mathcal{F}_4\cap\mathcal{G}_4$; purple: $\mathcal{F}_4\cap\mathcal{G}_5$ and $\bar{\mathcal{F}}_4\cap\bar{\mathcal{G}}_5$; orange: $\mathcal{F}_4\cap\bar{\mathcal{F}}_4$; dark green: $\bar{\mathcal{F}}_5\cap\bar{\mathcal{G}}_5$. The circles denote the points where the cut locus fails to be C^1.

6. $0<E_1<D_1$ (CASE $\boldsymbol{B}_+$)

When $\frac{|E_1|}{|D_1|}<1$, the cut locus does not depend on the values of the two invariants C_2 and A only. Indeed, we notice that the fourth bang front $\bar{\mathcal{F}}_4$ may intersect $\bar{\mathcal{G}}_4$, as condition (41) is always verified, and (42) holds for every $p_y^0\le\frac{3E_1}{2D_1}+\frac{1}{2}$. In particular, if $3\frac{E_1}{D_1}\ge1$, then every $p_y^0\in[-1,1]$ satisfies the condition, whereas if $3\frac{E_1}{D_1}<1$, then $\frac{3E_1}{2D_1}+\frac{1}{2}<1$ and only some Γ_{-f} geodesics intersect a Γ_{-g} geodesic before their fourth switching time. Then, the last invariant that determines the shape of the cut locus is the ratio $\frac{3E_1}{D_1}$. We now study all the cases in details.

6.1. $C_2<0$.

$A > 0$. As usual, we first concentrate on the geodesics of the set Γ_f. As observed in Section 3.3.1, for every $p_y^0 \in [-1, -\frac{E_1}{D_1})$ the geodesic with initial covector $(1, p_y^0, 1/\rho_0)$ intersects, at the (reparametrised) time $\mathcal{T}_{int} = 7 - \frac{1}{2}p_y^0 + \frac{3E_1}{2D_1} + \mathcal{O}(\rho_0)$, the geodesic (of the set Γ_f) with initial covector $(1, -\frac{3E_1}{2D_1} - \frac{1}{2}p_y^0, 1/\widetilde{\rho}_0)$, where $\widetilde{\rho}_0 = \rho_0 + \frac{9}{4}A(p_y^0 + E_1D_1)\rho_0^3 + \mathcal{O}(\rho_0^4)$. This intersection belongs to the cut locus, and is, up to higher order terms, a horizontal segment of length $\sim \big(1 - \frac{E_1}{D)1}\big)\zeta$.

Fix some $\zeta = \rho_0 + \mathcal{O}(\rho_0^2)$. By comparing the expression of suspensions of the fronts (equations (18)-(19) and (49)), it is possible to verify that, at time

$$\boldsymbol{T} = 8\zeta + \Big(\frac{8}{3}C_2 - 4A\Big)\zeta^3 - \frac{3(E_1 + D_1/3)^2}{2D_1}\zeta^4 + \mathcal{O}(\zeta^5)$$

the three fronts $\mathcal{F}_4$, $\mathcal{F}_5$ and $\bar{\mathcal{G}}_4$ meet; more precisely, the intersection involves the Γ_f geodesic with initial covector $(1, \gamma, 1/\rho_0)$, the Γ_f geodesic with initial covector $(1, \eta, 1/\widetilde{\rho}_0)$ and the Γ_{-g} geodesic with initial covector $(\mu, -1, 1/\widehat{\rho}_0)$, with

$$\gamma = -1 + 4C_2\zeta^2 + 4(E_2 + D_2/3)\zeta^3 + \mathcal{O}(\zeta^4) \qquad \rho_0 = \zeta - \big(C_2 + \frac{3}{2}A\big)\zeta^3 + \mathcal{O}(\zeta^4)$$

$$\eta = \frac{1}{2} - \frac{3E_1}{2D_1} + \mathcal{O}(\zeta) \qquad \widetilde{\rho}_0 = \zeta - \big(C_2 - \frac{3}{2}A\eta\big)\zeta^3 + \mathcal{O}(\zeta^4)$$

$$\mu = -1 + 8A\zeta^2 + \big(5E_1 + \frac{3E_1^2}{2D_1} + \frac{3D_1}{2}\big)\zeta^3 + \mathcal{O}(\zeta^4) \qquad \widehat{\rho}_0 = \zeta - \big(C_2 - \frac{3}{2}A\big)\zeta^3 + \mathcal{O}(\zeta^4).$$

Summing up these elements, we can describe the cut locus of the geodesics of the set Γ_f.

- the geodesics with $p_y^0 \in [-1, \frac{1}{2} - \frac{3E_1}{2D_1})$ lose global optimality due to the intersection of $\mathcal{F}_4$ with $\mathcal{F}_5$, as described in Section 3.3.1.
- the geodesics with $p_y^0 \in (\frac{1}{2} - \frac{3E_1}{2D_1}, 1]$ lose global optimality during their fifth bang arc, by intersecting with the fourth bang of geodesics of the set Γ_{-g}. The suspension (and the value of the intersection time) of this intersection are provided in Appendix A.2-θ).

As anticipated before, the form of the cut locus of the geodesics of the set Γ_{-f} depends on the value of $\frac{E_1}{D_1}$. If $\frac{3E_1}{D_1} \geq 1$, then all $\gamma \in [-1, 1]$ satisfy equation (42); this means that every geodesic in Γ_{-f} intersects the fourth front of the geodesics in Γ_{-g}, and the suspension of the intersection is, up to the third order in ζ, a horizontal segment of vertical coordinate equal to $-4A\zeta^3 + \mathcal{O}(\zeta^4)$ (see equation (43)). For what concerns the geodesics of the sets $\Gamma_{\pm g}$, we can adapt the reasonings done in Section 5.1: more precisely, the geodesics of the set Γ_g lose their global optimality when intersecting the fourth front of geodesics of the sets Γ_{-f} or Γ_{-g}. The suspension of such intersections are respectively provided in equations (27) and (44). The geodesic of the set Γ_{-g} lose their global optimality when intersecting the geodesics of the sets Γ_f (equations (27) and (47)), Γ_g and Γ_{-f} (equation (26).

By direct computation of the tangents to the curves, we see that junction between the intersections $\mathcal{F}_5 \cap \bar{\mathcal{G}}_4$ and $\mathcal{G}_4 \cap \bar{\mathcal{G}}_4$ is C^1. The form of the cut locus is illustrated in Figure 10 (right).

Let us now assume that $\frac{3E_1}{D_1} < 1$, which implies that equation (42) is satisfied only for $y_y^0 \geq \frac{3E_1}{2D_1} + \frac{1}{2} < 1$. All geodesics with initial covector $(-1, p_y^0, 1/\zeta)$, $p_y^0 \leq \frac{3E_1}{2D_1} + \frac{1}{2}$, intersect, at the (reparametrised) time $\mathcal{T} = 7 + p_y^0 + \mathcal{O}(\zeta^2)$, the fourth bang arc of Γ_{-g} geodesics. On the other hand, the geodesics with $p_y^0 \in [1 + 4C_2\zeta^2, 1]$ lose their global optimality by intersecting the fourth front of $\mathcal{G}_4$, as shown in Section 5.1.

To find the cut locus for the geodesics with initial covector $p_y^0 \in [\frac{1}{2} + \frac{3E_1}{2D_1}, 1 + 4C_2\zeta^2]$, we must study the front $\bar{\mathcal{F}}_5$. Indeed, the front $\bar{\mathcal{F}}_4$ cannot intersect $\mathcal{F}_4$ or $\mathcal{F}_5$, because $A > 0$, and we can neglect eventual intersections with the fronts $\mathcal{G}_5$ and $\bar{\mathcal{G}}_5$, which are not optimal.

Equation (20) shows that the suspension of the front $\bar{\mathcal{F}}_5$ is contained in a horizontal strip of width $\mathcal{O}(\zeta^4)$ centred around $\{y = -4A\zeta^3\}$. This suggests to study its intersection with the fourth bang front of the trajectories Γ_g (see Appendix A.2-ι) for details). In particular, comparing the expressions of the fronts $\mathcal{G}_4$, $\bar{\mathcal{F}}_5$ and $\bar{\mathcal{G}}_4$, we can show that the Γ_g geodesic with initial adjoint

vector $(\beta, 1, 1/\rho_0)$, the Γ_{-f} geodesic with initial adjoint vector $(-1, \eta, 1/\widetilde{\rho}_0)$ and the Γ_{-g} geodesic with initial adjoint vector $(\gamma, -1, 1/\widehat{\rho}_0)$, with

$$\beta = 1 - 8A\zeta^2 + \mathcal{O}(\zeta^3)$$
$$\eta = \frac{3E_1}{2D_1} + \frac{1}{2}$$
$$\gamma = -1 + \frac{3}{2}\frac{(E_1 + D_1)^2}{D_1}\zeta^3 + \mathcal{O}(\zeta^4)$$

and $\rho_0, \widetilde{\rho}_0, \widehat{\rho}_0 = \zeta + \mathcal{O}(\zeta^2)$, meet at the time $\boldsymbol{T} = 8\zeta + (-4A + 8/3C_2)\zeta^3 + \mathcal{O}(\zeta^5)$.

By straightforward computation, we can see that the junction of this part of the cut locus with the intersection $\mathcal{G}_4 \cap \bar{\mathcal{F}}_4$ is C^1, but this is not the case for the one with $\mathcal{G}_4 \cap \bar{\mathcal{G}}_4$.

Summing, up, differently from the case $\frac{3E_1}{D_1} \geq 1$, the suspension of the cut locus is *disconnected*, with one connected component made by only one branch, and the other one made by three branches, one of which is not C^1. Its shape is illustrated in Figure 10 (right). The formation of the cut locus in this last case is shown in Figure 11.

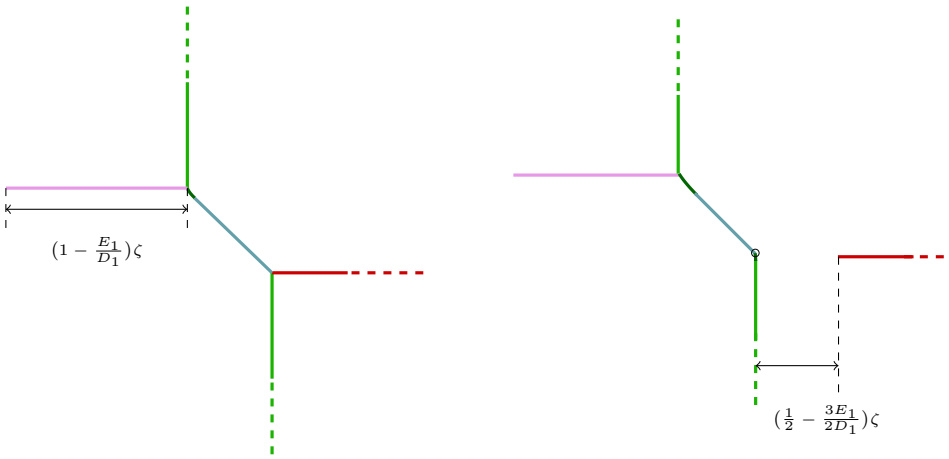

FIGURE 10. Suspension of the cut locus for the case B_+ with $C_2 < 0$ and $A > 0$. On the left, $\frac{3E_1}{D_1} \geq 1$, on the right $\frac{3E_1}{D_1} < 1$: pink: $\mathcal{F}_4 \cap \mathcal{G}_4$. Pink: $\mathcal{F}_4 \cap \mathcal{G}_4$; red: $\bar{\mathcal{F}}_4 \cap \bar{\mathcal{G}}_4$; green: $\mathcal{G}_4 \cap \bar{\mathcal{F}}_4$ and $\bar{\mathcal{G}}_4 \cap \mathcal{F}_4$; sugarpaper: $\mathcal{G}_4 \cap \bar{\mathcal{G}}_4$; dark green: $\mathcal{F}_5 \cap \bar{\mathcal{G}}_4$ and $\bar{\mathcal{F}}_5 \cap \mathcal{G}_4$. The circle shows the point where the suspension is not C^1.

$A < 0$. We recall that, if $A < 0$, the intersection of the fronts $\mathcal{F}_5$ and $\bar{\mathcal{G}}_4$ is no more possible. Our first concern is then to understand how the geodesics of the set Γ_f with $p_y^0 \geq \frac{1}{2} - \frac{3E_1}{2D_1}$ lose optimality. Studying the expression of the fronts, we can verify that the Γ_f geodesic with initial covector $(1, \beta, 1/\rho_0)$, the Γ_f geodesic with initial covector $(1, q_0, 1/\rho_0)$ and the Γ_{-f} geodesic with initial covector $(-1, -\gamma, 1/\rho_0)$, where

$$\beta = -1 - (4C_2 + 8A)\zeta^2 + \big(3/2E_1^2/D_1 + E_1 - 4E_2 + 1/6D_1 - 4/3D_2\big)\zeta^3$$
$$q_0 = \frac{1}{2} - \frac{3E_1}{2D_1}$$
$$\gamma = -1 - 4C_2\zeta^2 - \big(3/2E_1^2/D_1 + E_1 - 4E_2 + 1/6D_1 - 4/3D_2\big)\zeta^3.$$

meet at time

$$\boldsymbol{T} = 8\zeta + \Big(\frac{8}{3}C_2 + 4A\Big)\zeta^3\ (+0\zeta^4) + \mathcal{O}(\zeta^5)$$

It is easy to verify that the first and the third geodesics have not passed their fourth switching time yet, while the second one has already. This suggests to investigate the intersections of the front $\mathcal{F}_5$ corresponding to geodesics with $p_y^0 \geq \frac{1}{2} - \frac{3E_1}{2D_1}$ with the front $\bar{\mathcal{F}}_4$ (see Appendix A.2-ε)). This intersection is indeed part of the cut locus.

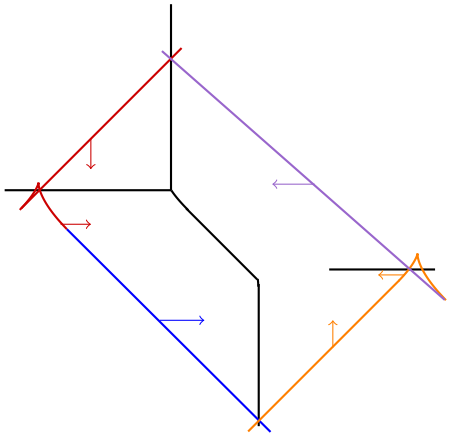

FIGURE 11. The formation of the cut locus in the case B_+ with $C_2 < 0$, $A > 0$ and $\frac{3E_1}{D_1} < 1$. The arrows show how the fronts deplace as time increases.

Again, for other intersections involving the fronts of the geodesics of the set Γ_{-f}, we must distinguish the two cases $\frac{3E_1}{D_1} \geq 1$ and $\frac{3E_1}{D_1} < 1$.

In the first case, the cut locus is connected and made of five C^1 branches. More precisely:

- the Γ_f geodesics with $p_y^0 \in [-1, -1-4(2A+C_2)\zeta^2)$ lose their optimality before the fourth switching time, by intersecting the fourth bang arc of some Γ_{-f} geodesics; those with initial covector $p_y^0 \in (-1-(4C_2+8A)\zeta^2, \frac{1}{2} - \frac{3E_1}{2D_1})$ lose optimality by means of the self intersection $\mathcal{F}_4 \cap \mathcal{F}_5$; finally, those with $p_y^0 \in (\frac{1}{2} - \frac{3E_1}{2D_1}, 1]$ lose optimality after the fourth switching time, intersecting the fourth bang arc of the Γ_{-f} geodesics.
- the geodesics of the set Γ_{-f} with $p_y^0 \in [1+4C_2\zeta^2, 1]$ lose optimality by intersecting $\mathcal{F}_5$; those with $p_y^0 \in (1+4(2A+C_2)\zeta^2, 1+4C_2\zeta^2)$, by intersecting $\mathcal{F}_4$; for $p_y^0 \in [-1, 1+4(2A+C_2)\zeta^2]$, intersecting the front $\bar{\mathcal{G}}_4$.
- the geodesics of the kind $\Gamma_{\pm g}$ lose optimality during the fourth bang arc, by intersecting, respectively, the fronts $\bar{\mathcal{F}}_4$ and $\mathcal{F}_4$.

The cut locus is depicted in Figure 12 (left).

In the case $\frac{3E_1}{D_1} < 1$, the suspension of the cut locus is disconnected and made by two connected components. With respect to the preceding case, there is no difference in what concerns the geodesics of the set Γ_g, those of the set Γ_f with $p_y^0 \geq -1-4(2A+C_2)\zeta^2$, and those of the set Γ_{-g}.

The geodesics of the set Γ_{-f} with initial adjoint covector $p_y^0 \leq \frac{1}{2} + \frac{3E_1}{2D_1}$ lose optimality by intersecting the fourth arc of geodesics Γ_{-g}; the suspension is given by (43) and constitutes one connected component of the cut locus. The geodesics with $p_y^0 \in [\frac{1}{2} + \frac{3E_1}{2D_1}, 1]$ lose optimality by intersecting the geodesics with strategies Γ_f (whose second component of the initial covector lies in the interval $[-1-4C_2\zeta^2+4\big(E_1+\frac{D_1}{3}\big)\zeta^3, -1-4C_2\zeta^2+4\big(E_2+\frac{D_2}{3}-E_1+\frac{D_1}{3}\big)\zeta^3]$); in particular, those with $p_x^0 \in [1+4(2A+C_2)\zeta^2, 1]$ lose optimality before their fourth switching time, the other ones after the fourth switching time.

The suspension of the intersection $\mathcal{F}_4 \cap \bar{\mathcal{F}}_5$ is given in equation (45) . In particular, its tangent for $p_y^0 = \frac{1}{2} + \frac{3E_1}{2D_1}$) is $-\frac{2D_1}{3(E_1+D_1)}$, which shows that the junction with $\mathcal{F}_4 \cap \bar{\mathcal{F}}_4$ is not C^1.

6.2. $C_2 > 0$. To describe the cut locus when $C_1 = 0$, $D_1 > E_1 > 0$ and $C_2 > 0$, we can rely on the analysis carried out up to now. Indeed, the main differences with the cases studied in Section 5.2 involve the cut locus of the geodesics of the sets $\Gamma_{\pm f}$.

As could be easily guessed, the shape of the cut locus depends on the relative values of the invariants A and C_2 and on the value of $\frac{3E_1}{D_1}$.

$A > C_2$. As already proved, the geodesics of the set Γ_f with initial covector $(1, p_y^0, 1/\rho_0)$ and $p_y^0 \in \big[-1, \frac{1}{2} - \frac{E_1}{D_1}\big]$ lose their optimality because of the intersection of the fronts $\mathcal{F}_4$ and $\mathcal{F}_5$.

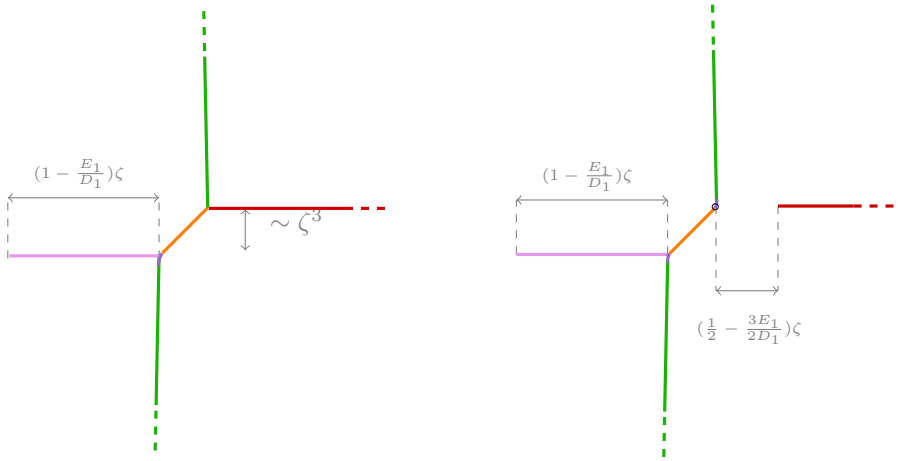

FIGURE 12. Suspension of the cut locus for the case B_+ with $C_2<0$ and $A<0$. On the left, $\frac{3E_1}{D_1}\geq 0$: pink: $\mathcal{F}_4\cap\mathcal{F}_5$; purple: $\mathcal{F}_5\cap\bar{\mathcal{F}}_4$; red: $\bar{\mathcal{F}}_4\cap\bar{\mathcal{G}}_4$; green: $\mathcal{G}_4\cap\bar{\mathcal{F}}_4$ and $\bar{\mathcal{G}}_4\cap\mathcal{F}_4$; orange: $\mathcal{F}_4\cap\bar{\mathcal{F}}_4$. On the right $\frac{3E_1}{D_1}<0$: : pink: $\mathcal{F}_4\cap\mathcal{F}_5$; purple: $\mathcal{F}_5\cap\bar{\mathcal{F}}_4$ and $\bar{\mathcal{F}}_5\cap\mathcal{F}_4$; red: $\bar{\mathcal{F}}_4\cap\bar{\mathcal{G}}_4$; green: $\mathcal{G}_4\cap\bar{\mathcal{F}}_4$ and $\bar{\mathcal{G}}_4\cap\mathcal{F}_4$; orange: $\mathcal{F}_4\cap\bar{\mathcal{F}}_4$. As usual, the circle indicates non-smooth junctions.

As $A>0$, it is likely that the other geodesics of the set Γ_f lose optimality when they meet the fifth front of the trajectories of the set Γ_{-g}; recall indeed that the three fronts $\mathcal{F}_4,\mathcal{F}_5$ and $\bar{\mathcal{G}}_4$ meet at the point $\big(-4A\zeta^3-\frac{4}{3}(2E_1+\mathcal{d})\zeta^4, 4A\zeta^3+\big(E_1+\frac{3E_1^2}{2D_1}-\frac{D_1}{2}+\frac{2}{3}\mathcal{c}\big)\zeta^4\big)$ (see page 27). In order to analyse such intersection, we proceed as done before, by imposing the equality between equations (19) and (50), obtaining the system

(35)
$$\begin{cases}\Big(4A+4g_0C_2+T_3-\frac{8}{3}C_2\Big)\zeta^3-\Big(2D_2g_0^2+4E_2g_0-\frac{4}{3}D_1(p_y^0)^3-2E_1(p_y^0)^2-2E_1-\frac{2}{3}D_2-T_4\Big)\zeta^4=\mathcal{O}(\zeta^5)\\ \Big(T_3-\frac{2}{3}C_2+2C_2g_0^2+4A\Big)\zeta^3-\Big(\frac{4}{3}D_2g_0^3+2E_2g_0^2+2D_1(p_y^0)^2+4E_1(p_y^0)+2E_2-\frac{2}{3}D_1-T_4\Big)\zeta^4=\mathcal{O}(\zeta^5).\end{cases}$$

(we recall that g_0 is the first component of the initial covector of the geodesics of the set Γ_g). As already seen when studying the intersections $\mathcal{G}_5\cap\bar{\mathcal{F}}_5$ and $\mathcal{F}_5\cap\bar{\mathcal{G}}_4$, simply equating the jets of order three and four, and neglecting higher order ones, we obtain that the system is satisfied for $g_0=1$, $T_3=-4A-\frac{4}{3}C_2$, and the two pairs of solutions

$$p_y^0=\frac{1}{2}-\frac{3}{2}\frac{E_1}{D_1}\qquad T_4=-\frac{3}{2}\Big(E_1+\frac{D_1}{3}\Big)^2+4E_2+\frac{4}{3}D_2$$
$$p_y^0=-1\qquad T_4=4(E_2-E_1)+\frac{4}{3}(D_1+D_2),$$

that is, it seems that the suspension of the intersection between the two fronts is composed by two points. Differently from the preceding sections, here we are interested in finding a solution of the system for values of p_y^0 greater than or equal to $\frac{1}{2}-\frac{3E_1}{2D_1}$.

We proceed as we did before: subtracting the two equations in the system (35) and setting $g_0=1+\eta(p_y^0,\zeta)$ and $\boldsymbol{T}=8\zeta-(4A+\frac{4}{3}C_2+T(p_y^0,\zeta))\zeta^3+\mathcal{O}(\zeta^4)$, we obtain the equation

(36) $$\eta(p_y^0,\zeta)^2(-3C_2+(3D_2+3E_2+2D_2\eta(p_y^0,\zeta))\zeta)+\zeta(1+p_y^0)^2(3E_1+D_1(2p_y^0-1))+\zeta^2R=0,$$

where R is some continuous function of the variables p_y^0,g_0,T and ζ (in particular, uniformly bounded for $g_0,p_y^0\in[-1,1]$, T in some sufficiently small neighbourhood of $-\frac{3}{2}\big(E_1+\frac{D_1}{3}\big)^2+4E_2+\frac{4}{3}D_2$ and ζ small enough).

The polynomial $y^2(-3C_2+(3D_2+3E_2+2D_2y)\zeta)$ has a double root in $y=0$ and a simple root in $y=\frac{3C_2}{2D_2\zeta}-\frac{3}{2}-\frac{3E_2}{2D_2}$. Since the function $\zeta(1+p_y^0)^2(3E_1+D_1(2p_y^0-1))$ is increasing with p_y^0

for $p_y^0 \geq -\frac{E_1}{D_1}$, for every $p_y^0 \in \left[\frac{1}{2} - \frac{3E_1}{2D_1}, 1\right]$ there exists $\bar\zeta > 0$ such that $\zeta(1+p_y^0)^2(3E_1 + D_1(2p_y^0 - 1)) + \zeta^2 R > 0$ for $0 < \zeta < \bar\zeta$ and g_0, T belonging to a small open neighbourhood of the point $\left(1, -\frac{3}{2}\left(E_1 + \frac{D_1}{3}\right)^2 + 4E_2 + \frac{4}{3}D_2\right)$. In particular, for every $p_y^0 \in \left[\frac{1}{2} - \frac{3E_1}{2D_1}, 1\right]$ there exists $\bar\zeta > 0$ such that equation (36) has a solution $\eta(p_y^0, \zeta)$ for every $0 < \zeta < \bar\zeta$. It is easy to find an asymptotic expansion for η; this provides the following asymptotic expansion for g_0 and T:

$$g_0 = 1 - \sqrt{\zeta}\sqrt{\frac{3(D_1 - E_1)^2}{2D_1C_2}}\sqrt{p_y^0 - \frac{1}{2} + \frac{3E_1}{2D_1}} + \mathcal{O}\left(p_y^0 - \frac{1}{2} + \frac{3E_1}{2D_1}, \zeta\right)$$

$$T = -4\sqrt{\zeta}\sqrt{\frac{3}{2}\frac{C_2(D_1 - E_1)^2}{D_1}}\sqrt{p_y^0 - \frac{1}{2} + \frac{3E_1}{2D_1}} + \mathcal{O}\left(p_y^0 - \frac{1}{2} + \frac{3E_1}{2D_1}, \zeta\right)$$

The suspension of the intersection can be recovered by substituting these values into equation (50):

$$x = -4(A + C_2)\zeta^3 + 4\zeta^{7/2}\sqrt{\frac{3}{2}\frac{C_2(D_1 - E_1)^2}{D_1}}\sqrt{p_y^0 - \frac{1}{2} + \frac{3E_1}{2D_1}} + \mathcal{O}(\zeta^4)$$

$$y = 4A\zeta^3 + \mathcal{O}(\zeta^4)$$

Summing up, we can conclude that the geodesics of the set Γ_f with $p_y^0 \in \left[-1, \frac{1}{2} - \frac{3E_1}{2D_1}\right]$ lose their optimality at the self-intersection between $\mathcal{F}_4$ and $\mathcal{F}_5$, and those with $p_y^0 \in \left(\frac{1}{2} - \frac{3E_1}{2D_1}, 1\right]$ lose optimality after their fourth switching time, by intersecting with the (fifth front) of the geodesics of the set Γ_{-g}.

For what concerns the cut locus of the geodesics of the set Γ_{-f}, it depends on the value of $\frac{3E_1}{D_1}$; indeed, if $\frac{3E_1}{D_1} \geq 1$, then all Γ_{-f} geodesics lose their optimality before the fourth switching time; if instead $\frac{3E_1}{D_1} < 1$, then only the geodesics with $p_y^0 \in \left[-1, \frac{1}{2} + \frac{3E_1}{2D_1}\right]$ lose their optimality by intersecting with (the fourth arc of) the geodesics of the set Γ_{-g}, whereas those with $p_y^0 \in \left(\frac{1}{2} + \frac{3E_1}{2D_1}, 1\right]$ lose their optimality after the fourth switching time, by intersecting the geodesics of the set Γ_g, as already seen in Section 6.1.

The remaining part of the cut locus is completely analogous of the one studied in Section 5.2, therefore we do not repeat its description. We can conclude that, if $\frac{3E_1}{D_1} \geq 1$, the cut locus is connected and composed by a single branch, whereas if $\frac{3E_1}{D_1} < 1$, the cut locus is composed by two connected components. In both cases, it is piecewise C^1. The cut locus is shown in Figure 13.

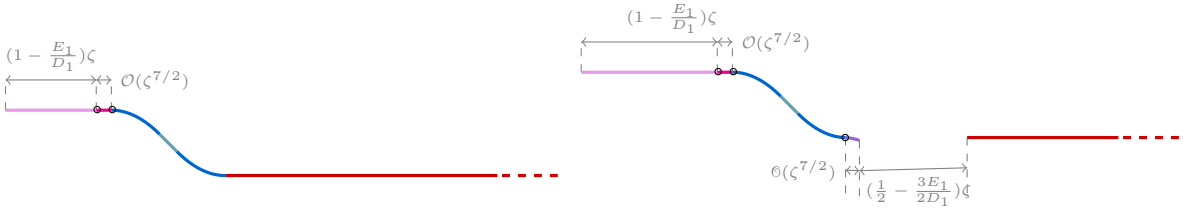

FIGURE 13. Suspension of the cut locus for the case B_+ with $C_2 > 0$ and $A > C_2$. On the left, $\frac{3E_1}{E_1} \geq 1$, on the right $\frac{3E_1}{E_1} < 1$: pink: $\mathcal{F}_4 \cap \mathcal{F}_5$; magenta: $\mathcal{F}_5 \cap \bar{\mathcal{G}}_5$; red: $\bar{\mathcal{F}}_4 \cap \bar{\mathcal{G}}_4$; blue: $\mathcal{G}_4 \cap \bar{\mathcal{G}}_5$ and $\bar{\mathcal{G}}_4 \cap \mathcal{G}_5$; sugarpaper: $\mathcal{G}_4 \cap \bar{\mathcal{G}}_4$; purple $\mathcal{G}_5 \cap \bar{\mathcal{F}}_5$. The circles point out the non-smooth junctions.

$0 < A < C_2$. This case is very similar to the precedent one, with the sole exception that, as already remarked in Section 5.2, the fronts $\mathcal{G}_4$ and $\bar{\mathcal{G}}_4$ do not intersect, while $\mathcal{G}_5$ and $\bar{\mathcal{G}}_5$ do.

Thus, if $\frac{3E_1}{D_1} \geq 1$, the cut locus is made by the concatenation of the following intersections

$$\mathcal{F}_4 \cap \mathcal{F}_5 \quad \mathcal{F}_5 \cap \bar{\mathcal{G}}_5 \quad \mathcal{G}_4 \cap \bar{\mathcal{G}}_5 \quad \mathcal{G}_5 \cap \bar{\mathcal{G}}_5 \quad \bar{\mathcal{G}}_4 \cap \mathcal{G}_5 \quad \bar{\mathcal{F}}_4 \cap \bar{\mathcal{G}}_4$$

and it is piecewise C^1.

If $\frac{3E_1}{D_1} < 1$, the suspension of the cut locus is disconnected; one connected component is made by the concatenation of the intersections

$$\mathcal{F}_4 \cap \mathcal{F}_5 \quad \mathcal{F}_5 \cap \bar{\mathcal{G}}_5 \quad \mathcal{G}_4 \cap \bar{\mathcal{G}}_5 \quad \mathcal{G}_5 \cap \bar{\mathcal{G}}_5 \quad \bar{\mathcal{G}}_4 \cap \mathcal{G}_5 \quad \bar{\mathcal{F}}_f \cap \mathcal{G}_5$$

It is piecewise smooth; the other connected component is the intersection $\bar{\mathcal{F}}_4 \cap \bar{\mathcal{G}}_4$. The two cases are illustrated in Figure 14.

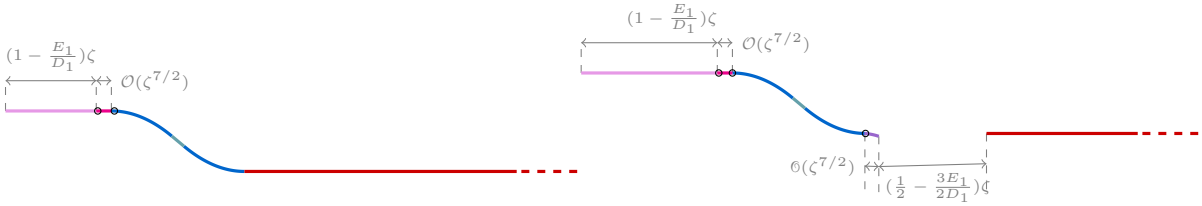

FIGURE 14. Suspension of the cut locus for the case B_+ with $C_2 > 0$ and $A > C_2$. On the left, $\frac{3E_1}{E_1} \geq 1$, on the right $\frac{3E_1}{E_1} < 1$: pink: $\mathcal{F}_4 \cap \mathcal{F}_5$; magenta: $\mathcal{F}_5 \cap \bar{\mathcal{G}}_5$; red: $\bar{\mathcal{F}}_4 \cap \bar{\mathcal{G}}_4$; blue: $\mathcal{G}_4 \cap \bar{\mathcal{G}}_5$ and $\bar{\mathcal{G}}_4 \cap \mathcal{G}_5$; sugarpaper: $\mathcal{G}_4 \cap \bar{\mathcal{G}}_4$; purple $\mathcal{G}_5 \cap \bar{\mathcal{F}}_5$. The circles point out the non-smooth junctions.

$-C_2 < A < 0$. As usual, we first investigate the geodesics of the set Γ_f. As already studied in the preceding sections, those with initial covector $p_y^0 \in [-1, -1 - 8A\zeta^2]$ lose optimality by intersecting the front $\mathcal{G}_5$ (see Appendix A.2-κ)), and those with $p_y^0 \leq \frac{1}{2} - \frac{3E_1}{2D_1}$ lose optimality because of the self intersection between $\mathcal{F}_4$ and $\mathcal{F}_5$. What about the Γ_f geodesics with $p_y^0 \geq \frac{1}{2} - \frac{3E_1}{2D_1}$? First of all, we notice that the point

$$\Big(4(A - C_2)\zeta^3 - (4E_2 + \frac{8}{3}E_1 + \frac{4}{3}\mathcal{d} - \frac{4}{3}D_2)\zeta^4, 4A\zeta^3 - (2D_1q_0^2D_1 + 4E_1q_0 - \frac{2}{3}\mathcal{c})\zeta^4\Big)$$

is the intersection of the geodesic with initial covector $(1, \beta, 1/\widetilde{\rho}_0)$, the one with initial covector $(1, q_0, 1/\rho_0)$ and the one with initial covector $(\gamma, 1, 1/\widehat{\rho}_0)$, with

$$\begin{aligned}
\beta &= -1 - 8A\zeta^2 + \mathcal{O}(\zeta^3) & \widetilde{\rho}_0 &= \zeta - (C_2 + \frac{3}{2}A)\zeta^3 + \mathcal{O}(\zeta^4)\\
q_0 &= \frac{1}{2} - \frac{3E_1}{2D_1} & \rho_0 &= \zeta + \big(\frac{3}{4D_1}A(D_1 - 3E_1) - 8C_2\big)\zeta^3 + \mathcal{O}(\zeta^4)\\
\gamma &= 1 - \frac{\big(3E_1 + D_1\big)^2}{3D_1}\zeta^3 + \mathcal{O}(\zeta^4) & \widehat{\rho}_0 &= \zeta - (C_2 - \frac{3}{2}A)\zeta^3 + \mathcal{O}(\zeta^4).
\end{aligned}$$

The former two belong to the set Γ_f, the latter to the set Γ_g. The intersection time is $\boldsymbol{T} = 8\zeta + \big(4A - \frac{4}{3}C_2\big)\zeta^3$. This suggest us to investigate the intersection between the fronts $\mathcal{F}_5$ and $\mathcal{G}_5$. To do so, as usual, we impose the equality between the jets of the front $\mathcal{F}_5$ (equation (19)) and the jets of the front $\mathcal{G}_5$ (equation (50)), where in the latter we substitute g_0 with the power series $\sum_{k\geq 0}\gamma_k\rho_0^k$. We find that, for the equalities to hold true, it must be

$$\gamma_0 = 1, \qquad \gamma_1 = \gamma_2 = 0, \qquad \gamma_3 = -\frac{4}{3}D_1q_0^3 - 2E_1q_0^2 + 2D_1q_0 - 2E_1 - \frac{2}{3}D_1.$$

In particular, if $q_0 \geq \frac{1}{2} - \frac{3E_1}{2D_1}$, then $\gamma_3 \leq 0$ and $\gamma \leq 1$.

The suspension of the intersection is given by

$$\begin{cases} x = 4(A - C_2)\zeta^3 + \big(\frac{4}{3}(D_2 - \mathcal{c}) - \frac{8}{3}E_1 - 4E_2\big)\zeta^4 \\ y = 4A\zeta^3 - \big(2D_1q_0^2 + 4E_1q_0 - \frac{2}{3}\mathcal{c}\big)\zeta^4 \end{cases} \tag{37}$$

which is a vertical segment, up to fifth order terms in ζ. The intersection time is $\boldsymbol{T} = 8\zeta + \big(4A - \frac{4}{3}C_2\big)\zeta^3 - (2E_1 + \frac{4}{3}D_1q_0^3 + 2E_1q_0^2 + 4E_2 - \frac{4}{3}D_2)\zeta^4 + \mathcal{O}(\zeta^5)$.

Concerning the geodesics of the set Γ_{-f}, we still must distinguish the two cases $\frac{3E_1}{D_1} \geq 1$ and $\frac{3E_1}{D_1} < 1$. In the first one, all geodesics lose optimality before the fourth switching time: those

with $p_y^0 \in [-1, 1+8A\rho_0^2]$ by intersecting $\bar{\mathcal{G}}_4$, the ones with $p_y^0 \in [1+8A\rho_0^2, 1]$ by intersecting $\mathcal{G}_5$ (see Appendix A.2-β)). If $\frac{3E_1}{D_1} < 1$, then the geodesics with $p_y^0 \leq \frac{1}{2} + \frac{3E_1}{2D_1}$ lose optimality before the fourth switching time, intersecting $\bar{\mathcal{G}}_4$; for $p_y^0 \in \left[\frac{1}{2} + \frac{3E_1}{2D_1}, 1 + 8A\rho_0^2\right]$, they lose optimality after the fourth switching time, intersecting the fifth arc of some Γ_{-g} geodesic. The suspension of this intersection can be recovered by applying a suitable transformation and permutation of the invariants to (37), and gives

$$\begin{cases} x = -4(A - C_2)\zeta^3 + \left(\frac{4}{3}(D_2 + \mathscr{c}) - \frac{8}{3}E_1 - 4E_2\right)\zeta^4 \\ y = -4A\zeta^3 - \left(2D_1(p_y^0)^2 - 4E_1 p_y^0 + \frac{2}{3}\mathscr{c}\right)\zeta^4 \end{cases}$$

The rest of the cut locus is, as in the case A_+, $-C_2 < A < 0$, given by the intersection of $\mathcal{G}_4 \cap \bar{\mathcal{G}}_4$.

Summing up, if $\frac{3E_1}{D_1} \geq 1$, the suspension of the cut locus is connected and given by three C^1 branches; if $\frac{3E_1}{D_1} < 1$, the cut locus is composed by two connected components. The two cases are depicted in Figure 15.

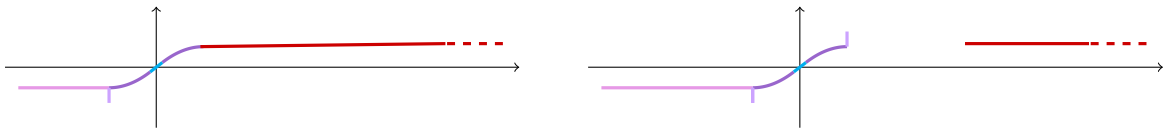

FIGURE 15. Cut locus for the case B_+ with $-C_1 < A < 0$. On the left, $\frac{3E_1}{D_1} \geq 1$, on the right $\frac{3E_1}{D_1} < 1$: rose: $\mathcal{F}_4 \cap \mathcal{F}_5$; purple: $\mathcal{F}_4 \cap \mathcal{G}_5$ and $\bar{\mathcal{F}}_4 \cap \bar{\mathcal{G}}_5$; lilac $\bar{\mathcal{F}}_5 \cap \mathcal{G}_5$ and $\bar{\mathcal{F}}_5 \cap \bar{\mathcal{G}}_5$; red: $\bar{\mathcal{F}}_4 \cap \bar{\mathcal{G}}_4$; cyan: $\mathcal{G}_5 \cap \bar{\mathcal{G}}_5$.

$A < -C_2 < 0$. This last case can be deduced by gathering the arguments used to study the precedent ones. In particular, the only difference with the case just analysed ($-C_2 < A < 0$) involves the "central part" of the (suspension of the) cut locus, which is made by the concatenation of the intersections $\mathcal{F}_4 \cap \mathcal{G}_5$, $\mathcal{F}_4 \cap \bar{\mathcal{F}}_4$ and $\bar{\mathcal{F}}_4 \cap \bar{\mathcal{G}}_5$. More precisely:

- the Γ_f geodesics with $p_y^0 \in [-1, -1 - 8(A + C_2)\zeta^2]$ lose optimality by intersection with the fourth bang arc $\bar{\mathcal{F}}_4$; those with $p_y^0 \in [-1 - 8(A + C_2)\zeta^2, -1 - 8A\zeta^2]$, by intersection with the fifth bang arc $\mathcal{G}_5$; for $p_y^0 \in \left[-1 - 8A\zeta^2, \frac{1}{2} - \frac{3E_1}{2D_1}\right]$, because of the self intersection between $\mathcal{F}_4$ and $\mathcal{F}_5$; finally, those with $p_y^0 \in \left[\frac{1}{2} - \frac{3E_1}{2D_1}, 1\right]$ lose optimality after the fourth switching time, by intersection with $\mathcal{G}_5$, as described above.
- analogously, the Γ_{-f} geodesics with $p_y^0 \in [1+8(A+C_2)\zeta^2, 1]$ lose optimality by intersection with the fourth bang arc $\mathcal{F}_4$, and those with $p_y^0 \in [1+8A\zeta^2, 1+8(A+C_2)\zeta^2]$ by intersection with the fifth bang arc $\bar{\mathcal{G}}_5$. For $p_y^0 \leq 1 + 8A\zeta^2$, we must distinguish the cases: if $\frac{3E_1}{D_1} \geq 1$, then all geodesics lose optimality by intersecting $\bar{\mathcal{G}}_4$, whereas, if $\frac{3E_1}{D_1} < 1$, only the geodesics with $p_y^0 \leq \frac{1}{2} + \frac{3E_1}{2D_1}$ lose optimality in this way; those with $p_y^0 \in \left[\frac{1}{2} + \frac{3E_1}{2D_1}, 1 + 8A\zeta^2\right]$ lose optimality after the fifth bang arc, by intersecting $\bar{\mathcal{G}}_5$ (see equation 6.2).

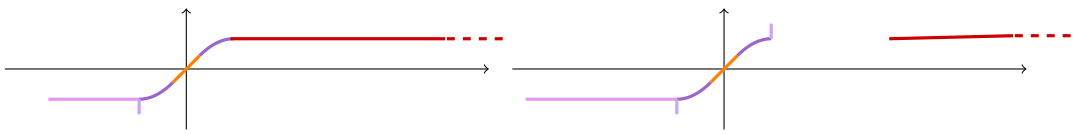

FIGURE 16. Cut locus for the case B_+ with $-C_1 < A < 0$. On the left, $\frac{3E_1}{D_1} \geq 1$, on the right $\frac{3E_1}{D_1} < 1$: rose: $\mathcal{F}_4 \cap \mathcal{F}_5$; purple: $\mathcal{F}_4 \cap \mathcal{G}_5$ and $\bar{\mathcal{F}}_4 \cap \bar{\mathcal{G}}_5$; lilac $\bar{\mathcal{F}}_5 \cap \mathcal{G}_5$ and $\bar{\mathcal{F}}_5 \cap \bar{\mathcal{G}}_5$; red: $\bar{\mathcal{F}}_4 \cap \bar{\mathcal{G}}_4$; orange: $\mathcal{F}_4 \cap \bar{\mathcal{F}}_4$.

7. $-D_1 < E_1 < 0$ (CASE $\boldsymbol{B_-}$)

At last, we consider the case in which $D_1 > -E_1 > 0$. As already remarked at the beginning of Section 6, the cut time of the geodesics of the set Γ_f with $p_y^0 \leq -\frac{E_1}{D_1}$ must be less than or equal to the fourth switching time, which actually is the conjugate time. The same happens for the geodesics of the set Γ_{-f} with $p_y^0 \geq \frac{E_1}{D_1}$.

A coarse analysis reveals that the major differences between the case B_- and the case B_+ involve the geodesics of the set Γ_f, as, if $\frac{3E_1}{D_1} < -1$, then a part of the front $\mathcal{F}_4$ intersects the front $\mathcal{G}_4$. Assume indeed that $\frac{3E_1}{D_1} < -1$, and consider the self intersection of the front of the geodesics of the set Γ_f (equation (21)); from the fact that $\gamma_0 \leq \eta_0$, we see that γ_0 must be greater than or equal to $-\frac{3E_1}{D_1} - 2$ (which is strictly greater than -1): the geodesics with initial covector $p_y^0 \leq -\frac{3E_1}{D_1} - 2$ are not involved in the self intersection. On the other hand, (41) states that the intersection between the fourth bang fronts of Γ_f and Γ_g trajectories may occur only if $\gamma_0 \leq -\frac{3E_1}{D_1} - 2$. From equation (22), we see that the intersection $\mathcal{F}_4 \cap \mathcal{F}_5$ is, approximately, a horizontal segment joining the points $\big((\frac{E_1}{D_1} - 1)\zeta, 4A\zeta^3\big)$ and $\big((\frac{3E_1}{D_1} + 1)\zeta, 4A\zeta^3\big)$, while the intersection $\mathcal{F}_4 \cap \mathcal{G}_4$ is a horizontal segment joining the points $\big((\frac{3E_1}{D_1} + 1)\zeta, 4A\zeta^3\big)$ and $\big(-4(A+C_2)\zeta^3, 4A\zeta^3\big)$. This suggests to consider only the fourth bang arc front of Γ_f trajectories when studying the cut locus close to the origin of the plane $\{z = 4\zeta^2\}$.

In instead $\frac{3E_1}{D_1} \geq -1$, then the behaviour of Γ_f trajectories is not much different from the one described in Section 6.

The other difference with the precedent cases is that $\frac{3E_1}{2D_1} + \frac{1}{2} < 1$, which implies that the intersection between a Γ_{-f} geodesics (of initial covector $(-1, p_y^0, 1/\rho_0)$) with a Γ_{-g} one is possible only if $p_y^0 \in \big[-1, \frac{3E_1}{2D_1} + \frac{1}{2}\big]$; as already seen in Section 6, the suspension of this intersection is, up to higher order terms in ζ, a segment of length $\frac{3}{2}(1 + \frac{E_1}{D_1})\zeta$ and constitutes a connected component of the cut locus. Then, in the case B_- the suspension of the cut locus is always disconnected.

A detailed analysis of the cut locus in the 12 different sub-cases of the case B_- is not necessary, as it can easily be deduced from the preceding cases. For the sake of completeness, we just give, here below, a brief description.

7.1. $C_2 < 0$.

$A > 0$. As already anticipated at the beginning of the section, if $\frac{3E_1}{D_1} \geq -1$ the cut locus is very similar to the one shown in Figure 10 (right). Indeed, all geodesics of the set Γ_f with initial covector $p_y^0 \in [-1, -\frac{3E_1}{2D_1} + \frac{1}{2}]$ lose optimality because of the self-intersection $\mathcal{F}_4 \cap \mathcal{F}_5$, as already seen before; those with $p_y^0 \in [-\frac{3E_1}{2D_1} + \frac{1}{2}, 1]$ intersect the fourth bang arc of Γ_{-g} geodesics (see A.2-θ)). The suspension of the cut locus in this case is shown in Figure 17 (left).

The geodesics of the set Γ_{-f} whose second component of the initial covector belongs to the interval $[-1, \frac{3E_1}{2D_1} + \frac{1}{2}]$ lose optimality when they intersect the fourth bang front $\bar{\mathcal{G}}_4$ (equation (43)); the suspension of this intersection is, up to higher order terms in ζ, a segment of length $\frac{3}{2}(1 + \frac{E_1}{D_1})\zeta$ and constitute one connected component of the cut locus. On the other hand, the Γ_{-f} geodesics with $p_y^0 \geq \frac{3E_1}{2D_1} + \frac{1}{2}$ lose optimality after the fourth switching time, by intersecting the front $\mathcal{G}_4$.

Finally, the geodesics of the sets $\Gamma_{\pm g}$ lose optimality during their fourth bang arc. The cut locus is shown in Figure 17 (left).

As already remarked, when $\frac{3E_1}{D_1} < -1$ only the Γ_f geodesics with initial covector $p_y^0 \in [-\frac{3E_1}{D_1} - 2, 1]$ are involved in the self-intersection $\mathcal{F}_4 \cap \mathcal{F}_5$; those with $p_y^0 \in [-1 + 8A\rho_0^2, -\frac{3E_1}{D_1} - 2]$ lose optimality when intersecting the front $\mathcal{G}_4$. The cut locus is depicted in Figure 17 (right).

$A < 0$. As when $\frac{3E_1}{D_1} \geq -1$ the cut locus is almost identical to the one shown in Figure 12, we describe in details only the case in which $\frac{3E_1}{D_1} < -1$. Nevertheless, both cases are illustrated in Figure 18. Consider a geodesic of the set Γ_f; we have that

- if $p_y^0 \in \big[-\frac{3E_1}{2D_1} + \frac{1}{2}, 1\big]$, then the geodesic loses optimality during its fifth bang arc, by intersection with the front $\bar{\mathcal{F}}_4$ (see Appendix A.2-ε));

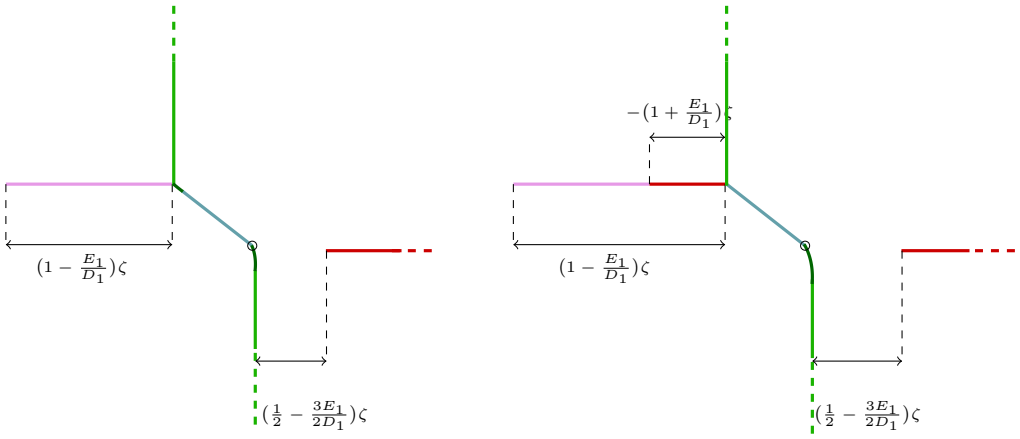

FIGURE 17. Cut locus for the case B_- with $C_2 < 0$ and $A > 0$. On the left, $-\frac{3E_1}{D_1} \leq 1$, on the right, $-\frac{3E_1}{D_1} > 1$: pink: $\mathcal{F}_4 \cap \mathcal{G}_4$; red: $\bar{\mathcal{F}}_4 \cap \bar{\mathcal{G}}_4$ and $\mathcal{F}_4 \cap \mathcal{G}_4$; green: $\mathcal{G}_4 \cap \bar{\mathcal{F}}_4$ and $\bar{\mathcal{G}}_4 \cap \mathcal{F}_4$; sugarpaper: $\mathcal{G}_4 \cap \bar{\mathcal{G}}_4$; dark green: $\mathcal{F}_5 \cap \bar{\mathcal{G}}_4$ and $\bar{\mathcal{F}}_5 \cap \mathcal{G}_4$. The circles denote the points where the junction between two intersections is not C^1.

– if $p_y^0 \in \big(-1, \frac{3E_1}{2D_1} + \frac{1}{2}\big]$, the geodesics loses optimality because of the self intersection of the fronts $\mathcal{F}_4$ and $\mathcal{F}_5$.

For what concerns the geodesics of the set Γ_{-f}, they lose optimality in the following way, according to the value of the initial covector:

– if $p_y^0 \in \big[-1, \frac{3E_1}{2D_1} + \frac{1}{2}\big]$, during their fifth bang arc, by intersection with the front $\bar{\mathcal{G}}_4$;
– for $p_y^0 \in \big[\frac{3E_1}{2D_1} + \frac{1}{2}, 1 + 4(2A + C_2)\zeta^2\big]$, during their fifth arc, by intersection with the front $\mathcal{F}_4$;
– for $p_y^0 \geq 1 + 4(2A + C_2)\zeta^2$, again by intersection with the front $\mathcal{F}_4$, but before their fourth switching time.

The geodesics belonging to the sets $\Gamma_{\pm g}$ lose optimality during their fourth bang arc, as shown in Figure 18 (right).

7.2. $C_2 > 0$.
$A > C_2$. If $\frac{3E_1}{D_1} \geq -1$ the cut locus is very similar to the one shown in Figure 13 (right), and is given by the concatenation of the following intersections

$$\mathcal{F}_4 \cap \mathcal{F}_5, \quad \mathcal{F}_5 \cap \bar{\mathcal{G}}_5, \quad \mathcal{G}_4 \cap \bar{\mathcal{G}}_5, \quad \mathcal{G}_4 \cap \bar{\mathcal{G}}_4, \quad \bar{\mathcal{G}}_4 \cap \bar{\mathcal{G}}_5, \quad \bar{\mathcal{F}}_5 \cap \mathcal{G}_5$$

plus the connected component $\bar{\mathcal{F}}_4 \cap \bar{\mathcal{G}}_4$.

On the other hand, if $\frac{3E_1}{D_1} < -1$, then the geodesics of the set Γ_f may eventually intersect those of the set Γ_{-g} only after their conjugate time; in particular, those with initial covector $p_y^0 \in [-\frac{3E_1}{D_1} - 2, 1]$ lose their optimality at the self intersection $\mathcal{F}_4 \cap \mathcal{F}_5$, while those with $p_y^0 \in [-1, -\frac{3E_1}{D_1} - 2]$ lose optimality when intersecting the front $\mathcal{G}_4$. The cut locus is thus given by the concatenation

$$\mathcal{F}_4 \cap \bar{\mathcal{F}}_5, \quad \mathcal{F}_4 \cap \mathcal{G}_4, \quad \mathcal{G}_4 \cap \bar{\mathcal{G}}_5, \quad \mathcal{G}_4 \cap \bar{\mathcal{G}}_4, \quad \bar{\mathcal{G}}_4 \cap \mathcal{G}_5, \quad \bar{\mathcal{F}}_5 \cap \mathcal{G}_5,$$

plus the connected component $\bar{\mathcal{F}}_4 \cap \bar{\mathcal{G}}_4$.

The cut locus (for $\frac{3E_1}{D_1} < -1$) is shown in Figure 19 (left).
$0 < A < C_2$. The only difference between this case and the precedent one is that the intersection $\mathcal{G}_4 \cap \bar{\mathcal{G}}_4$ does not participate to the cut locus, and that the intersection of the fronts $\mathcal{G}_4$ and $\bar{\mathcal{G}}_5$ is optimal only if the initial momentum of the Γ_g geodesic involved satisfies $p_x^0 \leq \frac{2A}{C_2} - 1$ (see for instance page 31).

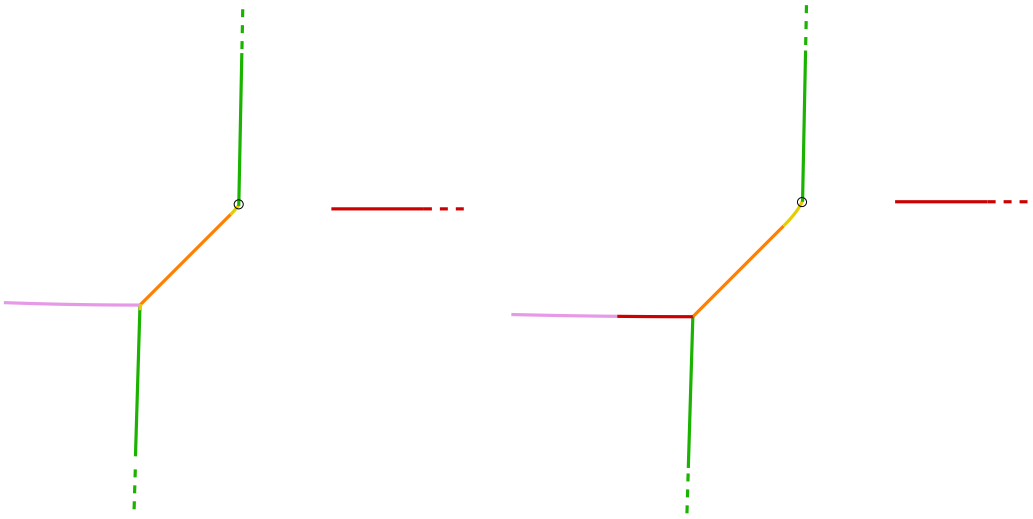

FIGURE 18. Cut locus for the case B_- with $C_2 < 0$ and $A < 0$. On the left, $-\frac{3E_1}{E_1} \leq 1$, on the right, $-\frac{3E_1}{D_1} > 1$; red: $\mathcal{F}_4 \cap \mathcal{G}_4$ and $\bar{\mathcal{F}}_4 \cap \bar{\mathcal{G}}_4$; pink: $\mathcal{F}_4 \cap \mathcal{F}_5$; green: $\mathcal{G}_4 \cap \bar{\mathcal{F}}_4$ and $\bar{\mathcal{G}}_4 \cap \mathcal{F}_4$; orange: $\mathcal{F}_4 \cap \bar{\mathcal{F}}_4$; yellow: $\mathcal{F}_4 \cap \bar{\mathcal{F}}_5$. The circles denote the points where the junction between two intersections is not C^1.

Then, if $\frac{3E_1}{D_1} \geq -1$, the suspension of the cut locus is analogous to the one shown in Figure 15 (right), and given by the concatenation of the intersections

$$\mathcal{F}_4 \cap \mathcal{F}_5, \quad \mathcal{F}_5 \cap \bar{\mathcal{G}}_5, \quad \mathcal{G}_4 \cap \bar{\mathcal{G}}_5, \quad \mathcal{G}_5 \cap \bar{\mathcal{G}}_5, \quad \bar{\mathcal{G}}_4 \cap \mathcal{G}_5, \qquad \mathcal{G}_5 \cap \bar{\mathcal{F}}_5$$

plus the connected component $\bar{\mathcal{F}}_4 \cap \bar{\mathcal{G}}_4$.

If $\frac{3E_1}{D_1} < -1$, the geodesics of the set Γ_f with initial momentum $p_y^0 \in [-\frac{3E_1}{D_1} - 2, 1]$ lose their optimality at the self intersection $\mathcal{F}_4 \cap \mathcal{F}_5$, while those with $p_y^0 \in [-1, -\frac{3E_1}{D_1} - 2]$ lose optimality when intersecting the front $\mathcal{G}_4$. The cut locus is thus given by the concatenation

$$\mathcal{F}_4 \cap \mathcal{F}_5, \quad \mathcal{F}_4 \cap \mathcal{G}_4, \quad \mathcal{G}_4 \cap \bar{\mathcal{G}}_5, \quad \mathcal{G}_5 \cap \bar{\mathcal{G}}_5, \quad \bar{\mathcal{G}}_4 \cap \mathcal{G}_5, \quad \bar{\mathcal{F}}_5 \cap \mathcal{G}_5,$$

and the connected component $\bar{\mathcal{F}}_4 \cap \bar{\mathcal{G}}_4$. This last case is shown in Figure 19 (right).

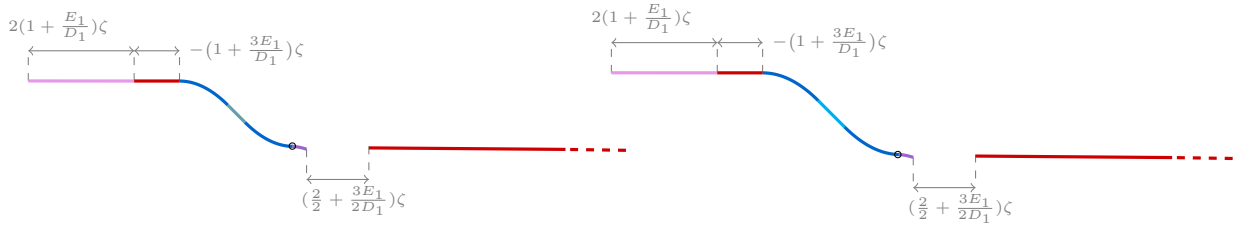

FIGURE 19. Cut locus for the case B_- with $C_2 > 0$, $A > 0$ and $\frac{3E_1}{E_1} < -1$. On the left, $A > C_2$, on the right $A < C_2$: pink: $\mathcal{F}_4 \cap \mathcal{F}_5$; purple: $\bar{\mathcal{F}}_5 \cap \mathcal{G}_5$; red: $\mathcal{F}_4 \cap \mathcal{G}_4$ and $\bar{\mathcal{F}}_4 \cap \bar{\mathcal{G}}_4$; blue: $\mathcal{G}_4 \cap \bar{\mathcal{G}}_5$ and $\bar{\mathcal{G}}_4 \cap \mathcal{G}_5$; sugarpaper: $\mathcal{G}_4 \cap \bar{\mathcal{G}}_4$; cyan: $\mathcal{G}_5 \cap \bar{\mathcal{G}}_5$. The circles show the points where the junction is not C^1.

$-C_2 < A < 0$. If $\frac{3E_1}{D_1} \geq -1$ the suspension of the cut locus is disconnected and completely analogous to the one depicted in Figure 15 (right): one connected component is made by the intersection of the geodesics of the set Γ_{-f} with initial momentum $p_y^0 \in \left[-1, -\frac{1}{2} - \frac{3E_1}{2D_1}\right]$ with the front $\bar{\mathcal{G}}_4$; the other connected component is made by 3 branches, meeting at the point $(4(A -$

$C_2)\zeta^3, 4A\zeta^3)$: the self intersection $\mathcal{F}_4 \cap \mathcal{F}_5$, the intersection $\mathcal{F}_5 \cap \mathcal{G}_5$ and the concatenation of the intersections

$$\mathcal{F}_4 \cap \mathcal{G}_5, \quad \mathcal{G}_5 \cap \bar{\mathcal{G}}_5, \quad \bar{\mathcal{F}}_5 \cap \bar{\mathcal{G}}_5.$$

If $\frac{3E_1}{D_1} < -1$, as seen above, then the self intersection $\mathcal{F}_4 \cap \mathcal{F}_5$ involves only the geodesics with initial momentum $p_y^0 \in \left[-\frac{3E_1}{D_1} - 2, 1\right]$; moreover, the intersection between the fifth front of the geodesics of the sets Γ_f and Γ_g does not occur. The cut locus is thus made by two connected components: one is the intersection $\bar{\mathcal{F}}_4 \cap \bar{\mathcal{G}}_4$; the other one, the concatenation of the intersections

$$\mathcal{F}_4 \cap \bar{\mathcal{F}}_5, \quad \mathcal{F}_4 \cap \mathcal{G}_4, \quad \mathcal{F}_4 \cap \mathcal{G}_5, \quad \mathcal{G}_5 \cap \bar{\mathcal{G}}_5, \quad \bar{\mathcal{F}}_4 \cap \bar{\mathcal{G}}_5 \quad \bar{\mathcal{F}}_5 \cap \bar{\mathcal{G}}_5.$$

This last case is shown in Figure 20 (left).
$-A < -C_2 < 0$. If $\frac{3E_1}{D_1} \geq -1$ the cut locus is completely analogous to the one depicted in Figure 16 (right).

If instead $\frac{3E_1}{D_1} < -1$, then the cut locus is thus made by two connected components: the intersection $\bar{\mathcal{F}}_4 \cap \bar{\mathcal{G}}_4$ and the concatenation of the intersections

$$\mathcal{F}_4 \cap \bar{\mathcal{F}}_5, \quad \mathcal{F}_4 \cap \mathcal{G}_4, \quad \mathcal{F}_4 \cap \mathcal{G}_5, \quad \mathcal{F}_4 \cap \bar{\mathcal{F}}_4, \quad \bar{\mathcal{F}}_4 \cap \bar{\mathcal{G}}_5 \quad \bar{\mathcal{F}}_5 \cap \bar{\mathcal{G}}_5.$$

This last case is illustrated in Figure 20 (right).

FIGURE 20. Cut locus for the case B_- with $C_2 > 0$, $A < 0$ and $\frac{3E_1}{D_1} < -1$. On the left, $-C_2 < A$, on the right $A < -C_2$; rose: $\mathcal{F}_4 \cap \mathcal{F}_5$; red: $\mathcal{F}_4 \cap \mathcal{G}_4$ and $\bar{\mathcal{F}}_4 \cap \bar{\mathcal{G}}_4$ purple: $\mathcal{F}_4 \cap \mathcal{G}_5$ and $\bar{\mathcal{F}}_4 \cap \bar{\mathcal{G}}_5$; lilac $\bar{\mathcal{F}}_5 \cap \bar{\mathcal{G}}_5$; orange: $\mathcal{F}_4 \cap \bar{\mathcal{F}}_4$.

8. Open Problems and final remarks

In this paper, all results hold true for the jets of the geodesics with respect to the small parameter ρ_0, up to the fourth order for the coordinates x, y and the fifth order for the coordinate z. Once the cut locus for the jets of the dynamics has been described, the natural question to be answered concerns the shape of the cut locus for the original system. As already observed in [7] for the generic case (in which $C_1 \neq 0$), all cut points of geodesics with initial covector (p_x^0, p_y^0, p_z^0) with $|p_x^0| \neq |p_y^0|$ correspond to transversal self-intersections of the wavefront (in the case of the cut locus) or to switching locus that are transversal to the wavefronts (for the conjugate locus), and are therefore stable. In the case considered in the present paper, this fact is still true for all geodesics with $|p_x^0| \neq |p_y^0|$ and for those with $|p_x^0| = 1$ and $p_y^0 \neq -\frac{E_1}{D_1}$: for these values of the adjoint vector, indeed, the front of the jet of the dynamics has a cusp.

Therefore, the cut loci computed above represent a good approximation for the cut loci of the true dynamics, except for the extremals with those particular value of the initial covector. To understand what happens in these cases, a stability analysis is in order. The question is particularly tricky, as the class in which study the stability of these singularities is not completely clear, as it is, for instance, for the caustics in sub-Riemannian geometry, which are stable in the class of Lagrangian maps (see [2, 12, 22]).

Another open problem concerns the study of the cut points of geodesics with final point (x_1, y_1, z_1) satisfying $|z_1| \leq \frac{x_1 y_1}{2}$. We recall that, for the Heisenberg system, such points are reached in optimal time $|x_1| + |y_1|$ by means of a trajectory with at most two bang arc and/or by a singular trajectory; the "lower part" of the unit sphere is thus made by the surface $\{(x, y, z) : |x| + |y| = 1 \text{ and } z \leq |xy|/2\}$.

To study the "lower part" of the sphere in the generic case, some remarks are in order. First of all, we notice that, under some generic assumptions, there is no singular extremal; indeed, singular extremals are characterised by the constraint $|F(\boldsymbol{\lambda}(t))| \equiv |G(\boldsymbol{\lambda}(t))| \equiv 0$ along the whole singular

interval. In particular, this implies that $\Theta(\lambda(t)) \equiv 0$ and that all time derivatives of Θ along the extremal are null on the interval, i.e.

$$\langle \boldsymbol{\lambda}(t), \mathrm{ad}^k_{u_1 f + u_2 g}[f,g](\boldsymbol{\xi}(t))\rangle = 0 \ \forall t \in I, \ \forall k \geq 0. \tag{38}$$

In particular, (38) gives a list of orthogonality constraints that the singular extremal and its associated control must satisfy; for a generic pair of vectors f, g, these constraints have maximal rank and thus impose that the covector is null, which is prohibited by PMP.

On the other hand, differently from the nilpotent case, the sign of Θ is allowed to change along an extremal, which could lead to controls switching several times between two particular controls sharing the same side of Q (see [7]). In order to have such a behaviour in short times, we must have $\Theta(\boldsymbol{\lambda}(0)) \ll 1$. Indeed, if $\Theta(\boldsymbol{\lambda}(0)) \sim 1$, then Θ cannot change sign in small time, because $\dot{\Theta}$ is bounded (and close to 0 at the initial time). This in particular shows that bang-bang extremals with several switches in small times may have only two behaviours: either the control switch from vertex to vertex of Q always in the same sense (that corresponds to Θ of constant sign along the extremal, and to the situation we analysed throughout the paper), or it switches several times between two vertices of Q sharing the same side (which correspond to the fact that both $|F|$ and $|G|$ stay close to 1).

A preliminary analysis (carried on for geodesics with three bang arcs) shows that the behaviour of such geodesics is dominated by the value of the invariants $\mathrm{ax}_{ij}, \mathrm{ay}_{ij}$ with $i, j = 1, 2$, and their combinations, and that the invariants A, C_1, C_2, D_1 and E_1 are not involved. It thus seems that the behaviour of the upper part and the lower one of the cut locus are not related (that is, we could have almost every possible combination). The question is surely interesting and will be the subject of future analyses of the authors'.

Appendix A. Some useful computations

A.1. **General scheme of computation of the suspensions.** In this section we give some more details on the method used to compute the suspensions of the fronts, that is, the analytic expression of sets of the form $\mathrm{Exp}(\boldsymbol{p}, \boldsymbol{T}) \cap \{z = 4\zeta^2\}$, for some fixed parameters $\boldsymbol{T}, \zeta$ and $\boldsymbol{p}$ belonging to some suitable domain in $\mathbb{R}^3$. In particular, we are detailing the computation of the fifth bang front of trajectories of the set Γ_f (that is, we fix $\boldsymbol{p} = (1, p_y^0, p_z^0)$ with $p_y^0 \in [-1, 1)$ such that $\mathbb{T}_4(p_y^0, p_z^0) \leq \boldsymbol{T}$, $\mathbb{T}_4$ denoting the fourth switching time of the geodesic with initial momentum $(1, p_y^0, p_z^0)$).

Fix a small positive parameter ζ and some time $\boldsymbol{T} = \sum_{k\geq 1} T_k \zeta^k$. Thanks to equation (14), the reparametrised time $\tau(\boldsymbol{T})$ along the geodesic with initial momentum $(1, p_y^0, p_z^0)$ satisfies

$$\boldsymbol{T} = \rho_0 \tau + \int_0^\tau \rho_4(\tau)\rho_0^4 + \rho_5(\tau)\rho_0^5 \, d\tau + \mathcal{O}(\rho_0^6), \tag{39}$$

where $\rho_0 = 1/p_z^0$. We develop τ as $\tau = \mathscr{T}_4 + \sum_{k\geq 0} \delta_k \rho_0^k$, $\mathscr{T}_4$ denoting the (reparametrised) fourth switching time of the considered geodesic, and the coefficient δ_k being smooth functions of p_y^0 and ρ_0; to find them, we develop ρ_0 is powers of ζ as follows

$$\rho_0 = \zeta + r_2\zeta^2 + r_3\zeta^3 + \cdots, \tag{40}$$

then we solve equation (39) at every order in ζ. This provides the expressions for δ_k as functions of the switching times $\mathscr{T}_k$ (that is, of p_y^0) and the coefficients $T_2, T_3, r_2, r_3, \ldots$.

Afterwards, we compute $z(\tau)$, where we substitute ρ_0 with its development (40), and we set $z(\tau) = 4\zeta^2 + \mathcal{O}(\zeta^7)$. Solving this equation at every order in ζ, we obtain the expression of r_k, $k \geq 2$.

The suspension of the front is thus obtained by computing $x(\tau)$ and $y(\tau)$, where ρ_0 is written as a polynomial in ζ, with the coefficients r_k just computed.

A.2. **Intersections between regular bang-bang geodesics with different initial control.** In this Section, we just provide the existence conditions, the intersection times and the expression of the suspensions on the plane $\{z = 4\zeta^2\}$ of the intersections between bang-bang geodesics.

These results are obtained following the same procedure described for the intersection between a fourth bang arc of a Γ_f geodesics with the fourth bang arc of a Γ_g geodesic (page 20).

α) $\bar{\mathcal{F}}_4 \cap \bar{\mathcal{G}}_4$ may be easily recovered from the computation at page 20, by applying suitably Lemmas 1-2. In particular, we deduce that such intersections may occur only if $C_1 \leq 0$ and, if $C_1 = 0$, if

$$E_1 + \frac{2 - p_y^0}{3} D_1 \geq 0 \tag{41}$$

$$E_1 + \frac{1 - 2p_y^0}{3} D_1 \geq 0, \tag{42}$$

where p_y^0 is the second component of the initial momentum of the trajectory with initial velocity equal to $-f$. The intersection occurs at (reparametrised) time $\mathcal{T}$ such that

$$\mathscr{T}_4 - \mathcal{T} = -2(1 + p_y^0)C_1\rho_0^2 - 2(1 + p_y^0)\Big(E_1 + \frac{1 - 2p_y^0}{3} D_1\Big)\rho_0^3 \mathcal{O}(\rho_0^4),$$

and the suspension of the intersection at $z = 4\zeta^2$ is given by

$$\begin{cases} x = (1 - p_y^0)\zeta - \big((1 - 12p_y^0 - 5(p_y^0)^2)\frac{A}{4} - (p_y^0 + 3)C_2\big)\zeta^3 + \mathcal{O}(\zeta^4) \\ y = -4A\zeta^3 + \big(\frac{2}{3}D_1(p_y^0)^2 - 2(E_1 + \frac{D_1}{3})p_y^0 + \boldsymbol{c}\big)\zeta^4 + \mathcal{O}(\zeta^5). \end{cases} \tag{43}$$

β) $\mathcal{G}_4 \cap \bar{\mathcal{F}}_4$ This case can be obtained from the precedent one, by a rotation of $\pi/2$ around the $z-$axis and a suitable permutation of the invariants. We consider a Γ_g geodesic with initial covector $(p_x^0, 1, 1/\rho_0)$, and a Γ_{-f} geodesic with initial covector $(-1, \beta, 1/\widetilde{\rho}_0)$, where β and $\widetilde{\rho}_0$ are power series in ρ_0. Fix $\boldsymbol{T} = (7 + p_x^0)\rho_0 + \mathcal{O}(\rho_0^2)$ and look at the intersection of the two geodesics at time $\boldsymbol{T}$. As we find

$$\beta = 1 + 2(p_x^0 + 1)C_2\rho_0^2 + \mathcal{O}(\rho_0^3),$$

this intersection occurs only if $C_2 \leq 0$. The intersection occurs at (reparametrised) time $\mathcal{T} = \mathscr{T}_4 + 2(1 - p_x^0)C_2\rho_0^2 + \mathcal{O}(\rho_0^3)$.

γ) $\mathcal{F}_4 \cap \bar{\mathcal{F}}_4$ In general, the intersection among geodesics with opposite initial velocity occur only close to the the vertical axis, that is, at a time $\boldsymbol{T} \sim 8/p_z(0)$; since we are considering fourth arcs, this means that the second component of the initial momentum must be close to ± 1. We then set $p_y^0 = -1 + \sum_{k\geq 1} \mu_k \rho_0^k$ for the trajectory of the set Γ_f, $p_y^0 = 1 + \sum_{k\geq 1} \beta_k \rho_0^k$ for the trajectory of the set Γ_{-f}. Equating the jets as usual, we find that the intersection occurs if $\beta_1 = \mu_1 = 0$ and $\mu_2 - \beta_2 = -8(A + C_2)$, which is admissible only if $A + C_2 \leq 0$.

The intersection occurs at (reparametrised) time

$$\mathcal{T} = \mathscr{T}_4 + \big(4C_2 + 8A + \mu_2\big)\rho_0^2$$

where $\mathscr{T}_4$ is the (reparametrised) fourth switching time of the first trajectory. As this makes sense only if $\mathcal{T} \leq \mathscr{T}_4$, this imposes $\mu_2 \leq 4(C_2 + 2A)$. The suspension of the intersection is given by

$$\begin{cases} x = -(4A + 4C_2 + \mu_2)\zeta^3 + \mathcal{O}(\zeta^4) \\ y = -(4A + 4C_2 + \mu_2)\zeta^3 + \mathcal{O}(\zeta^4). \end{cases}$$

δ) $\mathcal{G}_4 \cap \bar{\mathcal{G}}_4$ Repeating the same procedure as above, this intersection occurs only if $A \geq 0$, and the suspension of the intersection is given by

$$\begin{cases} x = -(4A - \gamma_2)\zeta^3 + \mathcal{O}(\zeta^4) \\ y = (4A - \gamma_2)\zeta^3 + \mathcal{O}(\zeta^4), \end{cases} \tag{44}$$

where the initial momentum of the Γ_{-g} trajectory is $(p_x^0, -1, \rho_0)$, with $p_x^0 = -1 + \gamma_2\rho_0^2 + \mathcal{O}(\rho_0^3)$. The intersection occurs at (reparametrised) time

$$\mathcal{T} = \mathscr{T}_4 + \big(4C_2 - 8A - \gamma_2\big)\rho_0^2.$$

ε) $\bar{\mathcal{F}}_5 \cap \mathcal{F}_4$ For ρ_0 and $\boldsymbol{T}$ fixed, we consider a trajectory of the set Γ_{-f} with initial covector $(-1, p_y^0, 1/\rho_0)$ and a trajectory of the set Γ_f with initial covector $(1, \beta, 1/\widetilde{\rho}_0)$, with $\beta = \sum_{k\geq 0} \beta_k \rho_0^k$ and $\widetilde{\rho}_0 = \rho_0 + \sum_{k\geq 2} \alpha_k \rho_0^k$. We assume that $\boldsymbol{T}$ is greater than the fourth switching time of the first geodesics, but smaller than the fourth switching time of the second one.

Imposing the equality of the jets at each order, we find that

$$\beta_0 = -1, \quad \beta_1 = 0, \quad \beta_2 = -4C_2 + (p_y^0 + 1)^2 C_1,$$
$$\mathbb{T}_4 - \boldsymbol{T} = -8(A + C_1)\rho_0^3 + \mathcal{O}(\rho_0^4),$$

where $\mathbb{T}_4$ denotes the fourth switching time of the trajectory belonging to the set Γ_f. This implies that, if $C_1 = 0$, the intersection occurs only if $C_2 \leq 0$ and $A \leq 0$.

If $C_1 = 0$, the suspension of the intersections to the plane $\{z = 4\zeta^2\}$ is given by

(45)
$$\begin{cases} x = -4A\zeta^3 + \big(-\frac{2}{3}D_1(p_y^0)^3 + (E_1 - D_1)(p_y^0)^2 + 2E_1 p_y^0 + \frac{1}{3}(D_1 - 5E_1 - 4d)\big)\zeta^4 + \mathcal{O}(\zeta^5) \\ y = -4A\zeta^3 - \big(2D_1(p_y^0)^2 - 4E_1 p_y^0 - \frac{2}{3}c\big)\zeta^4 + \mathcal{O}(\zeta^5). \end{cases}$$

Applying a rotation of π around the axis z (and p_z in the adjoint space) and the suitable permutation of the invariant, we obtain the expression of the suspension of the intersection $\mathcal{F}_5 \cap \bar{\mathcal{F}}_4$:

$$\begin{cases} x = 4A\zeta^3 + \big(\frac{2}{3}D_1(p_y^0)^3 + (E_1 - D_1)(p_y^0)^2 - 2E_1 p_y^0 + \frac{1}{3}(D_1 - 5E_1 - 4d)\big)\zeta^4 + \mathcal{O}(\zeta^5) \\ y = 4A\zeta^3 - \big(2D_1(p_y^0)^2 + 4E_1 p_y^0 - \frac{2}{3}c\big)\zeta^4 + \mathcal{O}(\zeta^5), \end{cases}$$

where p_y^0 denotes the second component of the initial momentum of the geodesic belonging to the set Γ_f. The existence conditions for such intersection are the same.

ζ) $\mathcal{G}_4 \cap \bar{\mathcal{G}}_5$ For ρ_0 and $\boldsymbol{T}$ fixed, we consider a trajectory of the set Γ_{-g} with initial covector $(p_x^0, -1, 1/\rho_0)$ and a trajectory of the set Γ_g with initial covector $(\beta, 1, 1/\widehat{\rho}_0)$, with $\beta = \sum_{k\geq 0} \beta_k \rho_0^k$. We assume that $\boldsymbol{T}$ is greater than the fourth switching time of the first geodesics, but smaller than the fourth switching time of the second one (denoted with $\mathbb{T}_4$ in the following).

Imposing the equality of the jets at each order, we find the constraints

$$\beta_0 = 1, \quad \beta_1 = 0, \quad \beta_2 = -(1 - p_x^0)^2 C_2,$$

so that this intersection occurs only if $C_2 \geq 0$. On the other hand, since $\mathbb{T}_4 - \boldsymbol{T} = 4A\rho_0^3 + \mathcal{O}(\rho_0^4)$, then this intersections occurs only if $A \geq 0$.

The suspension of the intersections to the plane $\{z = 4\zeta^2\}$ is given by

(46)
$$\begin{cases} x = -4(A + p_x^0 C_2)\zeta^3 + \big(2D_2(p_x^0)^2 + 4E_2 p_x^0 + \frac{2}{3}c\big)\zeta^4 + \mathcal{O}(\zeta^5) \\ y = (4A - (1 - p_x^0)^2 C_2)\zeta^3 + \big(\frac{2}{3}D_2(p_x^0)^3 + (E_2 - D_2)(p_x^0)^2 - 2E_2 p_x^0 + c'\big)\zeta^4 + \mathcal{O}(\zeta^5), \end{cases}$$

The leading term ($\mathcal{O}(\zeta^3)$) is an arc of parabola with vertex for $p_x^0 = 1$.

The intersection $\bar{\mathcal{G}}_4 \cap \mathcal{G}_5$ can be easily recovered from this one, by changing all signs in the suspension and applying a suitable permutation of the invariants. As, under such permutations, A and C_2 are unchanged, at the leading term the suspension is the symmetric of (46) with respect to the origin.

η) $\mathcal{G}_5 \cap \bar{\mathcal{G}}_5$ For ρ_0 and $\boldsymbol{T}$ fixed, we consider a trajectory of the set Γ_g with initial covector $(p_x^0, 1, 1/\rho_0)$ and a trajectory of the set Γ_{-g} with initial covector $(\beta, -1, 1/\widehat{\rho}_0)$, with $\beta = \sum_{k\geq 0} \beta_k \rho_0^k$.

These two trajectories intersects only if $p_x^0 - \beta_0 = \frac{2A}{C_2}$; in particular, this imposes $|A| < C_2$. The intersection occurs at time $\boldsymbol{T} = 8\rho_0 + \frac{4}{C_2}\Big(C_2^2(p_x^0)^2 - 2AC_2 p_x^0 - A^2 + \frac{2}{3}C_2^2\Big)\rho_0^3 + \mathcal{O}(\rho_0^4)$. The suspension of the intersections to the plane $\{z = 4\zeta^2\}$ is given by

$$\begin{cases} x = 4(A - C_2 p_x^0)\zeta^3 + \mathcal{O}(\zeta^4) \\ y = -4\frac{A}{C_2}\big(A - C_2 p_x^0\big)\zeta^3 + \mathcal{O}(\zeta^4). \end{cases}$$

The leading term is a segment of slope $-A/C_2$.

θ) $\mathcal{F}_5 \cap \bar{\mathcal{G}}_4$ For ρ_0 and $\boldsymbol{T}$ fixed, we consider a trajectory of the set Γ_f with initial covector $(1, p_y^0, 1/\rho_0)$ and a trajectory of the set Γ_{-g} with initial covector $(\beta, -1, 1/\widetilde{\rho}_0)$, with $\beta = \sum_{k\geq 0} \beta_k \rho_0^k$ and $\widetilde{\rho}_0 = \rho_0 + \sum_{k\geq 2} \alpha_k \rho_0^k$. We assume that $\boldsymbol{T}$ is greater than the fourth switching time of the first

geodesics, but smaller than the fourth switching time of the second one. Equating as usual the jets of the two geodesics, we find

$$\beta_0 = -1, \quad \beta_1 = 0, \quad \beta_2 = 8A - 4(1+p_y^0)C_1,$$
$$\mathbb{T}_4 - \boldsymbol{T} = \big(2A(1+p_y^0) + (1+p_y^0)C_1 + ((p_y^0)^2 + 2p_y^0 - 3)C_2\big)\rho_0^3 + \mathcal{O}(\rho_0^4),$$

where $\mathbb{T}_4$ denotes the fourth switching time of the Γ_{-g} trajectory. We can verify that, for $C_1 = 0$, $A > 0$ and $C_2 < 0$, this expression is always negative. Indeed, it is a concave parabola in p_y^0, which is positive for $p_y^0 = 1$ and $p_y^0 = -1$, so positive on the whole interval. This implies that, for $C_1 = 0$, the intersection occurs only if $C_2 \leq 0$ and $A \geq 0$.

For $C_1 = 0$, the suspension of the intersections to the plane $\{z = 4\zeta^2\}$ is

$$\begin{cases} x = -4A\zeta^3 + \big(\frac{2}{3}D_1(p_y^0)^3 + (E_1+D_1)(p_y^0)^2 + 2E_1p_y^0 - \frac{1}{3}(D_1 + 5E_1 + 4\mathcal{d})\big)\zeta^4 + \mathcal{O}(\zeta^5) \\ y = 4A\zeta^3 - \big(2D_1(p_y^0)^2 + 4E_1p_y^0 - \frac{2}{3}\mathcal{c}\big)\zeta^4 + \mathcal{O}(\zeta^5). \end{cases} \tag{47}$$

ι) $\bar{\mathcal{F}}_5 \cap \mathcal{G}_4$ The existence conditions, the intersection times and the suspension of the intersection at $z = 4\zeta^2$ can be obtained exactly as the precedent one. If $C_1 = 0$, it is given by

$$\begin{cases} x = 4A\zeta^3 + \big(-\frac{2}{3}D_1(p_y^0)^3 + (E_1+D_1)(p_y^0)^2 - 2E_1p_y^0 - \frac{1}{3}(D_1 + 5E_1 + 4\mathcal{d})\big)\zeta^4 + \mathcal{O}(\zeta^5) \\ y = -4A\zeta^3 - \big(2D_1(p_y^0)^2 - 4E_1p_y^0 - \frac{2}{3}\mathcal{c}\big)\zeta^4 + \mathcal{O}(\zeta^5) \end{cases}$$

(here p_y^0 denotes the second component of the initial covector of the Γ_{-f} geodesics). It is a small curve of length $\mathcal{O}(\zeta^4)$.

κ) $\mathcal{F}_4 \cap \mathcal{G}_5$ We consider a trajectory of the set Γ_g with initial covector $(p_x^0, 1, 1/\rho_0)$ and we intersect it with a geodesic of the set Γ_f with initial covector $(1, \beta, 1/\widetilde{\rho}_0)$, where $\beta = \sum_{k\geq 0}\beta_k\rho_0^k$ and $\widetilde{\rho}_0 = \rho_0 + \sum_{k\geq 2}\alpha_k\rho_0^k$.

The existence conditions, the intersection times and suspension of the intersection at $z = 4\zeta^2$ can be obtained by applying to the result of θ) a rotation of $\pi/2$ around the z and the p_z axes and the suitable permutation of the invariants. In particular, we obtain that such intersections occur only for $p_x^0 \geq 1 + \frac{2A}{C_2}$.

If $C_1 = 0$, the suspension on the plane $\{z = 4\zeta^2\}$ reads

$$\begin{cases} x = 4(A - p_x^0C_2)\zeta^3 + \big(2D_2(p_x^0)^2 - 4E_2p_x^0 - \frac{2}{3}\mathcal{d}_2\big)\zeta^4 + \mathcal{O}(\zeta^5) \\ y = (4A + (1-p_x^0)^2C_2)\zeta^3 + \big(-\frac{2}{3}D_2(p_x^0)^3 + (E_2 - D_2)(p_x^0)^2 - 2E_2p_x^0 + \frac{1}{3}(D_2 + 5E_2 + 4\mathcal{d}_2\big)\zeta^4 + \mathcal{O}(\zeta^5) \end{cases} \tag{48}$$

A.3. **Analytical expression of the fronts of the geodesics of the sets $\Gamma_{\pm g}$.** For the sake of clarity, we write here the expression of the suspensions of the part of the wavefront of the geodesics of the sets $\Gamma_{\pm g}$. They can be easily recovered from the corresponding expressions for the geodesics in the sets Γ_f (equations (18)-(19)) , by means of the usual rotation around the z axis and permutation of the invariants.

We fix a small $\zeta > 0$, $\boldsymbol{T} = 8\zeta + \sum_{k\geq 2}T_k\zeta^k$ and $p_y^0 = \pm 1 + \sum_{k\geq 1}\mu_k\rho_0^k$. For such parameters, the intersection of the fronts $\mathcal{G}_4$ and $\bar{\mathcal{G}}_4$ with the plane $z = 4\zeta^2$ are respectively given by

$$\begin{cases} x(\boldsymbol{T}) = \pm(T_2 \mp \mu_1)\zeta^2 \pm \big(T_3 + \frac{1}{6}(8C_1 - 16C_2 + 3(\mp T_2\mu_1 + \mu_1^2 \mp 2\mu_2))\big)\zeta^3 + \mathcal{O}(\zeta^4) \\ y(\boldsymbol{T}) = \mu_1\zeta^2 \pm (4A \pm \mu_2 - 4C_1)\zeta^3 + \mathcal{O}(\zeta^4 j). \end{cases} \tag{49}$$

On the other hand, if $\boldsymbol{T}$ is greater than the fourth switching time and less than the fifth one, we have

$$\begin{cases} x = 4(\pm A - g_0C_2)\zeta^3 + \big(2D_2g_0^2 \mp 4E_2g_0 - \frac{2}{3}\mathcal{c}_2\big)\zeta^4 + \mathcal{O}(\zeta^5) \\ y = \pm(T_1 - 8)\zeta \pm T_2\zeta^2 \pm \big(T_3 - \frac{2}{3}C_2 + 2C_2g_0^2 + 2(T_1-8)(A \mp C_2g_0) - \frac{8}{3}C_1\big)\zeta^3 + \Big(\pm T_4 \\ \qquad \mp\frac{4}{3}D_2g_0^3 + 2E_2g_0^2 \pm 2T_2(A \mp C_2g_0) - \frac{1}{3}(T_1-8)\left(\pm 6E_2g_0 - 3D_2g_0^2 + \mathcal{c}_2\right) - \frac{2}{3}(E_2 + 2\mathcal{d}_2)\Big)\zeta^4, \end{cases} \tag{50}$$

where g_0 denotes the first component of the initial covector (i.e, $g_0 = p_x^0$).

Appendix B. Useful formulas

B.1. **Permutations of the invariants.** Thanks to Lemma 1, we see that Γ_{-f} and $\Gamma_{\pm g}$ trajectories may be recovered from the Γ_f ones, by applying a rotation around the z axis and a suitable permutation of the invariants. For the sake of clarity, in this section we provide these permutations, for the main invariants.

Γ_g to obtain a Γ_g geodesic from a Γ_f one, we must perform a rotation of $\pi/2$ around the vertical axis, and apply the following transformations:

$$\begin{gathered} A \mapsto -A \\ C_1 \mapsto C_2 \qquad C_2 \mapsto C_1 \\ D_1 \mapsto D_2 \qquad D_2 \mapsto -D_1 \qquad E_1 \mapsto E_2 \qquad E_2 \mapsto -E_1 \end{gathered}$$

Γ_{-f} to obtain a Γ_{-f} geodesic from a Γ_f one, we must perform a rotation of π around the vertical axis, and apply the following transformations:

$$\begin{gathered} D_1 \mapsto -D_1 \qquad D_2 \mapsto -D_2 \qquad E_1 \mapsto -E_1 \qquad E_2 \mapsto -E_2 \\ c \mapsto -c \qquad d \mapsto -d \end{gathered}$$

Γ_{-g} to obtain a Γ_{-g} geodesic from a Γ_f one, we must perform a rotation of $3\pi/2$ around the vertical axis, and apply the following transformations:

$$\begin{gathered} A \mapsto -A \\ C_1 \mapsto C_2 \qquad C_2 \mapsto C_1 \\ D_1 \mapsto -D_2 \qquad D_2 \mapsto D_1 \qquad E_1 \mapsto -E_2 \qquad E_2 \mapsto E_1 \end{gathered}$$

B.2. **Jets of the geodesics.** Consider a geodesics of the set Γ_f, with initial adjoint covector $(1, p_y^0, 1/\rho_0)$. Let τ and $\mathscr{T}_3$ denote, respectively, the reparametrised time and the reparametrised third switching time, and set $\hat{\tau} = \tau - \mathscr{T}_3$. Then the jets of the geodesics are given by the following expressions:

$$\begin{aligned} x(\hat{\tau}) = {} & -(1+p_y^0)\rho_0 + \Big(Ap_y^0 - \frac{1}{6}C_1(1+p_y^0)^3 - 4C_2\Big)\rho_0^3 + \frac{1}{24}\Big(- 17(p_y^0)^4 \mathrm{ax}_{21} - 36(p_y^0)^3 \mathrm{ax}_{21} \\ & - 12\mathrm{ax}_{12}\left((p_y^0)^2(\hat{\tau}-2)^2 + 2(p_y^0)\left(\hat{\tau}^2 - 4\hat{\tau} - 8\right) + (\hat{\tau}-2)^2\right) - 6(p_y^0)^2\mathrm{ax}_{21} + 144(p_y^0)^2\mathrm{ax}_{22} \\ & - 8\mathrm{ax}_{11}\left((p_y^0)^3(3\hat{\tau}-2) + 3(p_y^0)^2(3\hat{\tau}+4) + (p_y^0)(9\hat{\tau}-6) + 3\hat{\tau} + 4\right) + 28(p_y^0)\mathrm{ax}_{21} + 15\mathrm{ax}_{21} \\ & - 80\mathrm{ax}_{22} - 12(p_y^0)^2\hat{\tau}^2\mathrm{ay}_{11} + 48(p_y^0)^2\hat{\tau}\mathrm{ay}_{11} - 48(p_y^0)^2\mathrm{ay}_{11} + 144(p_y^0)^2\mathrm{ay}_{21} - 8(p_y^0)\hat{\tau}^3\mathrm{ay}_{12} \\ & - 24(p_y^0)\hat{\tau}^2\mathrm{ay}_{11} + 48(p_y^0)\hat{\tau}^2\mathrm{ay}_{12} + 96(p_y^0)\hat{\tau}\mathrm{ay}_{11} - 96(p_y^0)\hat{\tau}\mathrm{ay}_{12} + 192(p_y^0)\mathrm{ay}_{11} + 64(p_y^0)\mathrm{ay}_{12} \\ & - 288(p_y^0)\mathrm{ay}_{22} - 8\hat{\tau}^3\mathrm{ay}_{12} - 12\hat{\tau}^2\mathrm{ay}_{11} + 48\hat{\tau}^2\mathrm{ay}_{12} + 48\hat{\tau}\mathrm{ay}_{11} - 96\hat{\tau}\mathrm{ay}_{12} - 48\mathrm{ay}_{11} \\ & - 256\mathrm{ay}_{12} - 80\mathrm{ay}_{21} + 15(p_y^0)^4\omega_{xx31} + 60(p_y^0)^3\omega_{xx31} + 90(p_y^0)^2\omega_{xx31} - 240(p_y^0)^2\omega_{xx32} \\ & - 240(p_y^0)^2\omega_{xy31} - 240(p_y^0)^2\omega_{yx31} + 60(p_y^0)\omega_{xx31} + 480(p_y^0)\omega_{xy32} + 480(p_y^0)\omega_{yx32} \\ & + 480(p_y^0)\omega_{yy31} + 15\omega_{xx31} - 80\omega_{xx32} - 80\omega_{xy31} - 80\omega_{yx31} - 960\omega_{yy32}\Big)\rho_0^4 + \mathcal{O}(\rho_0^5) \end{aligned} \tag{51}$$

$$\begin{aligned} y(\hat{\tau}) = {} & (2-\hat{\tau})\rho_0 + \big(C_1(p_y^0-1)^2 - 2A(p_y^0-1) + \frac{4}{3}C_2\big)\rho_0^3 + \frac{1}{6}\Big((-p_y^0-1)\hat{\tau}\big(3\hat{\tau}((p_y^0+1)\mathrm{ax}_{22} \\ & + (p_y^0+1)\mathrm{ay}_{21} - 4\mathrm{ay}_{22}) + 6\big(2(2\mathrm{ay}_{22} - (p_y^0+1)(\mathrm{ax}_{22}+\mathrm{ay}_{21})) + (p_y^0+1)^2\mathrm{ax}_{21}\big) + 2\hat{\tau}^2\mathrm{ay}_{22}\big) \\ & - 18(p_y^0-1)^3\mathrm{ax}_{21} + 18(p_y^0-1)^2\mathrm{ax}_{11} + 48p_y^0(p_y^0-1)^2\mathrm{ax}_{21} - 24(p_y^0-1)^2\mathrm{ax}_{21} \\ & + 18(p_y^0-1)^2\mathrm{ax}_{22} - 8(p_y^0-1)\mathrm{ax}_{12} - 48(p_y^0-1)\mathrm{ax}_{21} - 48p_y^0(p_y^0-1)\mathrm{ax}_{22} \\ & + 48(p_y^0-1)\mathrm{ax}_{22} - 32\mathrm{ax}_{21} + 48\mathrm{ax}_{22} + 18(p_y^0-1)^2\mathrm{ay}_{21} - 8(p_y^0-1)\mathrm{ay}_{11} \\ & - 48p_y^0(p_y^0-1)\mathrm{ay}_{21} + 48(p_y^0-1)\mathrm{ay}_{21} \\ & - 24(p_y^0-1)\mathrm{ay}_{22} + 64p_y^0\mathrm{ay}_{22} + 4\mathrm{ay}_{12} + 48\mathrm{ay}_{21} - 96\mathrm{ay}_{22} - 30(p_y^0-1)^3\omega_{xx31} \\ & + 30(p_y^0-1)^2\omega_{xx32} + 30(p_y^0-1)^2\omega_{xy31} - 40(p_y^0-1)\omega_{xy32} + 30(p_y^0-1)^2\omega_{yx31} \\ & - 40(p_y^0-1)\omega_{yx32} - 40(p_y^0-1)\omega_{yy31} + 60\omega_{yy32}\Big)\rho_0^4 + \mathcal{O}(\rho_0^5) \end{aligned} \tag{52}$$

(53)

$$
\begin{aligned}
z(\hat\tau) = {}& \frac{1}{2}\big(6 + p_y^0(\hat\tau - 2) + \hat\tau\big)\rho_0^2 + \frac{1}{6}\Big(- 3\mathrm{ax}_{32}\big((p_y^0)^2\left(\hat\tau^2 - 4\hat\tau - 4\right)\\
& + 2(p_y^0)\left(\hat\tau^2 + 4\hat\tau + 20\right) + \hat\tau^2 - 4\hat\tau - 20\big)\\
& - 2\mathrm{ax}_{31}\left((p_y^0)^3(\hat\tau + 10) + 3(p_y^0)^2(\hat\tau - 22) + 3(p_y^0)(\hat\tau + 26) + \hat\tau - 38\right) - 3(p_y^0)^2\hat\tau^2\mathrm{ay}_{31}\\
& + 12(p_y^0)^2\hat\tau\mathrm{ay}_{31} + 12(p_y^0)^2\mathrm{ay}_{31} - 2(p_y^0)\hat\tau^3\mathrm{ay}_{32} - 6(p_y^0)\hat\tau^2\mathrm{ay}_{31} + 12(p_y^0)\hat\tau^2\mathrm{ay}_{32}\\
& - 24(p_y^0)\hat\tau\mathrm{ay}_{31} - 24(p_y^0)\hat\tau\mathrm{ay}_{32} - 120(p_y^0)\mathrm{ay}_{31} - 16(p_y^0)\mathrm{ay}_{32} - 2\hat\tau^3\mathrm{ay}_{32} - 3\hat\tau^2\mathrm{ay}_{31}\\
& + 12\hat\tau^2\mathrm{ay}_{32} + 12\hat\tau\mathrm{ay}_{31} + 72\hat\tau\mathrm{ay}_{32} + 60\mathrm{ay}_{31} + 176\mathrm{ay}_{32}\Big)\rho_0^4\\
& + \frac{1}{48}\Big(17\hat\tau\mathrm{ax}_{21}(p_y^0)^4 - 106\mathrm{ax}_{21}(p_y^0)^4 + 9\hat\tau\omega_{xx31}(p_y^0)^4 + 102\omega_{xx31}(p_y^0)^4 + 36\hat\tau\mathrm{ax}_{21}(p_y^0)^3\\
& + 552\mathrm{ax}_{21}(p_y^0)^3 + 72\mathrm{ax}_{22}(p_y^0)^3 + 72\mathrm{ay}_{21}(p_y^0)^3 + 36\hat\tau\omega_{xx31}(p_y^0)^3 - 792\omega_{xx31}(p_y^0)^3 + 12\hat\tau^2\omega_{xx32}(p_y^0)^3\\
& - 48\hat\tau\omega_{xx32}(p_y^0)^3 - 72\omega_{xx32}(p_y^0)^3 12\hat\tau^2\omega_{xy31}(p_y^0)^3 - 48\hat\tau\omega_{xy31}(p_y^0)^3 - 72\omega_{xy31}(p_y^0)^3 + 12\hat\tau^2\omega_{yx31}(p_y^0)^3\\
& - 48\hat\tau\omega_{yx31}(p_y^0)^3 - 72\omega_{yx31}(p_y^0)^3 + 6\hat\tau\mathrm{ax}_{21}(p_y^0)^2 - 300\mathrm{ax}_{21}(p_y^0)^2 - 144\hat\tau\mathrm{ax}_{22}(p_y^0)^2 - 552\mathrm{ax}_{22}(p_y^0)^2\\
& + 4\hat\tau^3\mathrm{ay}_{11}(p_y^0)^2 - 24\hat\tau^2\mathrm{ay}_{11}(p_y^0)^2 + 48\hat\tau\mathrm{ay}_{11}(p_y^0)^2 - 144\hat\tau\mathrm{ay}_{21}(p_y^0)^2 - 552\mathrm{ay}_{21}(p_y^0)^2 - 96\mathrm{ay}_{22}(p_y^0)^2\\
& + 54\hat\tau\omega_{xx31}(p_y^0)^2 + 1332\omega_{xx31}(p_y^0)^2 + 36\hat\tau^2\omega_{xx32}(p_y^0)^2 + 96\hat\tau\omega_{xx32}(p_y^0)^2 + 744\omega_{xx32}(p_y^0)^2 + 36\hat\tau^2\omega_{xy31}(p_y^0)^2\\
& + 96\hat\tau\omega_{xy31}(p_y^0)^2 + 744\omega_{xy31}(p_y^0)^2 + 8\hat\tau^3\omega_{xy32}(p_y^0)^2 - 48\hat\tau^2\omega_{xy32}(p_y^0)^2 + 96\hat\tau\omega_{xy32}(p_y^0)^2 + 96\omega_{xy32}(p_y^0)^2\\
& + 36\hat\tau^2\omega_{yx31}(p_y^0)^2 + 96\hat\tau\omega_{yx31}(p_y^0)^2 + 744\omega_{yx31}(p_y^0)^2 + 8\hat\tau^3\omega_{yx32}(p_y^0)^2 - 48\hat\tau^2\omega_{yx32}(p_y^0)^2 + 96\hat\tau\omega_{yx32}(p_y^0)^2\\
& + 96\omega_{yx32}(p_y^0)^2 + 8\hat\tau^3\omega_{yy31}(p_y^0)^2 - 48\hat\tau^2\omega_{yy31}(p_y^0)^2 + 96\hat\tau\omega_{yy31}(p_y^0)^2 + 96\omega_{yy31}(p_y^0)^2 - 28\hat\tau\mathrm{ax}_{21}(p_y^0)\\
& - 440\mathrm{ax}_{21}(p_y^0) + 120\mathrm{ax}_{22}(p_y^0) + 8\hat\tau^3\mathrm{ay}_{11}(p_y^0) - 48\hat\tau^2\mathrm{ay}_{11}(p_y^0) - 192\hat\tau\mathrm{ay}_{11}(p_y^0) + 128\mathrm{ay}_{11}(p_y^0)\\
& + 2\hat\tau^4\mathrm{ay}_{12}(p_y^0) - 16\hat\tau^3\mathrm{ay}_{12}(p_y^0) + 48\hat\tau^2\mathrm{ay}_{12}(p_y^0) - 64\hat\tau\mathrm{ay}_{12}(p_y^0) + 16\mathrm{ay}_{12}(p_y^0) + 120\mathrm{ay}_{21}(p_y^0)\\
& + 288\hat\tau\mathrm{ay}_{22}(p_y^0) + 832\mathrm{ay}_{22}(p_y^0) + 36\hat\tau\omega_{xx31}(p_y^0) - 1272\omega_{xx31}(p_y^0) + 36\hat\tau^2\omega_{xx32}(p_y^0) - 144\hat\tau\omega_{xx32}(p_y^0)\\
& - 696\omega_{xx32}(p_y^0) + 36\hat\tau^2\omega_{xy31}(p_y^0) - 144\hat\tau\omega_{xy31}(p_y^0) - 696\omega_{xy31}(p_y^0) + 16\hat\tau^3\omega_{xy32}(p_y^0) - 96\hat\tau^2\omega_{xy32}(p_y^0)\\
& - 288\hat\tau\omega_{xy32}(p_y^0) - 1088\omega_{xy32}(p_y^0) + 36\hat\tau^2\omega_{yx31}(p_y^0) - 144\hat\tau\omega_{yx31}(p_y^0) - 696\omega_{yx31}(p_y^0) + 16\hat\tau^3\omega_{yx32}(p_y^0)\\
& - 96\hat\tau^2\omega_{yx32}(p_y^0) - 288\hat\tau\omega_{yx32}(p_y^0) - 1088\omega_{yx32}(p_y^0) + 16\hat\tau^3\omega_{yy31}(p_y^0) - 96\hat\tau^2\omega_{yy31}(p_y^0)\\
& - 288\hat\tau\omega_{yy31}(p_y^0) - 1088\omega_{yy31}(p_y^0) + 6\hat\tau^4\omega_{yy32}(p_y^0) - 48\hat\tau^3\omega_{yy32}(p_y^0) + 144\hat\tau^2\omega_{yy32}(p_y^0) - 192\hat\tau\omega_{yy32}(p_y^0)\\
& - 144\omega_{yy32}(p_y^0) + 4\Big((3\hat\tau^2 - 4\hat\tau - 22)(p_y^0)^3 + 3(3\hat\tau^2 + 8\hat\tau + 26)(p_y^0)^2 + 3(3\hat\tau^2 - 4\hat\tau - 46)(p_y^0) + 3\hat\tau^2 + 8\hat\tau + 50\Big)\mathrm{ax}_{11}\\
& + 4\left(\hat\tau^3 - 6\hat\tau^2 + (p_y^0)^2\left(\hat\tau^2 - 6\hat\tau + 12\right)\hat\tau + 12\hat\tau + 2(p_y^0)\left(\hat\tau^3 - 6\hat\tau^2 - 24\hat\tau + 16\right) + 16\right)\mathrm{ax}_{12} - 15\hat\tau\mathrm{ax}_{21}\\
& + 262\mathrm{ax}_{21} + 80\hat\tau\mathrm{ax}_{22} + 360\mathrm{ax}_{22} + 4\hat\tau^3\mathrm{ay}_{11} - 24\hat\tau^2\mathrm{ay}_{11} + 48\hat\tau\mathrm{ay}_{11} + 64\mathrm{ay}_{11} + 2\hat\tau^4\mathrm{ay}_{12} - 16\hat\tau^3\mathrm{ay}_{12} + 48\hat\tau^2\mathrm{ay}_{12}\\
& + 256\hat\tau\mathrm{ay}_{12} - 368\mathrm{ay}_{12} + 80\hat\tau\mathrm{ay}_{21} + 360\mathrm{ay}_{21} - 32\mathrm{ay}_{22} + 9\hat\tau\omega_{xx31} + 342\omega_{xx31} + 12\hat\tau^2\omega_{xx32}\\
& + 32\hat\tau\omega_{xx32} + 408\omega_{xx32} + 12\hat\tau^2\omega_{xy31} + 32\hat\tau\omega_{xy31} + 408\omega_{xy31} + 8\hat\tau^3\omega_{xy32} - 48\hat\tau^2\omega_{xy32} + 96\hat\tau\omega_{xy32}\\
& + 416\omega_{xy32} + 12\hat\tau^2\omega_{yx31} + 32\hat\tau\omega_{yx31} + 408\omega_{yx31} + 8\hat\tau^3\omega_{yx32} - 48\hat\tau^2\omega_{yx32} + 96\hat\tau\omega_{yx32} + 416\omega_{yx32} + 8\hat\tau^3\omega_{yy31}\\
& - 48\hat\tau^2\omega_{yy31} + 96\hat\tau\omega_{yy31} + 416\omega_{yy31} + 6\hat\tau^4\omega_{yy32} - 48\hat\tau^3\omega_{yy32} + 144\hat\tau^2\omega_{yy32} + 768\hat\tau\omega_{yy32} + 1776\omega_{yy32}\Big)\rho_0^5
\end{aligned}
$$

Consider a geodesics of the set Γ_f, with initial adjoint covector $(1, p_y^0, 1/\rho_0)$. Set now $\hat{\tau} = \tau - \mathscr{T}_4$. Then

$$
\begin{aligned}
x(\hat{\tau}) &= x(\mathscr{T}_4) + \hat{\tau}\rho_0 + \mathcal{O}(\rho_0^5)\\
y(\hat{\tau}) &= y(\mathscr{T}_4) + \mathcal{O}(\rho_0^5)\\
z(\hat{\tau}) &= z(\mathscr{T}_4) + 2\hat{\tau}(C_1 p_y^0 - A)\rho_0^4 + \hat{\tau}\big((p_y^0)^2 D_1 + 2E_2 p_y^0 - \frac{1}{3}c\big)\rho_0^5 + \mathcal{O}(\rho_0^6)
\end{aligned}
$$

B.3. **Switching times.**

$$
\begin{aligned}
\mathscr{T}_1 &= (p_x^0 - p_y^0) + \frac{4}{3}\mathrm{ax}_{31}(p_x^0 - p_y^0)^3\rho_0^2\\
&\quad + \frac{1}{24}\rho_0^3\left(15\mathrm{ax}_{21}(p_x^0 - p_y^0)^4 + 32p_x^0\mathrm{ax}_{11}(p_x^0 - p_y^0)^3 + 32p_y^0\mathrm{ax}_{21}(p_x^0 - p_y^0)^3 + 15\omega_{xx31}(p_x^0 - p_y^0)^4\right)
\end{aligned}
$$

$$
\begin{aligned}
\mathscr{T}_2 &= \mathscr{T}_1 + 2p_x^0 + \frac{2}{3}\left(12(p_x^0)^2\mathrm{ax}_{32}(p_x^0 - p_y^0) + 12p_x^0\mathrm{ax}_{31}(p_x^0 - p_y^0)^2 + 16(p_x^0)^3\mathrm{ay}_{32} + 12(p_x^0)^2\mathrm{ay}_{31}(p_x^0 - p_y^0)\right)\rho_0^2\\
&\quad + \frac{1}{24}\Big(32(p_x^0)^3\mathrm{ax}_{12}(p_x^0 - p_y^0) + 72(p_x^0)^2\mathrm{ax}_{11}(p_x^0 - p_y^0)^2 + 120(p_x^0)^2\mathrm{ax}_{22}(p_x^0 - p_y^0)^2\\
&\quad + 192(p_x^0)^2p_y^0\mathrm{ax}_{22}(p_x^0 - p_y^0) + 120p_x^0\mathrm{ax}_{21}(p_x^0 - p_y^0)^3 + 192p_x^0p_y^0\mathrm{ax}_{21}(p_x^0 - p_y^0)^2 + 16(p_x^0)^4\mathrm{ay}_{12}\\
&\quad + 32(p_x^0)^3\mathrm{ay}_{11}(p_x^0 - p_y^0) + 160(p_x^0)^3\mathrm{ay}_{22}(p_x^0 - p_y^0) + 256(p_x^0)^3p_y^0\mathrm{ay}_{22} + 120(p_x^0)^2\mathrm{ay}_{21}(p_x^0 - p_y^0)^2\\
&\quad + 192(p_x^0)^2p_y^0\mathrm{ay}_{21}(p_x^0 - p_y^0) + 240(p_x^0)^4\omega_{yy32} + 160(p_x^0)^3\omega_{xy32}(p_x^0 - p_y^0)\\
&\quad + 160(p_x^0)^3\omega_{yx32}(p_x^0 - p_y^0) + 160(p_x^0)^3\omega_{yy31}(p_x^0 - p_y^0) + 120(p_x^0)^2\omega_{xx32}(p_x^0 - p_y^0)^2 + 120(p_x^0)^2\omega_{xy31}(p_x^0 - p_y^0)^2\\
&\quad + 120(p_x^0)^2\omega_{yx31}(p_x^0 - p_y^0)^2 + 120p_x^0\omega_{xx31}(p_x^0 - p_y^0)^3\Big)\rho_0^3
\end{aligned}
$$

$$
\begin{aligned}
\mathscr{T}_3 &= \mathscr{T}_2 + 2p_x^0 + \left(\frac{8}{3}(p_x^0)^3\mathrm{ax}_{31} - 16(p_x^0)^2p_y^0\mathrm{ax}_{32} + 8p_x^0(p_y^0)^2\mathrm{ax}_{31} + 32(p_x^0)^3\mathrm{ay}_{32} - 16(p_x^0)^2p_y^0\mathrm{ay}_{31}\right)\rho_0^2\\
&\quad + \frac{1}{3}\rho_0^3\Big(-2(p_x^0)^4\mathrm{ax}_{11} + 10(p_x^0)^4\mathrm{ax}_{22} + 12(p_x^0)^3(p_y^0)\mathrm{ax}_{12} - 7(p_x^0)^3p_y^0\mathrm{ax}_{21} - 6(p_x^0)^2(p_y^0)^2\mathrm{ax}_{11}\\
&\quad - 18(p_x^0)^2(p_y^0)^2\mathrm{ax}_{22} + 9(p_x^0)(p_y^0)^3\mathrm{ax}_{21} - 24(p_x^0)^4\mathrm{ay}_{12} + 10(p_x^0)^4\mathrm{ay}_{21} + 12(p_x^0)^3(p_y^0)\mathrm{ay}_{11} + 36(p_x^0)^3(p_y^0)\mathrm{ay}_{22}\\
&\quad - 18(p_x^0)^2(p_y^0)^2\mathrm{ay}_{21} + 10(p_x^0)^4\omega_{xx32} + 10(p_x^0)^4\omega_{xy31} + 10(p_x^0)^4\omega_{yx31} + 120(p_x^0)^4\omega_{yy32} - 15(p_x^0)^3p_y^0\omega_{xx31}\\
&\quad - 60(p_x^0)^3p_y^0\omega_{xy32} - 60(p_x^0)^3p_y^0\omega_{yx32} - 60(p_x^0)^3p_y^0\omega_{yy31} + 30(p_x^0)^2(p_y^0)^2\omega_{xx32} + 30(p_x^0)^2(p_y^0)^2\omega_{xy31}\\
&\quad + 30(p_x^0)^2(p_y^0)^2\omega_{yx31} - 15p_x^0(p_y^0)^3\omega_{xx31}\Big)
\end{aligned}
$$

$$
\begin{aligned}
\mathscr{T}_4 &= \mathscr{T}_3 + 2p_x^0 + \Big(8(p_x^0)^3\mathrm{ax}_{31} - 8(p_x^0)^3\mathrm{ax}_{32} + 16(p_x^0)^2p_y^0\mathrm{ax}_{31} - 8(p_x^0)^2p_y^0\mathrm{ax}_{32} + 8p_x^0(p_y^0)^2\mathrm{ax}_{31} - 8(p_x^0)^3\mathrm{ay}_{31}\\
&\quad + \frac{32}{3}(p_x^0)^3\mathrm{ay}_{32} - 8(p_x^0)^2p_y^0\mathrm{ay}_{31}\Big)\rho_0^2\\
&\quad + \frac{1}{3}\Big(9(p_x^0)^4\mathrm{ax}_{11} - 4(p_x^0)^4\mathrm{ax}_{12} - 15(p_x^0)^4\mathrm{ax}_{21} + 15(p_x^0)^4\mathrm{ax}_{22} + 18(p_x^0)^3(p_y^0)\mathrm{ax}_{11} - 4(p_x^0)^3p_y^0\mathrm{ax}_{12}\\
&\quad - 21(p_x^0)^3p_y^0\mathrm{ax}_{21} + 6(p_x^0)^3p_y^0\mathrm{ax}_{22} + 9(p_x^0)^2(p_y^0)^2\mathrm{ax}_{11} + 3(p_x^0)^2(p_y^0)^2\mathrm{ax}_{21} - 9(p_x^0)^2(p_y^0)^2\mathrm{ax}_{22}\\
&\quad + 9p_x^0(p_y^0)^3\mathrm{ax}_{21} - 4(p_x^0)^4\mathrm{ay}_{11} + 2(p_x^0)^4\mathrm{ay}_{12} + 15(p_x^0)^4\mathrm{ay}_{21} - 20(p_x^0)^4\mathrm{ay}_{22} - 4(p_x^0)^3p_y^0\mathrm{ay}_{11}\\
&\quad + 6(p_x^0)^3(p_y^0)\mathrm{ay}_{21} + 12(p_x^0)^3p_y^0\mathrm{ay}_{22} - 9(p_x^0)^2(p_y^0)^2\mathrm{ay}_{21} - 15(p_x^0)^4\omega_{xx31} + 15(p_x^0)^4\omega_{xx32} + 15(p_x^0)^4\omega_{xy31}\\
&\quad - 20(p_x^0)^4\omega_{xy32} + 15(p_x^0)^4\omega_{yx31} - 20(p_x^0)^4\omega_{yx32} - 20(p_x^0)^4\omega_{yy31}\\
&\quad + 30(p_x^0)^4\omega_{yy32} - 45(p_x^0)^3(p_y^0)\omega_{xx31} + 30(p_x^0)^3(p_y^0)\omega_{xx32} + 30(p_x^0)^3p_y^0\omega_{xy31} - 20(p_x^0)^3p_y^0\omega_{xy32}\\
&\quad + 30(p_x^0)^3p_y^0\omega_{yx31} - 20(p_x^0)^3p_y^0\omega_{yx32} - 20(p_x^0)^3p_y^0\omega_{yy31} - 45(p_x^0)^2(p_y^0)^2\omega_{xx31} + 15(p_x^0)^2(p_y^0)^2\omega_{xx32}\\
&\quad + 15(p_x^0)^2(p_y^0)^2\omega_{xy31} + 15(p_x^0)^2(p_y^0)^2\omega_{yx31} - 15p_x^0(p_y^0)^3\omega_{xx31}\Big)\rho_0^3
\end{aligned}
$$

References

[1] A. Agrachev, G. Stefani, and P. Zezza. Strong optimality for a bang-bang trajectory. *SIAM Journal on Control and Optimization*, 41(4):991–1014, 2002.

[2] A. A. Agrachev, El-H. Chakir EL-Alaoui, J.-P. Gauthier, and I. Kupka. Generic singularities of sub-Riemannian metrics on R3. *Comptes-Rendus de l'Académie Sci., Paris*, pages 377–384, 1996.
[3] A. A. Agrachev and Yu. L. Sachkov. *Control Theory from the Geometric Viewpoint*. Springer-Verlag, 2004.
[4] A.A. Agrachev, D. Barilari, and U. Boscain. *A Comprehensive Introduction to Sub-Riemannian Geometry*. Studies in Advanced Mathematics. Cambridge University Press, 2019.
[5] A.A. Agrachev and J.P. Gauthier. On the Dido Problem and plane isoperimetric problems. *Acta Applicandae Mathematicae*, 57:287–338, 1999.
[6] E. A.L. Ali and G. Charlot. Local (sub)-Finslerian geometry for the maximum norms in dimension 2. *J. Dyn. Control. Syst*, (25):457–490, 2019.
[7] E. A.L. Ali and G. Charlot. Local contact sub-Finslerian geometry for maximum norms in dimension 3. *Mathematical Control & Related Fields*, 0, 2020.
[8] A.A. Ardentov, E. Le Donne, and Y.L. Sachkov. A sub-Finsler problem on the Cartan group. *Proc. Steklov Inst. Math.*, 304:42–59, 2019.
[9] D. Barilari, U. Boscain, E. Le Donne, and M. Sigalotti. Sub-Finsler geometry from the time-optimal control viewpoint for some nilpotent distributions. *J. Dyn. Control Syst.*, 3(3):547–575, 2017.
[10] B. Bonnet, J.-P. Gauthier, and F. Rossi. Generic singularities of the 3D-contact sub-Riemannian conjugate locus. *Comptes Rendus Mathematique*, 357(6):520–527, 2019.
[11] E. Breuillard and E. Le Donne. On the rate of convergence to the asymptotic cone for nilpotent groups and subfinsler geometry. *Proc. Natl. Acad. Sci. USA*, 110(48):19220–19226, 2013.
[12] El-H. Chakir E-Alaoui, J.-P. Gauthier, and I. Kupka. Small sub-Riemannian balls on R3. *Journal of dynamical and control systems*, 2(3):359–421.
[13] J. N. Clelland and C. G. Moseley. Sub-Finsler geometry in dimension three. *Differential Geometry and its Applications*, 24(6):628 – 651, 2006.
[14] J. N. Clelland, C. G. Moseley, and G. R. Wilkens. Geometry of sub-Finsler Engel manifolds. *Asian J. Math*, 11(4):699 – 726, 2007.
[15] M. Golubitsky and V. Guillemin. *Stable Mappings and Their Singularities*. Graduate texts in mathematics. Springer, 1974.
[16] F. Harrache. *Les métriques sous-Finslériennes en dimension 3*. PhD thesis, Ecole doctorale 548. in preparation.
[17] F. Jean. *Control of Nonholonomic Systems: from Sub-Riemannian Geometry to Motion Planning*. Springer-Briefs in Mathematics. Springer, 2014.
[18] L. V. Lokutsievskiy. Convex trigonometry with applications to sub-Finsler geometry. *Sbornik: Mathematics*, 210(8):1179–1205, 2019.
[19] R. Montgomery. *A Tour of Subriemannian Geometries, Their Geodesics and Applications*. American Mathematical Society, 2006.
[20] L. Poggiolini and G. Stefani. State-local optimality of a bang-bang trajectory: a Hamiltonian approach. *System and Control Letters*, 53, 2004.
[21] J.W. Rutter. *Geometry of Curves*. Chapman Hall/CRC Mathematics Series. CRC Press, 2018.
[22] L. Sacchelli. Short geodesics losing optimality in contact sub-Riemannian manifolds and stability of the 5-dimensional caustic. *SIAM Journal on Control and Optimization*, 57(4):2362–2391, 2019.
[23] M. Sigalotti. Bounds on time-optimal concatenations of arcs for two-input driftless 3D systems. In *Proceedings of the 21st IFAC Control Conference*, 2020.

LIS, UMR CNRS 7020, Université de Toulon, Aix Marseille University, France

Laboratoire de Conception et Conduite des Systémes de Production, Université Mouloud Mammeri, Tizi-Ouzou, Algeria
Email address: fazia.harrache@lis-lab.fr

LIS, UMR CNRS 7020, Université de Toulon, Aix Marseille University, France
Email address: francesca.chittaro@univ-tln.fr

Laboratoire de Conception et Conduite des Systémes de Production, Université Mouloud Mammeri, Tizi-Ouzou, Algeria
Email address: aidene@ummto.dz